Quantum Phases For Two-body Spin-invariant Nearest Neighbor Interactions

by

Beiyan Jin

A thesis submitted to the Department of Chemistry

in conformity with the requirements for

the degree of Doctor of Philosophy

Queen's University

Kingston, Ontario, Canada

March, 1998

Abstract

We build a family of Hamiltonians which include all two-body spin-invariant nearest neighbor interactions for a class of lattices. We study the phase structure for the pure two-body interactions in the family and label quantum phases with good quantum numbers. Possible quantum phases and phase transitions are investigated in lattices with cubic symmetry.

We are especially interested in the superconducting phase and its adjacent quantum phases in these systems. The relationship between the superconducting phase and the antisymmetrized geminal power function, which has a very close relation to the superconducting ground state in the microscopic theory of Bardeen, Cooper and Schrieffer for the conventional superconductivity, is addressed. This is done to gain a better understanding about the physical mechanism of superconducting pairing and thus the physical mechanism of high-temperature superconductivity in the CuO_2 based superconducting materials.

Aiming at a viable alternative to the wave-function approach, we analyze the lower bound method of reduced density matrix theory, a method which obtains a lower bound to the ground state energy of a many-body system as well as an ap-

proximation to the corresponding reduced density matrix. Two numerical algorithms based on a main theorem giving necessary and sufficient conditions for the optimum are presented. Numerical procedures for these algorithms are programmed to solve the central optimization program in the lower bound method. We consider their convergence properties which are very crucial for the lower bound method to become a computationally feasible method in large scale.

Direct lower bound calculations are carried out for the first time in one-dimensional rings. The entries of both the two-body and the three-body density matrices are used as variational parameters in these computations. The results obtained show that the three-body density matrix is the best choice for the lower bound method in these one-dimensional systems. The lower bound method with the three-body density matrix effectively provides a solution to the n-representability problem.

It is predicted that direct lower bound calculations in two-dimensional square lattices and other more complicated systems will be very successful too.

Statement of Originality

The original contributions presented in this thesis are summarized as follows:

- Quantum phases for pure two-body interactions. Pure two-body spin-invariant nearest neighbor interactions for a class of lattices are built and analyzed. Quantum phases for these interactions are studied.

- The antisymmetrized geminal power wave-functions and the superconducting ground states. Possible ground states, which can be described by the antisymmetrized geminal power wave-functions and thus are superconducting ground states in lattices with cubic symmetry, are studied.

- The lower bound method of reduced density matrix theory. The central optimization problem in the lower bound method of reduced density matrix theory is studied. Two numerical algorithms are presented to solve the central optimization problem with a fast speed of convergence.

- Application of the lower bound method of reduced density matrix theory. Direct lower bound calculations with the entries of both the two-body and the three-body density matrices as variational parameters are performed in one-dimensional rings.

Acknowledgements

I would like to express my sincere gratitude to my thesis supervisor Dr. Robert Erdahl. Without his conscientious guidance and advice, this work could never have been done. I learned a lot of mathematics from him which will benefit me for the rest of my life.

I would like to express my sincere gratitude to my co-supervisor Dr. Vedene Smith for all his advice and help. I feel proud to have been given the opportunity to be in Smith's group.

I also wish to extend my thanks to my colleagues in the Mathematics and Statistics Department and in the Chemistry Department for all kinds of help and interesting discussions.

Financial support from Queen's University and Dr. Erdahl are gratefully acknowledged. Thanks should also go to the Chemistry Department for giving me the chance to work as a teaching assistant.

Throughout the course of this research, the love, encouragement and understanding of my wife Hongshi Yu have meant much more to me than I can put in words. Last but not least, I thank my 17 months old daughter Daphne Jin. She has been a source of joy in the past two years, even before she came into this world.

Dedication

To my parents,

Xiuju Tong

and

Xunmin Jin,

with love and respect.

Contents

List of Figures

List of Tables

List of Important Symbols

BCS: Bardeen-Cooper-Schrieffer.

SC: Superconductivity.

FM: Ferromagnetic.

AFM: Anti-ferromagnetic.

AGP: Antisymmetrized geminal power.

ODLRO: Off-diagonal long-range order.

FCI: Full configuration interaction.

H^1: A linear space of pure 1-body spin-invariant interactions.

H^2: A linear space of pure 2-body spin-invariant interactions.

S_{H^2}: A unit sphere of pure 2-body spin-invariant interactions.

$\hat{h}^V$: Valence Hamiltonian.

$\hat{h}^I$: Ionic Hamiltonian.

$\hat{h}^M$: Mixed Hamiltonian.

$\hat{N}^{I,V}$: Operator that counts ionic and valence sites.

$H_B(\psi_g)$: Basin of attraction for ground state ψ_g.

$\mathbf{\Lambda}$: A vector space that designates a lattice.

$|\mathbf{\Lambda}|$: The total number of lattice sites in $\mathbf{\Lambda}$.

n_I: The total number of ionic sites.

$n_I(e)$: The number of empty ionic sites.

$n_I(d)$: The number of doubly occupied ionic sites.

n_V: The total number of valence sites.

$n_V^{\uparrow}$: The number of valence sites with spin up.

$n_V^{\downarrow}$: The number of valence sites with spin down.

$<\mathbf{i},\mathbf{j}>$: A pair of nearest neighbor sites in a lattice.

n_{ne}: The number of nearest neighbor sites in a lattice.

$\vec{S}$: Spin operator.

$|0>$: Vacuum state.

T_{PH}: Particle-hole transformation.

$\hat{e}$: Identity operator.

$\hat{d}$: The von Neumann density operator.

$\hat{d}^n$: The density operator for an n-particle system.

d^p: p-body density matrix.

D^p: A convex set of p-body density matrices.

d_n^p: n-representable p-body density matrix.

D_n^p: A convex set of n-representable p-body density matrices.

S: Pauli subspace.

$\square$: Symbol indicating the end of a proof.

Chapter 1

Introduction

In this chapter, we will first give a brief review on the recent development of studies on high-temperature superconductivity. We will focus on studies of two theoretical models, the Heisenberg model and the Hubbard model for 2D square lattices. The relationship between these models and high-temperature superconductivity will be addressed. Then, we will give a brief introduction to the lower bound method of reduced density matrix theory.

1.1 High-T_c Superconductivity and the 2D Square Lattices

1.1.1 Conventional Superconductivity versus High-T_c Superconductivity

With respect to superconductivity (SC), one can discern two fields of interest. The first one, the field of conventional SC, has its origin in 1911. In that year, Kamerlingh-Onnes discovered the phenomenon of SC, in mercury, which has a critical temperature, T_c, of 4.19 K [1]. Since then, other materials have been found to be superconductors. Until 1986, the highest T_c value was 23.2 K which was found in the alloy Nb_3Ge in 1973 [2]. It was widely felt that this value could at best be improved by only a degree or two in some exotic metallic alloy. To this point, all superconducting materials found were metals or alloys. The theory of Bardeen, Cooper and Schrieffer in 1957, referred to as BCS theory, was generally accepted as the microscopic theory which shows that the condensate of coherent electron pairs (known as the Cooper pairs) induced by the electron-phonon interaction is responsible for SC [3].

However, in 1986 Bednorz and Müller observed a T_c of 30 K in a class of cuprates, based on the parent compound La_2CuO_4 [4]. This is the starting point of the second field of SC: the field of high-T_c superconductivity. Ever since, several other superconducting materials with higher T_cs were found and recently, Gao et al. reported the highest T_c value so far of 164 K in a material which contains optimally doped

$HgBa_2Ca_2Cu_3O_{8+x}$ [5].

The practical importance of a T_c above the boiling point of nitrogen, 77.4 K, is that instead of liquid helium (with boiling point of 4.2 K), liquid nitrogen can be used for keeping the system at the appropriate temperature. This is much easier not only because of the higher boiling point but also because of the latent heat of nitrogen, which is about 10^5 times the latent heat of helium.

From a theoretical point of view, the conventional electron-phonon interaction appears not to be the origin of SC in these new superconducting materials, thus leaving the fundamental physics open to investigation. Indeed, it is becoming apparent that many of the properties of these new materials are unusual and a proper understanding will require developing and extending concepts from many areas of condensed matter physics. Nevertheless, the superconducting state appears to be associated with a pairing of electrons, and hence the overall superconducting behavior of the new systems will be similar in many respects to the conventional systems. In fact most of the familiar phenomena which are a manifestation of the superconducting state—persistent currents, Josephson tunneling, vortex lattice—have been established in the new systems.

1.1.2 The Oxide Superconductors and the 2D Square Lattices

Among the new superconductors, there is a class of oxide materials which have attracted the most attention. The most striking feature of these materials is that in

their crystal structures, one always observes parallel Cu-O planes. Both experimental evidence and theoretical analysis have shown that these parallel Cu-O planes in the cuprates dominate the material from the electronic, superconducting and structural points of view and are the cause of the highly anisotropic normal-state and superconducting properties [6]. The interaction between the adjacent Cu-O planes is much weaker than within each Cu-O plane. Thus it is widely believed that the study of one such separated Cu-O plane may reveal the fundamental physics in the whole system.

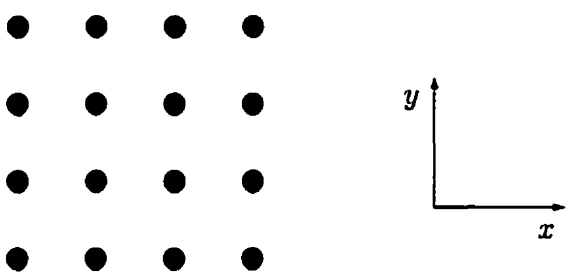

Figure 1.1: A 2-dimensional Square Lattice

Many models have been suggested to study the Cu-O plane. A review of theoretical models for the superconducting state and the superconducting pairing can be found in reference [7]. Among these models are a series of 1-band models for a 2-dimensional square lattice schematically shown in figure 1.1. Here, the square lattice refers to the positions (sites) of the Cu atoms in a Cu-O plane (x-y plane), the z axis is chosen as the quantization axis, and the 1-band is a result of the fact that each Cu atom in the Cu-O plane contributes one spatial orbital to the system. 1-band models are the simplest models and are the starting point for more sophisticated models.

1.2 Two Important Models for 2-dimensional Square Lattices

The spin-$\frac{1}{2}$ Heisenberg model and the Hubbard model on square lattices are the most basic models that are studied in high-T_c superconductivity.

1.2.1 The Spin-$\frac{1}{2}$ Heisenberg Model

The Heisenberg Hamiltonian takes its name from an early paper on ferromagnetism by Heisenberg [8]. In a 2-electron system with a spin-free Hamiltonian, let ${}^1E$ and ${}^3E$ denote the energies for the lowest singlet and triplet states, respectively, the coupling constant J, also called exchange integral, can be defined as $J = ({}^3E - {}^1E)$ [9]. Obviously with $J < 0$, one has parallel spin alignment in the ground state (ferromagnetism); whereas with $J > 0$, one has antiparallel spin alignment in the ground state (antiferromagnetism). The Heisenberg operator, which is equivalent to the Hamiltonian for the 2-electron system, is given by

$$H_{Heisenberg} = \frac{1}{4}({}^1E + 3{}^3E) + J\vec{S}_1 \cdot \vec{S}_2. \tag{1.1}$$

Here $\vec{S}_1$ and $\vec{S}_2$ are spin operators for the two electrons. Later, this idea was generalized to many-particle systems with any spin in any dimension.

The magnetic properties of the oxide materials have been of particular interest since the discovery in some parent (undoped) oxide materials that the Cu ions carry unpaired spins [10, 11] and these Cu spins order antiferromagnetically [12]-[15], with

the consequent possibility that the magnetic fluctuation may be responsible for superconductivity.

The spin-$\frac{1}{2}$ antiferromagnetic Heisenberg model describes a system which consists of interacting magnetic particles—the spins-$\frac{1}{2}$ —which are situated on the sites of a square lattice. The corresponding Hamiltonian is

$$H_{Heisenberg} = J \sum_{<i,j>} \vec{S}_i \cdot \vec{S}_j = J \sum_{<i,j>} S_i^z S_j^z + J \sum_{<i,j>} (S_i^x S_j^x + S_i^y S_j^y). \qquad (1.2)$$

Here $\vec{S}_i$ is the spin operator corresponding to site i and J is the coupling constant between spins on every pair of nearest neighbor sites $< i, j >$. With $J > 0$, this model is assumed to describe 2D antiferromagnetism in an isolated Cu-O plane of the undoped oxide materials. The key question to answer is: does this model have a ground state characterized by a 2-dimensional antiferromagnetic (AFM) long-range order? In order to answer this question, a lot of effort has been made. Manousakis reviewed this subject in 1991 [16].

In the right side of the second equality in Eq. (1.2), the first term is called the classical term which can be solved exactly. Its ground state is the well-known Néel state which is characterized by the AFM long-range order. The second term is called the quantum fluctuation term which reduces or even destroys the AFM long-range order. Despite its simplicity, this Heisenberg model lacks an exact solution. Numerical calculations with various techniques, such as exact diagonalization [17], Monte Carlo simulation [18], series expansion [19], spin-wave theory [20] and resonating-valence-bond model [21], all suggested that its ground state possesses an AFM long-range order. The spin fluctuation is not strong enough to destroy the long-range order, but

significantly reduces the value of the order parameter. The suggested numerical value of the order parameter agrees well with the experimental result [16]. It seems that the Heisenberg model gives a good description of spin dynamics in the undoped oxide materials.

It is widely believed that an appropriate model for such 2D spin fluctuations, when supplied with a hopping term that describes the hopping of a magnetic particle from one site to its nearest neighbor sites, would be an appropriate model to describe the superconducting states in the doped oxide materials.

1.2.2 The 1-band Hubbard Model

Led by the close proximity of the antiferromagnetic and superconducting phases in the oxide materials, Anderson proposed to describe the physics of the cuprates by the large-U, 1-band, Hubbard model on a square lattice [22]. The Hubbard Hamiltonian is given by

$$H_{hubbard} = t \sum_{<\mathrm{i}\mathrm{j}>} (a_{\mathrm{i}}^{+} a_{\mathrm{j}} + a_{\mathrm{j}}^{+} a_{\mathrm{i}} + b_{\mathrm{i}}^{+} b_{\mathrm{j}} + b_{\mathrm{j}}^{+} b_{\mathrm{i}}) + U \sum_{\mathrm{i}} a_{\mathrm{i}}^{+} a_{\mathrm{i}} b_{\mathrm{i}}^{+} b_{\mathrm{i}}, \qquad (1.3)$$

here a_{i}, b_{i} are annihilation operators for site i with spin up (z axis) and down respectively. In this expression, the first term is called the hopping term since it describes the hopping of an electron from site i to its nearest neighbor site j or vice versa with the same spin. The second term represents the on-site Coulomb repulsion between a pair of electrons ($U > 0$).

The best evidence relating superconductivity to the Hubbard model comes from the neutron diffraction experiments [14]. These experiments not only show the an-

tiferromagnetism in the undoped materials but also show that magnetic fluctuations can survive into the superconducting phase.

In the strong coupling limit, i.e., $U >> |t|$, the Hubbard Hamiltonian can be transformed into an effective Hamiltonian, called the Hubbard-Anderson Hamiltonian, by a unitary transformation [23]. The same result can also be obtained by second-order perturbation theory, in which the hopping term is treated as a perturbation [24]. It can be shown that, at exact half-filling, i.e., the number of electrons equals the number of sites in a lattice, the Hubbard-Anderson Hamiltonian is equivalent to the Heisenberg Hamiltonian, which has a ground state with the AFM long-range order. Since magnetic interactions may be responsible for superconductivity, Anderson has suggested the so-called Hubbard hypothesis [22] :

The fundamental physics of the oxide superconductors is contained in the Hamiltonian in Eq. (1.3) on a square lattice for small numbers of holes.

Since the properties of the Hubbard model are not yet under good theoretical control, there is no proof or disproof, and the testing of this hypothesis is regarded as a key issue. There are various versions of the Hubbard model, some of which claim ultimately to give superconductivity via spin fluctuations. But no generally accepted conclusion has been achieved yet. Anderson has recently reviewed this subject [25].

1.3 The Lower Bound Method of Reduced Density Matrix Theory

1.3.1 The Reduced Density Matrix

In quantum mechanics, there are two ways to describe a state. One is to use a wave-function and the other is to use a density operator.

For a pure state which can be described by a wave-function ψ, the corresponding density operator is defined as

$$\hat{d} = |\psi><\psi| . \tag{1.4}$$

Let $< \cdot, \cdot >$ denote the trace scalar product for operators on Fock space. If $|\psi>$ is normalized, i.e., $<\psi|\psi>= 1$, we have

$$<\hat{e}, \hat{d}>= 1, \tag{1.5}$$

where $\hat{e}$ is an identity operator. The mean value of a Hermitian operator $\hat{A}$ on the state can be calculated with $\hat{d}$ as

$$<\hat{A}>=<\hat{A}, \hat{d}>=<\psi|\hat{A}|\psi> . \tag{1.6}$$

For a non-pure state which is an ensemble of r pure states described by $\{\psi_1, \psi_2, \cdots, \psi_r\}$, the corresponding density operator is defined as

$$\hat{d} = \sum_i^r p_i \hat{d}_i = \sum_i^r p_i \, |\psi_i><\psi_i|, \tag{1.7}$$

here the coefficients $p_1, p_2, \cdots, p_r$ satisfy the following conditions

$$0 \le p_i \le 1, \quad \text{and} \quad \sum_i^r p_i = 1. \tag{1.8}$$

Obviously, the pure state density operator defined in Eq. (1.4) is a special ensemble density operator. The mean value of $\hat{A}$ on the mixed state can be computed by

$$<\hat{A}>=<\hat{A},\hat{d}>=\sum_{i}^{r} p_i <\hat{A},\hat{d}_i> . \tag{1.9}$$

A set C is said to be convex if for every c_1, $c_2 \in C$ and every real number α, $0 < \alpha < 1$, the point $\alpha c_1 + (1-\alpha)c_2 \in C$ [26]. Obviously, all density operators defined in Eq. (1.7) form a convex set of positive semi-definite operators $\hat{D}$. For an n-fermion system, such a convex set is usually denoted as $\hat{D}^n$. Any $\hat{d}^n \in \hat{D}^n$ is called an n-body density operator. d^n, a matrix representation for $\hat{d}^n$ in the linear space of n-fermion states, is called an n-body density matrix. The convex set of all positive semi-definite n-body density matrices is denoted as D^n.

In atomic, molecular and solid systems, most interactions can be expressed as a sum of interactions between two identical particles and thus are 2-body. In such systems, most of the physical properties can be obtained by computing the expectation value of a 2-body operator. The density operator contains enough information to evaluate the expectation value for an arbitrary operator. It seems that the density operator contains 'too much' information and a simplified version should be adopted. Thus comes the reduced density matrix.

For $\hat{d}$, the p-body density matrix d^p can be defined as

$$d^p(i_1,i_2,\cdots,i_p;j_1,j_2,\cdots,j_p) = Tr\left[a_{i_1}a_{i_2}\cdots a_{i_p}\hat{d}a^+_{j_1}a^+_{j_2}\cdots a^+_{j_p}\right], \tag{1.10}$$

where Tr is the trace on Fock space, $i_1, i_2, \cdots, i_p$ represent single particle states and $a_{i_1}, \cdots, a_{i_p}$ the annihilation operators for these states. All p-body density matrices

form a positive semi-definite convex set denoted by D^p. In Eq. (1.10), $\hat{d}$ is called a representation for the corresponding p-body density matrix. In an n-fermion system, given an p-body density matrix d^p, there need not be an n-body density operator $\hat{d}^n$ so that Eq. (1.10) holds. d^p with at least one representation $\hat{d}^n$ is called an n-representable or a reduced p-body density matrix. It is usually denoted as d_n^p. All reduced p-body density matrices form a positive semi-definite convex set denoted as D_n^p [27, 28].

Any p-body Hermitian operator $\hat{A}^p$ can be expressed as

$$\hat{A}^p = \sum_{\substack{i_1<i_2<\cdots<i_p \\ j_1<j_2<\cdots<j_p}} A_{[a_{i_1}^+,\cdots,a_{i_p}^+;a_{j_1},\cdots,a_{j_p}]} a_{i_1}^+ a_{i_2}^+ \cdots a_{i_p}^+ a_{j_1} a_{j_2} \cdots a_{j_p}. \tag{1.11}$$

The expectation value of $\hat{A}^p$ on $\hat{d}^n$ is

$$\begin{aligned} <\hat{A}^p> &= <\hat{A}^p, \hat{d}^n> \\ &= \sum_{\substack{i_1<i_2<\cdots<i_p \\ j_1<j_2<\cdots<j_p}} A_{[a_{i_1}^+,\cdots,a_{i_p}^+;a_{j_1},\cdots,a_{j_p}]} Tr\left[a_{j_1} a_{j_2} \cdots a_{j_p} \hat{d}^n a_{i_1}^+ a_{i_2}^+ \cdots a_{i_p}^+\right]. \end{aligned} \tag{1.12}$$

If we use A to represent a matrix whose entries are given by $A_{[a_{i_1}^+ \cdots a_{i_p}^+, a_{j_1},\cdots,a_{j_p}]}$, the above formula can be simplified as

$$<\hat{A}^p> = Tr[A d_n^p], \quad \text{with} \quad d_n^p \in D_n^p. \tag{1.13}$$

This shows that the expectation value for a p-body operator can be obtained from the p-body reduced density matrix.

The most important property of D_n^p is that it is n-representable. That means for any $d_n^p \in D_n^p$, there is at least one n-body density operator $\hat{d}^n$ which can give rise to d_n^p according to Eq. (1.10). This is a key problem in reduced density matrix theory.

1.3.2 n-representability Conditions

$d^p \in D^p$ describes a p-particle state in a p-particle system, whereas $d_n^p \in D_n^p$ describes a p-particle state in an n-particle system. So,

$$D_n^p \subset D^p. \tag{1.14}$$

In a system with up to p-body interactions, in order to obtain information directly from the p-body reduced density matrix, we must first find D_n^p or equivalently answer the following question: What conditions must D^p satisfy in order to be n-representable? These conditions are called n-representability conditions. If the full set of n-representability conditions for D_n^p is obtained, one can get rid of the wavefunction and obtain all the physical properties, which are associated with up to p-body operators, directly from D_n^p.

There have been several early attempts to calculate the properties of n-particle systems using the entries of $d^2 \in D^2$ as variational parameters [29]-[31]. As no n-representability condition was considered, the results obtained were far away from the true value. For example, the optimized energy for the Li atom is about 30% lower than the observed value [32]. These calculations indicated that certain constraints must be put on D^2 in order to obtain physically meaningful results and consequently led to the discovery of the n-representability problem.

The concept of n-representability was first raised in 1961 by Coleman [33]. Since then a lot of effort has been made to investigate the n-representability conditions, especially the conditions for D_n^2 [28], [34]-[37]. Although the full set of necessary

and sufficient n-representability conditions is not known explicitly, progress has been made and several important necessary conditions have been discovered. For example, the famous d, q and g conditions are necessary conditions for D_n^2, which require that the d matrix whose entries are given by $Tr[(a_1a_2)^+\hat{d}a_3a_4]$, the q matrix given by $Tr[(a_1^+a_2^+)^+\hat{d}a_3^+a_4^+]$ and the g matrix given by $Tr[(1+a_1^+a_2)^+\hat{d}(1+a_3^+a_4)]$ be positive semi-definite.

Generally speaking, so far, we know much more about the wave-function than the reduced density matrix and the n-representability problem is still very difficult to deal with. The cause of the difficulties arises from the non-smooth behavior of the boundary for the convex set D_n^p [37]. This may have something to do with the rigidity of the system or the non-smooth behavior of the system during phase transitions . The physical meaning behind the n-representability problem may be much more than just reducing the number of variables. Löwdin and Coleman reviewed the development of reduced density matrix theory and the n-representability problem in 1987 [32, 38].

1.3.3 Yang's Off-Diagonal Long-Range Order

One of the most important properties of the 2-body reduced density matrix is the off-diagonal long-range order (ODLRO), which relates the 'large' eigenvalues of d_n^2 to superconductivity.

The essence of the BCS theory is the pairing instability and the formation of a coherent pair condensate [3]. Yang attempted to answer a deeper version of this question: What is the essence of superconductivity which has somehow been correctly

captured by the BCS theory? His answer is that it is the ODLRO, a property of the 2-body reduced density matrix in fermion systems [39]. For an n-fermion system, the upper bound for the eigenvalues of a 2-body reduced density matrix defined in Eq. (1.10) was found to be n for an even n or $n-1$ for an odd n [28, 39]. A eigenvalue of order n for d_n^2 is called a large eigenvalue. Yang showed that it is when $d_n^2 \in D_n^2$ has large eigenvalues that a fermion system manifests certain long-range order such as present in superconductivity.

In the coordinate space, the off-diagonal entries of the 2-body reduced density matrix can be expressed as

$$d_n^2(\mathbf{r}, \mathbf{r}') = Tr[\hat{d}^n a_{\mathbf{r}}^+ b_{\mathbf{r}}^+ a_{\mathbf{r}'} b_{\mathbf{r}'}], \tag{1.15}$$

where $a_{\mathbf{r}}^+$, $b_{\mathbf{r}}^+$, when acting on the vacuum state $|0>$, create a particle at position $\mathbf{r}$ with spin up and down, respectively. If $d_n^2(\mathbf{r}, \mathbf{r}')$ does not go to zero as $|\ \mathbf{r}-\mathbf{r}'\ |$ becomes large, this fermion system is said to be in a state which possesses the ODLRO. This is a pure quantum effect involving the off-diagonal elements of the reduced density matrix which has no classical analogue.

The ODLRO is an idea which has been proposed earlier by Penrose and Onsager [40] and was confirmed later by Bloch [41]. It follows from Yang's argument that the largest possible eigenvalue of $d_n^2 \in D_n^2$ is attained when the associated wave-function is an antisymmetrized geminal power (AGP) function. AGP functions are very important in superconductivity as they are the projections onto an n-particle space of the wave-function used by Badreen, Cooper and Schrieffer in their microscopic theory

of superconductivity [42]. The BCS superconducting ground state is of the form

$$\prod_{\mathbf{k}}(\alpha_{\mathbf{k}} + \beta_{\mathbf{k}} B_{\mathbf{k}}^{+})|0>, \tag{1.16}$$

where the action of $B_{\mathbf{k}}^{+} = a_{\mathbf{k}\uparrow}^{+} a_{-\mathbf{k}\downarrow}^{+}$ on the vacuum state $|0>$ creates a singlet electron pair between two spatial orbitals labeled by a pair vectors $\mathbf{k}$ and $-\mathbf{k}$ in a reciprocal lattice space, and $\alpha_{\mathbf{k}}$, $\beta_{\mathbf{k}}$ are corresponding coefficients. The projection onto the n-particle space of such a ground state is proportional to

$$|\psi_{AGP}>= (\sum_{\mathbf{k}} \beta'_{\mathbf{k}} B_{\mathbf{k}}^{+})^{\frac{n}{2}}|0>, \tag{1.17}$$

where $\beta'_{\mathbf{k}}$ is a coefficient. As an antisymmetrized $\frac{n}{2}$-th power of the two-electron wave-function (geminal)

$$|g>= (\sum_{\mathbf{k}} \beta'_{\mathbf{k}} B_{\mathbf{k}}^{+})|0>, \tag{1.18}$$

ψ_{AGP} is called an antisymmetrized geminal power (AGP) function and usually denoted as g^n.

Yang made the following statements based on either proofs or conjectures [39]:

a) In fermion systems, there is only one route by which d_n^2 can exhibit the ODLRO and this route was chosen by the BCS superconductors.

b) The existence of the ODLRO is a sufficient condition for quantization of magnetic flux.

c) From the flux quantization, the Meissner effect and superconductivity almost certainly follow.

From these statements, it is expected that the ODLRO will be a property not only of the BCS superconductors, but also of any alternate type of superconductivity which may be found. Now the concept of the ODLRO has frequently been used as a criterion for superconducting states in superconductivity studies.

1.3.4 The Lower Bound Method of Reduced Density Matrix Theory

In an n-fermion system with a 2-body Hamiltonian $\hat{h}$, the lower bound method of reduced density matrix theory consists in finding a minimizer d^2_* that minimizes the following energy expression:

$$E(d^2) = Tr[d^2 h], \quad d^2 \in D^2_0, \tag{1.19}$$

here h is the matrix representation for $\hat{h}$ in the same basis set as the 2-body density matrix d^2 and D^2_0 is a convex set of approximately n-representable 2-body density matrices.

If the constraint set $D^2_0 \subset D^2$ satisfies all the n-representability conditions, i.e., $D^2_0 = D^2_n$, then d^2_* will be the exact 2-body reduced density matrix corresponding to the exact ground state of the system and $E(d^2_*)$ will be the exact ground state energy. Unfortunately, only several known necessary conditions can be used as constraints. As a result, too much freedom to the variational parameters is given and therefore, the optimized ground state energy $E(d^2_*)$ lies below the exact ground state energy obtained from the full configuration interaction (FCI) wave-function calculation with

the same set of 1-particle states. Thus the lower bound method of reduced density matrix theory is a method which obtains a lower bound to the ground state energy of a many-particle system, as well as an approximation to the corresponding reduced density matrix.

In principle, this method can be used for systems with p-body interactions for any $p \leq n$. In practice, however, it has only been used for systems with up to 2-body interactions. As $d^2 \in D_0^2$ contains fewer independent variables than $d^n \in D^n$ (unless n is very small), variational calculations for d^2 will be much easier than for d^n. This is the main reason why people want to use the reduced density matrix to replace the wave-function in variational calculations.

There have been several attempts to calculate the properties of an n-particle system using the entries of d^2 as variational parameters. In earlier attempts, fewer conditions were used, which were reasonable for simpler systems [44]- [47]. The first lower bound formula was derived by Bopp [44] and it was successfully applied to three-electron ions. Later, conditions important for many-body systems were introduced to further restrict the variation [48]- [50]. In recent attempts, this method was applied to the Be atom [51] and several nuclear systems [52] with varying degrees of success. In the case of the Be atom, the lower bound obtained is extremely tight.

Generally speaking, the more the condition set imposed is close to complete, the tighter the lower bound. But the tightness of the lower bound is also dependent upon the specific system considered. For example, with the same set of conditions as constraints, the computed lower bound for the Be atom agreed with the FCI ground

state energy using 1s, 2s, 2p orbitals to eight figures [51], but for some nuclear systems, the lower bounds obtained have been off by up to 15% [52].

In the variational calculation of the lower bound method, constraints from these known necessary n-representability conditions are usually very difficult to enforce. As a result, only a few manageable conditions have been used. And even with these conditions, the speed of convergence in the constrained variation is not very fast. A very efficient numerical method for this kind of variation has to be discovered before such a method is computationally feasible in large scale.

In 1979, Erdahl proposed a theorem giving necessary and sufficient conditions for the optimum of the optimization problem defined in Eq. (1.19). Preliminary numerical computations based on this theorem are very encouraging [53].

The status of all direct lower bound calculations is still in a pioneering stage.

Chapter 2

The Phase Structure for Pure Two-body Spin-invariant Nearest Neighbor Interactions

In this chapter, first we will construct a family of Hamiltonians which includes all pure 2-body spin-invariant nearest neighbor interactions (defined in section 2.1) in a class of lattices where all pairs of nearest neighbor sites are equivalent. Then, we will investigate the phase structure for these Hamiltonians.

2.1 Pure 2-body Spin-invariant Nearest Neighbor Interactions

For a fermion system with up to 2-body interactions, the Hamiltonian can be generally expressed as

$$\hat{h} = \alpha\hat{e} + \sum_{i,j} f_{i,j} a_i^+ a_j + \sum_{i<j,i'<j'} g_{i,j;i',j'} a_i^+ a_j^+ a_{i'} a_{j'}, \tag{2.1}$$

here $\hat{e}$ is an identity operator, $a_i^+, \cdots, a_i, \cdots$ are creators and annihilators for 1-particle states and α, $f_{i,j}$, $g_{i,j;i',j'}$ are corresponding coefficients. In this expression, $\{a_i^+ a_j\}$ are called 1-body operators. They represent interactions involving one particle only. $\{a_i^+ a_j^+ a_{i'} a_{j'}\}$ are called 2-body operators and they represent interactions involving two particles. Thus the three parts in Eq. (2.1) are called scalar, 1- and 2-body interactions, respectively. In the Hubbard Hamiltonian in Eq. (1.3), for example, the hopping term is 1-body and the on-site repulsion term is 2-body.

It is well-known that in atomic systems, 1-body interactions play a dominant role and the beautiful shell structure for electrons is explained by spherical symmetry, Pauli's principle and 1-body interactions. In this chapter, we will study how 2-body interactions and the Pauli's principle are the essential ingredient for phase separation in condensed matter. It is significant that 1-body interactions play no role in most model Hamiltonians used to explain phases such as the ferromagnetic (FM) and antiferromagnetic (AFM) phases. The single exception is the Hubbard model where the hopping term appears.

Our study of 2-body interactions in lattices is inspired by extensive studies show-

ing that 2-body interactions are responsible for high-T_c superconductivity [7]. There are various kinds of model Hamiltonians for 2-dimensional square lattices. But even for the simplest models, such as the Heisenberg or Hubbard models, both theoretical and numerical studies are difficult because of the large number of particles involved. The Hubbard model with strong Coulomb repulsion in Eq. (1.3) has been suggested as the simplest Hamiltonian that may contain the basic ingredients needed to explain superconductivity in the 2D systems [22]. So far no generally accepted result concerning the mechanism for high-T_c superconductivity has been obtained.

We want to study a family of Hamiltonians which are simple, but may still reveal some key phenomena of the real systems. We consider a class of 1-band models where all pairs of nearest neighbor sites are equivalent and each lattice site contributes one spatial orbital to the system. 1-dimensional rings with equal distance between every pair of nearest neighbor sites, 2-dimensional square lattices, 3-dimensional cubic lattices all belong to this class of lattices. They will be referred to as lattices with cubic symmetry or 1-, 2-, and 3-dimensional cubic lattices in this thesis. 2-dimensional hexagonal lattices also belong to this class of lattices. Let an arbitrarily chosen z axis be the quantization axis. Any lattice site can be empty, occupied by one electron with spin up (z axis) or down, or occupied by two electrons.

We consider pure 2-body spin-invariant nearest neighbor interactions. Here, nearest neighbor means that electrons on a site interact with only electrons on sites which are nearest neighbors. Spin-invariant means that there is no explicit spin-spin interaction between electrons. Thus the Hamiltonian will commute with the total spin

operator of the system. In other words, the Hamiltonian is invariant under the action of the spin group for the system. Let's define the trace scalar product on Fock space between two operators $\hat{A}$, $\hat{B}$ as $<\hat{A},\hat{B}>$. By removing a proper scalar, any 1-body operator $\hat{h}^1$ can be made orthogonal to $\hat{e}$ with

$$<\hat{e},\hat{h}^1>=0. \tag{2.2}$$

Such a traceless 1-body operator $\hat{h}^1$ is called a pure 1-body operator. Similarly, any 2-body operator $\hat{h}^2$ which is orthogonal to both $\hat{e}$ and any 1-body operator $\hat{h}^1$ with

$$\begin{aligned} <\hat{e}\,,\hat{h}^2> &= 0, \\ <\hat{h}^1,\hat{h}^2> &= 0 \end{aligned} \tag{2.3}$$

is called as a pure 2-body operator. Interactions associated with pure 1- and 2-body operators are called pure 1- and 2-body interactions, respectively.

With $\hat{h}^1$ and $\hat{h}^2$, $\hat{h}$ in the Hamiltonian in Eq. (2.1) can be rewritten as

$$\hat{h}=\alpha\hat{e}+\hat{h}^1+\hat{h}^2. \tag{2.4}$$

The reason behind such a classification is that both pure 1-body and pure 2-body operators form a carrier space for the irreducible representation of real canonical transformations [54]. As a result, pure 2-body operators may have certain common special properties that are quite different from those of pure 1-body operators.

In this thesis, our main interest is pure 2-body interactions. The main advantage of pure 2-body interactions over their conventional counterparts comes from their orthogonality to both scalar and pure 1-body interactions. Such an orthogonality removes the ambiguity by separating scalar and 1-body interactions completely from

pure 2-body interactions and thus makes pure 2-body interactions show much more clearly their 'true' characteristics. Most importantly, the introduction of pure 2-body interactions makes the investigation of phase structure for 2-body interactions much easier and thus can help us to obtain phase structure information that otherwise may not be obtained. It can be shown that the Heisenberg Hamiltonian in Eq. (1.2), which models both the FM and AFM phases on square lattices, is pure 2-body. We believe that in strongly correlated systems with up to 2-body interactions, it is the pure 2-body (rather than 1-body) interactions that play a key role in determining the fundamental physics and this is especially true for systems full of collective behavior. Perturbations from 1-body interactions may make the sharp picture of quantum phases for pure 2-body interactions become fuzzy. But the fundamental physics, such as coherent pairings and long-range orders will not be altered.

So in our investigation, the main question to answer is: To what extent can the phase structure for pure 2-body spin-invariant nearest neighbor interactions on the lattices be explained by a simple picture as in the atomic case?

2.2 Construction of Hamiltonians

2.2.1 Pure 1-body Nearest Neighbor Interactions

Because of the equivalence of all the nearest neighbor site pairs in a lattice, any element $\hat{h}$ in the family of Hamiltonians can be expressed as

$$\hat{h} = \sum_{<\mathbf{i},\mathbf{j}>} \hat{h}_{<\mathbf{i},\mathbf{j}>}. \tag{2.5}$$

Here $\hat{h}_{<\mathbf{i},\mathbf{j}>}$ is the interaction between the nearest neighbor sites $\mathbf{i}$ and $\mathbf{j}$. The notation $<\mathbf{i},\mathbf{j}>$ will be used throughout this thesis to represent a pair of nearest neighbor sites. Obviously $\hat{h}_{<\mathbf{i},\mathbf{j}>}$ must be Hermitian, symmetric with respect to $\mathbf{i}$ and $\mathbf{j}$ and spin-invariant.

In order to construct pure 2-body interactions, we first need to build a complete basis set for pure 1-body operators associated with $<\mathbf{i},\mathbf{j}>$. Let $\mathbf{\Lambda}$ be a vector space that designates a lattice with $|\mathbf{\Lambda}|$ sites and $a_\mathbf{i}$, $b_\mathbf{i}$ annihilation operators on site $\mathbf{i}$ with spin up (z axis) and down respectively. The spin operators for site $\mathbf{i}$ can be defined as $S_\mathbf{i}^+ = a_\mathbf{i}^+ b_\mathbf{i}$, $S_\mathbf{i}^- = b_\mathbf{i}^+ a_\mathbf{i}$ and $S_\mathbf{i}^z = \frac{1}{2}(a_\mathbf{i}^+ a_\mathbf{i} - b_\mathbf{i}^+ b_\mathbf{i})$. The total spin operator for site $\mathbf{i}$ is given by $\vec{S}_\mathbf{i}^2 = S_\mathbf{i}^z S_\mathbf{i}^z + \frac{1}{2}(S_\mathbf{i}^+ S_\mathbf{i}^- + S_\mathbf{i}^- S_\mathbf{i}^+)$. Let $s(i)$, $m_s(i)$ be the quantum numbers for the total spin and its z-component on site $\mathbf{i}$, the spin eigenstates $|\theta^{[s(i),m_s(i)]}>$ are given by

$$\begin{aligned} |\theta^{[0,0]}> &= |0>, \qquad |\theta^{[\frac{1}{2},\frac{1}{2}]}> = a_\mathbf{i}^+|0>, \\ |\theta^{[\frac{1}{2},-\frac{1}{2}]}> &= b_\mathbf{i}^+|0>, \quad |\theta^{[0,0]}> = a_\mathbf{i}^+ b_\mathbf{i}^+|0> . \end{aligned} \tag{2.6}$$

The spin operators associated with $<\mathbf{i},\mathbf{j}>$ are given by

$$\begin{aligned} S^{+}_{<\mathbf{i},\mathbf{j}>} &= S^{+}_{\mathbf{i}} + S^{+}_{\mathbf{j}}, \\ S^{-}_{<\mathbf{i},\mathbf{j}>} &= S^{-}_{\mathbf{i}} + S^{-}_{\mathbf{j}}, \\ S^{z}_{<\mathbf{i},\mathbf{j}>} &= \tfrac{1}{2}(S^{z}_{\mathbf{i}} + S^{z}_{\mathbf{j}}). \end{aligned} \tag{2.7}$$

It is easy to verify that these spin operators satisfy the following commutation relationships

$$\begin{aligned} [S^{z}_{<\mathbf{i},\mathbf{j}>},\, S^{+}_{<\mathbf{i},\mathbf{j}>}] &= S^{+}_{<\mathbf{i},\mathbf{j}>}, \\ [S^{z}_{<\mathbf{i},\mathbf{j}>},\, S^{-}_{<\mathbf{i},\mathbf{j}>}] &= -S^{-}_{<\mathbf{i},\mathbf{j}>}, \\ [S^{+}_{<\mathbf{i},\mathbf{j}>},\, S^{-}_{<\mathbf{i},\mathbf{j}>}] &= 2S^{z}_{<\mathbf{i},\mathbf{j}>}. \end{aligned} \tag{2.8}$$

Thus, $\{S^{+}_{<\mathbf{i},\mathbf{j}>}, S^{-}_{<\mathbf{i},\mathbf{j}>}, S^{z}_{<\mathbf{i},\mathbf{j}>}\}$ are the infinitesimal generators for a $SU(2)$ group which we will denote by $SU(2)_{<\mathbf{i},\mathbf{j}>}$. Operators associated with $<\mathbf{i},\mathbf{j}>$ can be labeled by the irreducible representations of this group as

$$\begin{aligned} [S^{z}_{<\mathbf{i},\mathbf{j}>},\, Q^{[s,m_s]}_{<\mathbf{i},\mathbf{j}>}] &= m_s Q^{[s,m_s]}_{<\mathbf{i},\mathbf{j}>}, \\ [S^{+}_{<\mathbf{i},\mathbf{j}>},\, Q^{[s,m_s]}_{<\mathbf{i},\mathbf{j}>}] &= [(s-m_s)(s+m_s+1)]^{1/2} Q^{[s,m_s+1]}_{<\mathbf{i},\mathbf{j}>}, \\ [S^{-}_{<\mathbf{i},\mathbf{j}>},\, Q^{[s,m_s]}_{<\mathbf{i},\mathbf{j}>}] &= [(s+m_s)(s-m_s+1)]^{1/2} Q^{[s,m_s-1]}_{<\mathbf{i},\mathbf{j}>}, \end{aligned} \tag{2.9}$$

where $[s, m_s]$ labels an irreducible representation of $SU(2)_{<\mathbf{i},\mathbf{j}>}$. Any spin-invariant operator belongs to $[0,0]$, the identity irreducible representation.

The complete basis set for pure 1-body operators associated with $<\mathbf{i},\mathbf{j}>$ can be labeled by $[s, m_s]$ as

$<i,j>$ Symmetry

$$
\begin{aligned}
(+) \qquad & Q^{[0,0]}_{1,<i,j>} &&= e_{a_i} + e_{b_i} + e_{a_j} + e_{b_j}, \\
(+) \qquad & Q^{[0,0]}_{2,<i,j>} &&= a_i^+ a_j + b_i^+ b_j + a_j^+ a_i + b_j^+ b_i, \\
(-) \qquad & P^{[0,0]}_{1,<i,j>} &&= e_{a_i} + e_{b_i} - (e_{a_j} + e_{b_j}), \\
(-) \qquad & P^{[0,0]}_{2,<i,j>} &&= (a_i^+ a_j - a_j^+ a_i) + (b_i^+ b_j - b_j^+ b_i), \\
(-) \qquad & P^{[1,1]}_{3,<i,j>} &&= -\sqrt{\tfrac{1}{2}}(a_i^+ b_j - a_j^+ b_i), \\
(-) \qquad & P^{[1,0]}_{3,<i,j>} &&= a_i^+ a_j + b_j^+ b_i - a_j^+ a_i - b_i^+ b_j, \\
(-) \qquad & P^{[1,-1]}_{3,<i,j>} &&= \sqrt{\tfrac{1}{2}}(b_i^+ a_j - b_j^+ a_i), \\
(+) \qquad & P^{[1,1]}_{4,<i,j>} &&= -\sqrt{\tfrac{1}{2}}(a_i^+ b_j + a_j^+ b_i), \\
(+) \qquad & P^{[1,0]}_{4,<i,j>} &&= a_i^+ a_j - b_j^+ b_i + a_j^+ a_i - b_i^+ b_j, \\
(+) \qquad & P^{[1,-1]}_{4,<i,j>} &&= \sqrt{\tfrac{1}{2}}(b_i^+ a_j + b_j^+ a_i), \\
(-) \qquad & P^{[1,1]}_{5,<i,j>} &&= -\sqrt{\tfrac{1}{2}}(a_i^+ b_i - a_j^+ b_j), \\
(-) \qquad & P^{[1,0]}_{5,<i,j>} &&= \tfrac{1}{2}(e_{a_j} - e_{a_i} + e_{b_i} - e_{b_j}), \\
(-) \qquad & P^{[1,-1]}_{5,<i,j>} &&= \sqrt{\tfrac{1}{2}}(b_i^+ a_i - b_j^+ a_j), \\
(+) \qquad & P^{[1,1]}_{6,<i,j>} &&= -\sqrt{\tfrac{1}{2}}(a_i^+ b_i + a_j^+ b_j), \\
(+) \qquad & P^{[1,0]}_{6,<i,j>} &&= \tfrac{1}{2}(e_{a_i} + e_{a_j} - e_{b_i} - e_{b_j}), \\
(+) \qquad & P^{[1,-1]}_{6,<i,j>} &&= \sqrt{\tfrac{1}{2}}(b_i^+ a_i + b_j^+ a_j),
\end{aligned}
\tag{2.10}
$$

with

$$
e_{a_i} = a_i^+ a_i - a_i a_i^+. \tag{2.11}
$$

Here, the $\pm$ sign indicates whether the operator is symmetric or antisymmetric with respect to i and j.

Among these pure 1-body operators, only $Q^{[0,0]}_{1,<i,j>}$ and $Q^{[0,0]}_{2,<i,j>}$ have the correct

symmetry, i.e., they are Hermitian, symmetric with respect to i and j and spin-invariant. If we denote by $H^1_{<i,j>}$ the 2-dimensional linear space spanned by $Q^{[0,0]}_{1,<i,j>}$ and $Q^{[0,0]}_{2,<i,j>}$, then all the pure 1-body spin-invariant nearest neighbor interactions associated with $<i,j>$ are contained in $H^1_{<i,j>}$. $H^1 = \sum_{<i,j>} H^1_{<i,j>}$ will be a 2-dimensional linear space of all pure 1-body spin-invariant nearest neighbor interactions in the lattice.

2.2.2 Pure 2-body Nearest Neighbor Interactions

Pure 2-body operators can be obtained by coupling pure 1-body operators. Without going into details, the linear space of pure 2-body operators, associated with $<i,j>$ and with the correct symmetry, is 5-dimensional. A basis set is given by

$<i,j>$ Symmetry

$$
\begin{aligned}
&(+) \qquad Q^{[0,0]}_{3,<i,j>} = e_{a_i} e_{b_i} + e_{a_j} e_{b_j}, \\
&(+) \qquad Q^{[0,0]}_{4,<i,j>} = a^+_i b^+_i b_j a_j + a^+_j b^+_j b_i a_i, \\
&(+) \qquad Q^{[0,0]}_{5,<i,j>} = e_{a_i} e_{a_j} + e_{b_i} e_{b_j} + e_{a_i} e_{b_j} + e_{a_j} e_{b_i}, \\
&(+) \qquad Q^{[0,0]}_{6,<i,j>} = e_{a_i} e_{a_j} + e_{b_i} e_{b_j} + 4(a^+_i b_i b^+_j a_j + a^+_j b_j b^+_i a_i), \\
&(+) \qquad Q^{[0,0]}_{7,<i,j>} = (e_{a_i} + e_{b_i} + e_{a_j} + e_{b_j}) Q^{[0,0]}_{2,<i,j>}.
\end{aligned}
\tag{2.12}
$$

If this linear space is denoted by $H^2_{<i,j>}$, then $H^2 = \sum_{<i,j>} H^2_{<i,j>}$ is also 5-dimensional. This is the linear space of pure 2-body spin-invariant nearest neighbor interactions in the lattice. It is significant that all pure 2-body spin-invariant nearest neighbor interactions for these models can be characterized by five real coefficients.

It is worth noting that the Heisenberg Hamiltonian

$$H_{Heisenberg} = J \sum_{<i,j>} \vec{S}_i \cdot \vec{S}_j = J \sum_{<i,j>} \{S_i^z S_j^z + \frac{1}{2}(S_i^+ S_j^- + S_i^- S_j^+)\} \quad (2.13)$$
$$= \frac{J}{16} \sum_{<i,j>} \{e_{a_i} e_{a_j} + e_{b_i} e_{b_j} - (e_{a_i} e_{b_j} + e_{a_j} e_{b_i}) - 8(a_i^+ b_j^+ b_i a_j + a_j^+ b_i^+ b_j a_i)\}$$

belongs to H^2, and the Hubbard Hamiltonian

$$H_{Hubbard} = t \sum_{<i,j>} (a_i^+ a_j + a_j^+ a_i + b_i^+ b_j + b_j^+ b_i) + U \sum_i a_i^+ a_i b_i^+ b_i \quad (2.14)$$

belongs to $H^1 \oplus H^2$, a 7-dimensional linear space of all up to 2-body spin-invariant nearest neighbor interactions in the lattice.

The most striking feature differentiating the pure 1-body interaction from the pure 2-body interaction is their different behavior under particle-hole transformations. Let T_{PH} represent the particle-hole transformation that changes creators to annihilators and annihilators to creators. The action of T_{PH}, for example, on operator a^+bc^+d is $T_{PH}(a^+bc^+d) = ab^+cd^+$. It is easy to verify that under the action of T_{PH}, any pure 1-body interaction in H^1 changes its sign whereas any pure 2-body interaction in H^2 is invariant. The invariance of H^2 under the particle-hole transformation is very important to the study of the phase structure for pure 2-body interactions.

2.3 Labeling Quantum Phases for Pure 2-body Nearest Neighbor Interactions

2.3.1 Classification of Pure 2-body Interactions

Pure 2-body interactions in H^2 can be classified according to their behavior in the

Fock space. Let

$$\hat{h}^V = J \sum_{<i,j>} e_{a_i} e_{a_j} + e_{b_i} e_{b_j} - (e_{a_i} e_{b_j} + e_{a_j} e_{b_i}) - 8(a_i^+ b_j^+ b_i a_j + a_j^+ b_i^+ b_j a_i); \tag{2.15}$$

$$\hat{h}^I = \alpha_1^I \hat{h}_1^I + \alpha_2^I \hat{h}_2^I, \tag{2.16}$$

with

$$\begin{aligned} \hat{h}_1^I &= \textstyle\sum_{<i,j>} (a_i^+ b_i^+ b_j a_j + a_j^+ b_j^+ b_i a_i), \\ \hat{h}_2^I &= \textstyle\sum_{<i,j>} (e_{a_i} e_{a_j} + e_{b_i} e_{b_j} + e_{a_i} e_{b_j} + e_{a_j} e_{b_i}); \end{aligned} \tag{2.17}$$

$$\hat{h}^M = \alpha_M \sum_{<i,j>} (e_{a_i} + e_{b_i} + e_{a_j} + e_{b_j})(a_i^+ a_j + b_i^+ b_j + a_j^+ a_i + b_j^+ b_i); \tag{2.18}$$

and

$$\hat{h}^{N^{I,V}} = \alpha_{N^{I,V}} N^{I,V} = \alpha_{N^{I,V}} \sum_i e_{a_i} e_{b_i}, \tag{2.19}$$

where J, α_1^I, α_2^I, α_M and $\alpha_{N^{I,V}}$ are arbitrary real coefficients. Then any $\hat{h} \in H^2$ can be expressed as

$$\hat{h} = \hat{h}^V + \hat{h}^I + \hat{h}^M + \hat{h}^{N^{I,V}}. \tag{2.20}$$

The physical meaning for such a classification will be given in the following section.

2.3.2 Pair Preservation and Good Quantum Numbers

In our models, each lattice site usually corresponds to a valence orbital of an atom or a molecule. For example, each site in a 2-dimensional square lattice corresponds to a valence d orbital of a Cu atom in the CuO plane. Since the net charge on a lattice is zero when the orbital is occupied by one electron and nonzero in other cases, any lattice site occupied by one electron is called valence and an empty or a doubly occupied lattice site is called ionic. Two electrons occupying the same site

form an electron pair called an on-site pairing. Now we will discuss in detail the effect of various 2-body interactions on these lattice sites. It is easy to see that

$$\begin{aligned}
\hat{h}^V_{<i,j>}|0> &= 0, \quad \hat{h}^V_{<i,j>}a_i^+b_i^+a_j^+b_j^+|0> = 0, \\
\hat{h}^V_{<i,j>}a_i^+b_i^+|0> &= 0, \quad \hat{h}^V_{<i,j>}a_j^+b_j^+|0> = 0, \\
\hat{h}^V_{<i,j>}a_i^+|0> &= 0, \quad \hat{h}^V_{<i,j>}a_i^+a_j^+b_j^+|0> = 0, \\
\hat{h}^V_{<i,j>}b_i^+|0> &= 0, \quad \hat{h}^V_{<i,j>}a_i^+b_j^+b_j^+|0> = 0, \\
\hat{h}^V_{<i,j>}a_j^+|0> &= 0, \quad \hat{h}^V_{<i,j>}a_j^+b_i^+a_i^+|0> = 0, \\
\hat{h}^V_{<i,j>}b_j^+|0> &= 0, \quad \hat{h}^V_{<i,j>}b_j^+a_i^+b_i^+|0> = 0,
\end{aligned} \tag{2.21}$$

and

$$\begin{aligned}
\hat{h}^V_{<i,j>}a_i^+a_j^+|0> &= 4Ja_i^+a_j^+|0>, \\
\hat{h}^V_{<i,j>}b_i^+b_j^+|0> &= 4Jb_i^+b_j^+|0>, \\
\hat{h}^V_{<i,j>}(a_i^+b_j^+ + b_i^+a_j^+)|0> &= 4J(a_i^+b_j^+ + b_i^+a_j^+)|0>, \\
\hat{h}^V_{<i,j>}(a_i^+b_j^+ - b_i^+a_j^+)|0> &= -12J(a_i^+b_j^+ - b_i^+a_j^+)|0> .
\end{aligned} \tag{2.22}$$

Thus, the action of $\hat{h}^V_{<i,j>}$ on any configuration is zero unless both i and j are valence. So the Heisenberg Hamiltonian $\hat{h}^V$, also called a valence Hamiltonian, is zero in the ionic subspace where all sites are ionic and its ground state is a valence state where all sites are valence. Similarly, it can be shown that the action of $\hat{h}^I_{<i,j>}$ on any configuration is zero unless both i and j are ionic. As a result, $\hat{h}^I$ is called an ionic Hamiltonian and it is zero in the valence subspace where all sites are valence. When

both i and j are ionic, we have

$$\begin{aligned}
\hat{h}^I_{2,<i,j>}|0> &= 4|0>, & \hat{h}^I_{2,<i,j>}a_i^+b_i^+a_j^+b_j^+|0> &= 4a_i^+b_i^+a_j^+b_j^+|0>, \\
\hat{h}^I_{2,<i,j>}a_i^+b_i^+|0> &= -4a_i^+b_i^+|0>, & \hat{h}^I_{2,<i,j>}a_j^+b_j^+|0> &= -4a_j^+b_j^+|0>, \\
\hat{h}^I_{1,<i,j>}|0> &= 0, & \hat{h}^I_{1,<i,j>}a_i^+b_i^+a_j^+b_j^+|0> &= 0, \\
\hat{h}^I_{1,<i,j>}a_i^+b_i^+|0> &= a_j^+b_j^+|0>, & \hat{h}^I_{1,<i,j>}a_j^+b_j^+|0> &= a_i^+b_i^+|0> .
\end{aligned} \tag{2.23}$$

Thus, in $\hat{h}^I_{<i,j>}$, the action of $\hat{h}^I_1$, called pair transport term, on any ionic configuration transports a pair of electrons from a doubly occupied ionic site to one of its nearest neighbor empty ionic sites. The action of $\hat{h}^I_2$ on any ionic configuration does not produce new configurations. Obviously, the ground state of $\hat{h}^I$ is an ionic state. The action of $\hat{h}^M_{<i,j>}$ on any configuration is zero if both i and j are ionic or valence, but is non-zero if one site is ionic and the other is valence. Thus $\hat{h}^M$, called mixed Hamiltonian, is zero in both the ionic and the valence subspaces, but is non-zero in any mixed subspace where some sites are ionic and others are valence. As

$$\begin{aligned}
\hat{h}^M_{<i,j>}a_i^+|0> &= -a_j^+|0>, & \hat{h}^M_{<i,j>}a_i^+a_j^+b_j^+|0> &= -a_j^+a_i^+b_i^+|0>, \\
\hat{h}^M_{<i,j>}a_j^+|0> &= -a_i^+|0>, & \hat{h}^M_{<i,j>}a_j^+a_i^+b_i^+|0> &= -a_i^+a_j^+b_j^+|0>,
\end{aligned} \tag{2.24}$$

the action of $\hat{h}^M_{<i,j>}$ switches the ionic and valence sites. As a result, the ground state of $\hat{h}^M$ is a mixed state where some sites are ionic and others are valence. The expectation value of $e_{a_i}e_{b_i}$ on any configuration will be +1 if i is ionic or -1 if i is valence. Thus $N^{I,V} = \sum_i e_{a_i}e_{b_i}$ counts the number of ionic and valence sites. In the subspace where every configuration has n_I ionic sites and n_V valence sites,

$$N^{I,V} = n_I - n_V \tag{2.25}$$

and thus $\hat{h}^{N^I,N^V}$ is equivalent to a constant. Later, we will see that $\hat{h}^{N^I,N^V}$ is very important in the investigation of phase structure for H^2, as it is directly related to some good quantum numbers of a system.

From the above analysis, we find the most important property of H^2: Any $\hat{h} \in H^2$ preserves the total number of on-site pairings. The action of $\hat{h}$ on any configuration may result in the exchange of a pairing site with an empty site or a pairing site with a valence site or an empty site with a valence site or a valence site with another valence site, but it does not break the on-site pairing. As a result, the number of doubly occupied ionic sites $n_I(d)$, the number of empty ionic sites $n_I(e)$, the number of valence sites with spin up $n_V^{\uparrow}$ and the number of valence sites with spin down $n_V^{\downarrow}$ are all good quantum numbers. Certainly the total number of valence sites $n_V = n_V^{\uparrow} + n_V^{\downarrow}$ and the total number of ionic sites $n_I = n_I(d) + n_I(e)$ are also good quantum numbers. As we deal with particle-conserving Hamiltonians, the total number of electrons $n = 2n_I(d) + n_V$ is also a good quantum number. Because of the spin invariance of H^2, the total spin and its z-component are good quantum numbers too. The eigenfunctions of any $\hat{h} \in H^2$ can be labeled by these quantum numbers.

2.3.3 Labeling Quantum Phases with a Unique Set of Quantum Numbers

To facilitate our investigation, the length of any $\hat{h} \in H^2$ is fixed to one, i.e., $< \hat{h}, \hat{h} >= 1$ on Fock space. Under this normalization condition, H^2 becomes the whole surface of a unit sphere in a 5-dimensional linear space. The degree of freedom

on the spherical surface, denoted by S_{H^2}, is four.

Theorem 2.1 *The ground state of any generic Hamiltonian $\hat{h} \in S_{H^2}$ can be labeled by a unique set of quantum numbers $\{n_I, n_V\}$.*

Proof: Assume that two sets of quantum numbers $\{n_I, n_V\}$, $\{n'_I, n'_V\}$ are associated with degenerate ground states $\phi_g^{n_I,n_V}$ and $\phi_g^{n'_I,n'_V}$ of $\hat{h} \in S_{H^2}$. Without loss of generality, we can assume that $n_I > n'_I$. Then $n_V < n'_V$ as $n_I + n_V = n'_I + n'_V = |\mathbf{\Lambda}|$ with $|\mathbf{\Lambda}|$ being the total number of sites. Thus $n'_I - n'_V < n_I - n_V$. If we use $\alpha N^{I,V} \in H^2$ as a perturbation with the coefficient α being small but positive, the degeneracy will be broken with the energy for $\phi_g^{n_I,n_V}$ being higher than that for $\phi_g^{n'_I,n'_V}$. Thus the ground state of any generic Hamiltonian in S_{H^2} is non-degenerate with respect to n_I and n_V and can be labeled by a unique set of $\{n_I, n_V\}$. □

According to theorem 2.1, S_{H^2} can be divided into a number of smaller areas in such a unique way that the ground state of any Hamiltonian in the interior of each area is associated with a unique set of $\{n_I, n_V\}$. There is no overlap among these areas and only Hamiltonians on the boundaries of these areas have a ground state associated with more than one set of $\{n_I, n_V\}$. Thus, the unit sphere S_{H^2} can be colored uniquely by quantum numbers $\{n_I, n_V\}$.

Quantum phases are important bulk properties of a system. A quantum phase for S_{H^2} is a stable state determined by a subset of Hamiltonians in S_{H^2}. The ground states for these Hamiltonians, called the Hamiltonians for the quantum phase, share the key characteristic of the quantum phase. Together, they describe the quantum phase. The boundary for the subset is called the phase boundary for the quantum

phase. As the Hamiltonian varies, the quantum phase will remain stable as long as the Hamiltonian does not go beyond the phase boundary.

According to this definition, we define for each of those smaller areas a quantum phase of S_{H^2}. Any $\hat{h}$ on the area is called a Hamiltonian for the quantum phase and the quantum phase is described by the ground states of its Hamiltonians. The boundary of the area is called the phase boundary. Obviously, the physical meaning for such a defined quantum phase is that: As a Hamiltonian varies on S_{H^2}, no matter in which direction it goes, the associated quantum phase will remain stable as long as the Hamiltonian does not go beyond the boundary of the phase. As the Hamiltonian goes across the phase boundary, the quantum phase will experience a sudden change from a state characterized by $\{n_I, n_V\}$ to another state characterized by a distinct set of $\{n_I', n_V'\}$. Such a defined quantum phase is certainly the one that will most likely exist from a physical point of view.

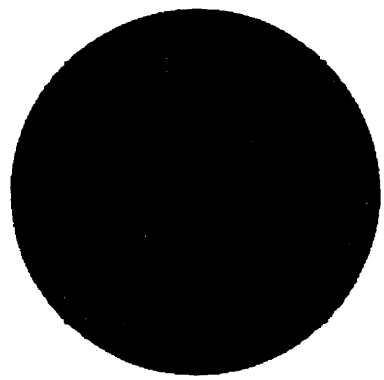

Figure 2.1: Labeling of Quantum Phases for S_{H^2} with $\{n_I, n_V\}$

In this way, quantum phases for S_{H^2} are labeled uniquely by $\{n_I, n_V\}$ as is

schematically shown in figure 2.1. It is very significant that such a simple picture of quantum phases is obtained by using only the very basic properties of pure 2-body nearest neighbor interactions in S_{H^2}. Certainly, not all possible values for $\{n_I, n_V\}$ need to occur on S_{H^2} and in each quantum phase, there may be fine phase structure. Such detailed information can only be obtained by further analyzing the Hamiltonian for a specific lattice.

The labeling of a quantum phase by a unique set of $\{n_I, n_V\}$ is very important. It tells us that instead of seeking a quantum phase in Fock space, we can separate the Fock space into a series of subspaces according to their quantum numbers n_I and n_V and study the quantum phase in each subspace. This definitely will simplify the investigation of phase structure dramatically.

2.3.4 Basins of Attraction

For ϕ, a ground state of $\hat{h} \in S_{H^2}$, we define the basin of attraction $H_B(\phi)$, a special subset of S_{H^2} to be given by:

$$\begin{aligned} (\hat{h} - c) \mid \phi > &= 0, \qquad \text{for } h \in H_B(\phi), \\ (\hat{h} - c) &\geq 0, \qquad \text{in Fock space,} \end{aligned} \tag{2.26}$$

with c being a constant.

Obviously, ϕ is the ground state of all interactions in $H_B(\phi)$. The bigger the basin, the more stable the ground state ϕ to perturbations in S_{H^2}. Thus the size of a basin of attraction represents the rigidity of the corresponding ground state to perturbations.

The dimensionality is the most important factor for a basin of attraction. If the

dimension of $H_B(\phi)$ reaches its highest possible value 4, the same as the dimension of S_{H^2}, $H_B(\phi)$ is said to be a basin of attraction with full dimension. A full-dimensional basin of attraction $H_B(\phi)$ indicates the existence of a Hamiltonian $\hat{h} \in H_B(\phi)$, such that under any small perturbation $\hat{h}' \in S_{H^2}$, $\hat{h} = \hat{h} + \hat{h}' \in H_B(\phi)$. Thus ϕ will remain unaltered under any perturbation from S_{H^2}. If $H_B(\phi)$ is not full-dimensional, ϕ can be altered under certain perturbation in S_{H^2}. If there is a generic $\hat{h} \in H_B(\phi)$ which is not on any phase boundary, according to theorem 2.1, ϕ has a unique set of $\{n_I, n_V\}$. Thus under perturbations, it can only be deformed in the subspace where every configuration has the same $\{n_I, n_V\}$.

Each smaller area on S_{H^2} containing all Hamiltonians for the corresponding quantum phase is called a basin of attraction for the quantum phase. Such a basin of attraction is certainly full-dimensional and it is the union of the basins of attraction for all ground states of the Hamiltonians for the quantum phase. It should be mentioned that a full-dimensional basin of attraction is only a necessary condition for a quantum phase. The full size of a basin of attraction depends not only on the dimensionality of the basin of attraction but also on the range of extension in each dimension.

Different quantum phases for S_{H^2} certainly have different basins of attraction. Any two basins of attraction $H_B(\phi_1)$, $H_B(\phi_2)$ can have a certain intersection or no intersection at all. No intersection means the two quantum phases do not share any common phase boundary and thus are not an adjacent phase pair. As a result, it is impossible for a phase transition between these quantum phases to happen. If $H_B(\phi_1)$ and $H_B(\phi_2)$ do have an intersection, the two quantum phases form an adjacent phase

pair and the phase transition between them may occur. The probability for such a phase transition to happen certainly depends upon the size of the intersection. The bigger the intersection, the more likely the phase transition occurs. Again, the dimensionality is the most important factor for the intersection. When the dimension of the intersection reaches its highest possible value 3, which is 1-dimension less than full-dimension, the two basins of attraction are said to have a common phase boundary with co-dimension one. Then, the phase transition between the two associated quantum phases is most likely to occur from a physical point of view.

The concept of basin of attraction is very useful in the investigation of phase structure.

2.4 The Phase Structure for S_{H^2} in Lattices with Cubic Symmetry

In this section, we study in detail the phase structure for S_{H^2} in lattices with cubic symmetry. These lattices can be 1-dimensional rings, 2-dimensional square lattices or 3-dimensional cubic lattices as noted previously. In our investigation, we especially want to know what kind of superconducting phases may exist, what kind of pairings play a key role there, and what quantum phases are adjacent to the superconducting phases.

2.4.1 Possible Quantum Phases of S_{H^2}

Here, we show what kind of quantum phases may exist in lattices with cubic symmetry.

Valence Quantum Phases

In the valence subspace, $\hat{h}^I$, $\hat{h}^M$ and $\hat{h}^{N^{I,V}}$ are either zero or a constant. If there is a valence ground state, it will be determined by $\hat{h}^V$. $\hat{h}^V$ is the Heisenberg Hamiltonian and its ground state ϕ_g^V is a valence state. As $\hat{h}^V$ is generic, ϕ_g^V can not be altered by any perturbation from $\{\hat{h}^I, \hat{h}^M, \hat{h}^{N^{I,V}}\}$. So $H_B(\phi_g^V)$ is full-dimensional.

The quantum phase determined by $\hat{h}^V$ is described by ϕ_g^V. It is called the FM quantum phase when the coupling constant $J < 0$ or the AFM quantum phase when $J > 0$. The FM ground state can be obtained exactly. It has all the spins of electrons aligned and thus is characterized by the FM long-range order. The AFM ground state can not be solved exactly using known techniques, except for the case of 1-dimensional rings. The AFM quantum phase is characterized by the AFM long-range order in 2- and 3-dimensional cubic lattices, but has no such a long-range order in 1-dimensional rings [16], [55]-[57].

Ionic Quantum Phases

Since $\hat{h}^V$, $\hat{h}^M$ and $\hat{h}^{N^{I,V}}$ are either zero or a constant in the ionic subspace, the ionic ground state, if there is one, is determined by $\hat{h}^I$. As the mean value of $\hat{h}^I_{<\mathbf{i},\mathbf{j}>}$ on any configuration can be negative only if both $\mathbf{i}$ and $\mathbf{j}$ are ionic sites and is zero

for other situations, the ground state ϕ_g^I of $\hat{h}^I$ is an ionic state.

Now, we will find out what these ionic ground states are. As

$$\begin{aligned} \hat{h}^I_{2,<i,j>}|0> &= 4|0>, \quad \hat{h}^I_{2,<i,j>}a_i^+b_i^+a_j^+b_j^+|0> = 4a_i^+b_i^+a_j^+b_j^+|0>, \\ \hat{h}^I_{2,<i,j>}a_i^+b_i^+|0> &= -4a_i^+b_i^+|0>, \quad \hat{h}^I_{2,<i,j>}a_j^+b_j^+|0> = -4a_j^+b_j^+|0>, \end{aligned} \tag{2.27}$$

the ground state of $\alpha_2^I\hat{h}_2^I$ is either the vacuum state $|0>$ (degenerate with the fully occupied state because of the invariance of S_{H^2} under particle-hole transformation) when $\alpha_2^I < 0$ or a Slater determinant called a checkerboard state when $\alpha_2^I > 0$. In such a Slater determinant, any on-site pairing site is surrounded by empty nearest neighbor sites and any empty site is surrounded by on-site pairing nearest neighbor sites. With circles and black disks to represent empty and on-site pairing sites in a square lattice, respectively, these ionic ground states are schematically shown in figure 2.2.

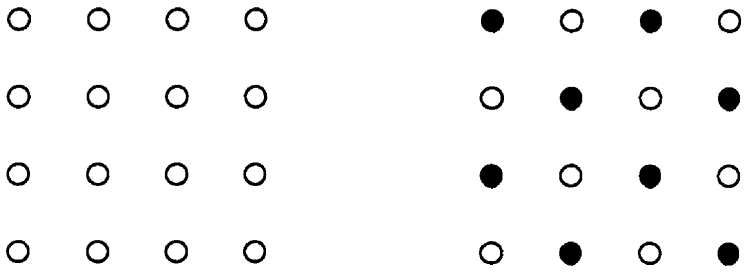

Figure 2.2: Vacuum and Checkerboard States

As $\hat{h}^I_{1,<i,j>}a_i^+b_i^+|0>= a_j^+b_j^+|0>$, all ionic configurations with the same number of electrons are connected together. Let $c_i = e^{i\theta_i}|c_i|$ be the coefficient for the i-th configuration in the ground state of $\hat{h}_1$, here $|c_i| = \sqrt{c_i^*c_i}$ is a real positive number and θ_i is real and referred to as the phase factor for the corresponding configuration. In

cubic lattices, $\theta_i - \theta_j$, referred to as the relative phase factor for any two configurations in the ground state of $\alpha_l^I \hat{h}_l^I$ can be determined easily. When $\alpha_l^I < 0$, the relative phase factor for any two configurations is zero; whereas when $\alpha_l^I > 0$, the relative phase factor for any two configurations is zero or π with the two configurations being connected by even or odd times transport of on-site electron pairs. With the same symbols as in figure 2.2, three ionic configurations are schematically given in figure 2.3. There, the coefficients for the first two configurations always have the same sign, whereas that for the third configuration has the same or opposite sign as the first two in the ground state with α_l^I being negative or positive, respectively. Although there is

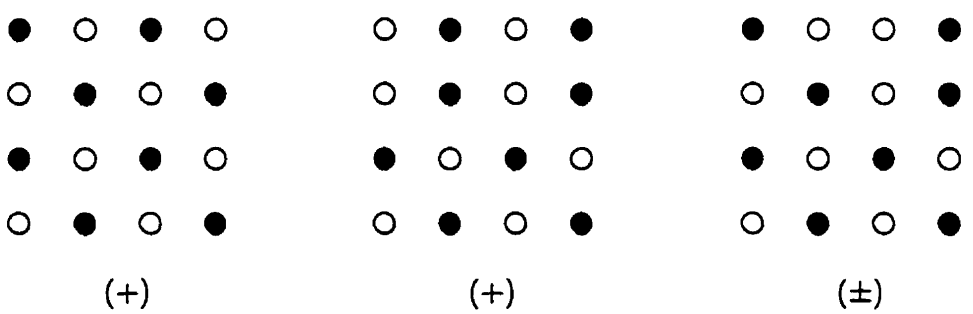

Figure 2.3: Phase Factor Setting for Three Ionic Configurations

more than one path in which two configuration can be connected by shifting electron pairs, the parity (odd or even times transport of an electron pair) of all possible paths connecting two configurations is the same. Thus the phase factor setting for configurations in the ground state is unique. This is a very special property for lattices with cubic symmetry. These two kinds of phase factor settings are referred to as constant and alternating phases, respectively. It is easy to see that in 2-dimensional hexagonal lattices, there is no way to make a similar phase factor setting preferred

by all interactions involved. This is usually called phase frustration.

Let m be the number of electron pairs and n_{ne} the number of nearest neighbor sites, the number of total configurations is $n_T = \binom{|\Lambda|}{m}$ and the number of non-zero interactions among these configurations is $n_{Int} = |\Lambda| n_{ne} \binom{|\Lambda|-2}{m-1}$. As the ratio n_{Int}/n_T reaches its maximum when $m = \frac{|\Lambda|}{2}$, the ground state of $\alpha_1^I \hat{h}_I^1$ is a half-filled state with a constant phase when $\alpha_1^I < 0$ or an alternating phase when $\alpha_1^I > 0$.

When $\alpha_2^I < 0$ and $\alpha_1^I = 8\theta\alpha_2^I$ with $\theta = \pm 1$, apart from a constant, $\hat{h}^I$ is the projection onto the ionic subspace of a positive semi-definite operator

$$\hat{h}_\theta = \sum_{<i,j>} Q^+_{\theta,<i,j>} Q_{\theta,<i,j>}, \tag{2.28}$$

with

$$Q_{\theta,<i,j>} = a_i^+ a_j + a_j^+ a_i - \theta(b_i^+ b_j + b_j^+ b_i). \tag{2.29}$$

$Q_{\theta,<i,j>}$ is a killer operator for the AGP function with a constant phase (CP) given by

$$|\psi_{CPAGP}> = \left\{ \sum_r a_r^+ b_r^+ \right\}^m |0>, \tag{2.30}$$

when $\theta = 1$, or an alternating phase (AP) given by

$$|\psi_{APAGP}> = \left\{ \sum_r e^{i\pi\cdot r} a_r^+ b_r^+ \right\}^m |0>, \tag{2.31}$$

when $\theta = -1$. That is

$$\begin{aligned} Q_{\theta,<i,j>}|\psi_{CPAGP}> &= 0 \qquad \text{for} \quad \theta = 1, \\ Q_{\theta,<i,j>}|\psi_{APAGP}> &= 0 \qquad \text{for} \quad \theta = -1. \end{aligned} \tag{2.32}$$

As equations in (2.32) hold for $m = 0, 1, \cdots, |\Lambda|$, the CPAGP or APAGP functions for any m in Eq. (2.30) or (2.31) are degenerate ground states for $\hat{h}_\theta$ and thus $\hat{h}^I$ with θ being 1 or -1, respectively.

From the above discussion, a general description for the ionic ground states is given as follows:

(1) With $\alpha_2^I < 0$ and $|\alpha_1^I| < 8|\alpha_2^I|$, the ground state is a vacuum state.

(2) With $\alpha_2^I < 0$ and $|\alpha_1^I| = 8|\alpha_2^I|$, the AGP functions in Eq. (2.30) or (2.31) with a constant phase when $\alpha_1 < 0$ or an alternating phase when $\alpha_1 > 0$ are degenerate ground states.

(3) For other values of α_1^I and α_2^I, the ground states can be classified into two categories: a constant phase when $\alpha_1^I < 0$ and an alternating phase when $\alpha_1^I > 0$. Both are half-filled states and the weight for each configuration in the ground state is determined by the ratio of α_1^I and α_2^I. As we vary this ratio gradually but keep the sign of α_1^I unchanged, the ground states will be deformed to each other smoothly within their own category and the two kinds of ground states are separated by the checkerboard ground state.

As $\hat{h}^I$ is generic, any perturbation from $\{\hat{h}^V, \hat{h}^M, \hat{h}^{N^I,V}\}$ obviously leaves these ionic ground states unchanged. Thus, the vacuum ground state has a full-dimensional basin of attraction and it describes a trivial vacuum quantum phase. Each half-filled ionic ground state has a basin of attraction which is 1-dimension less than full-dimension. The union of basins of attraction for the ionic ground states in each of the two categories is full-dimensional. Thus the two kinds of half-filled ionic ground states

characterized by the half-filled AGP functions with constant and alternating phases, respectively, describe two separated ionic quantum phases. As the AGP functions have the so-called off-diagonal long-range order and thus are superconducting states, we call the two corresponding quantum phases superconducting phases with constant and alternating phases, respectively.

Symmetry Between $\hat{h}^I$ and $\hat{h}^V$

Under the action of a canonical transformation T_C which changes a_i to a_i^+ and a_i^+ to a_i but leaves b_i^+ and b_i unchanged, $\hat{h}^V$ is transformed into a special ionic Hamiltonian

$$\begin{aligned} \hat{h}^I(V) &= J\{\sum_{<i,j>}[8(a_i^+ b_i^+ b_j a_j + a_j^+ b_j^+ b_i a_i + (e_{a_i}e_{a_j} + e_{b_i}e_{b_j} + e_{a_i}e_{b_j} + e_{a_j}e_{b_i})]\} \\ &= J(8\hat{h}_1^I + \hat{h}_2^I). \end{aligned} \tag{2.33}$$

Further analysis shows that: with negative J, the constant phase AGP function is the ground state of this transformed Hamiltonian, and with positive J, the ground state of $\hat{h}^I(V)$ is a half-filled ionic ground state with an alternating phase. Thus, under the action of T_C, the FM ground state in the valence subspace is transformed into the half-filled constant phase AGP function, and the AFM ground state is transformed into a half-filled ionic ground state with the alternating phase. Such a symmetry between $\hat{h}^I$ and $\hat{h}^V$ gives us a new alternative way to study the valence ground states in ionic subspace and this may be especially useful for the study of the AFM ground state.

Using this symmetry, we obtain the following theorem.

Theorem 2.2 *The only possible ground state of the Hamiltonian*

$$\hat{h}(\alpha) = \alpha\hat{h}^V + \hat{h}^I(V) \quad with \quad \alpha \geq 0 \tag{2.34}$$

is either an ionic state or a valence state.

Proof: Let ϕ^I, ϕ^V be the lowest ionic and valence energy states , ψ^I, ψ^V, ψ^B the ionic, valence and ionic-valence boundary parts of the lowest energy state $\phi^{I,V}$ in a mixed subspace and ψ^I_V the ionic image of ψ^V under the action of T_C. As $\hat{h}(\alpha)_{<i,j>}$ is zero in the ionic-valence boundary, the mean value of $\hat{h}(\alpha)$ on $\phi^{I,V}$ can be computed as

$$\begin{aligned} E_g^M &= <\phi^{I,V} \mid \hat{h}(\alpha) \mid \phi^{I,V}> \\ &= <\psi^I \mid \sum_{<i,j>\in\psi^I} \hat{h}^I_{<i,j>}(V) \mid \psi^I> + \alpha <\psi^V \mid \sum_{<i,j>\in\psi^V} \hat{h}^V_{<i,j>} \mid \psi^V> \\ &= <\psi^I \mid \sum_{<i,j>\in\psi^I} \hat{h}^I_{<i,j>}(V) \mid \psi^I> + \alpha <\psi^I_V \mid \sum_{<i,j>\in\psi^I_V} \hat{h}^I_{<i,j>}(V) \mid \psi^I_V> . \end{aligned} \tag{2.35}$$

When $\alpha = 1$, $\hat{h}(\alpha)$ is invariant under the action of T_C, thus

$$\begin{aligned} E_g^I &= <\phi^I \mid \hat{h}(\alpha) \mid \phi^I> = <\phi^V \mid \hat{h}(\alpha) \mid \phi^V> = E_g^V, \\ E_g^M &= <\phi^I\psi^I_V \mid \hat{h}^I(V) \mid \phi^I\psi^I_V> = <\psi^I\psi^I_V \mid \hat{h}(\alpha) \mid \psi^I\psi^I_V> . \end{aligned} \tag{2.36}$$

As the boundary between ψ^I_V and ψ^I is not optimized to give the lowest possible expectation value for $\hat{h}^I(V)$, the ionic state $|\psi^I\psi^I_V>$ is definitely not the ground state of $\hat{h}(\alpha)$. So E_g^M will be higher than both E_g^I and E_g^V. Thus for $\alpha = 1$, ϕ^I and ϕ^V are degenerate ground states of $\hat{h}(\alpha)$. Further it is easy to see that for $\alpha > 1$, ϕ^V is the ground state, and for $0 \leq \alpha < 1$, ϕ^I is the ground state. So mixed states can not be the ground states for $\hat{h}(\alpha)$. □

According to conjecture 2.1 in the next section, the ground state of any interaction from $\{\hat{h}^I, \hat{h}^V, \hat{h}^{N^{I,V}}\}$ can not be a mixed state. Thus if there is any mixed ground state, it must be determined by $\hat{h}^M$. As $\hat{h}^M$ is zero in both ionic and valence subspaces but non-zero in any mixed subspace, the ground state of $\hat{h}^M$ is a mixed state.

In the mixed subspace with $\{n_I, n_V\}$, as

$$\begin{aligned} \hat{h}^M_{<i,j>} a_i^+|0> &= -a_j^+|0>, \quad \hat{h}^M_{<i,j>} a_i^+ a_j^+ b_j^+|0> = -a_j^+ a_i^+ b_i^+|0>, \\ \hat{h}^M_{<i,j>} a_j^+|0> &= -a_i^+|0>, \quad \hat{h}^M_{<i,j>} a_j^+ a_i^+ b_i^+|0> = -a_i^+ a_j^+ b_j^+|0>, \end{aligned} \tag{2.37}$$

the action of $\hat{h}^M$ on any mixed state changes the ionic-valence boundary. As a result, all configurations with the same $n_I(d), n_I(e), n_V^\uparrow$ and $n_V^\downarrow$ but different ionic-valence boundaries are connected together. As $\hat{h}^M$ treats all ionic sites, as well as all valence sites, equally, its ground state may be degenerate.

The total number of configurations connected together by $\hat{h}^M$ is

$$n_T = \binom{|\Lambda|}{n_V}\binom{n_V}{n_V^\uparrow}\binom{n_I}{n_I(d)} \tag{2.38}$$

and the number of non-zero interactions among these configurations is

$$n_{Int} = |\Lambda| n_{ne} \binom{|\Lambda|-2}{n_V-1}\binom{n_V}{n_V^\uparrow}\binom{n_I}{n_I(d)}. \tag{2.39}$$

The ratio n_{Int}/n_T reaches its maximum when $n_V = \frac{|\Lambda|}{2}$. If there is a coherent phase factor setting for all configurations in the ground state of $\hat{h}^M$ favored by every pair interaction $\hat{h}^M_{<i,j>}$, here favor means that the expectation value for $\hat{h}^M_{<i,j>}$ is negative, non-zero interactions always lower the energy. Thus the ground states for $\hat{h}^M$ will be with half ionic and half valence sites.

Further analysis shows that in the mixed ground state for 2- and 3-dimensional cubic lattices, it is impossible to set phase factors for all configurations favored by every pair interaction $\hat{h}^M_{<i,j>}$. In a lattice, any two distinct paths connecting two sites form a closed path. Obviously, there is only one closed path in 1-dimensional rings and more than one closed path in 2- and 3-dimensional cubic lattices. Let circles and arrows represent the ionic and valence sites in a closed path of a lattice and $|\psi>$ be a Slater determinant for other sites. Two paths connecting $a_1^\dagger a_2^\dagger|\psi>$ and $a_1^\dagger a_3^\dagger|\psi>$ are schematically shown in figure 2.4. When $\alpha_M > 0$, $\hat{h}^M_{<1,4>}$, $\hat{h}^M_{<3,4>}$ and $\hat{h}^M_{<1,2>}$ in path 1 favor that the coefficients for $a_1^\dagger a_2^\dagger|\psi>$ and $a_1^\dagger a_3^\dagger|\psi>$ have the same sign, whereas in path 2, $\hat{h}^M_{<2,3>}$ favors that the coefficients for $a_1^\dagger a_2^\dagger|\psi>$ and $a_1^\dagger a_3^\dagger|\psi>$ have the opposite sign. When $\alpha_M < 0$, $\hat{h}^M_{<1,4>}$, $\hat{h}^M_{<3,4>}$ and $\hat{h}^M_{<1,2>}$ in path 1 favor that the coefficients for $a_1^\dagger a_2^\dagger|\psi>$ and $a_1^\dagger a_3^\dagger|\psi>$ have the opposite sign, whereas in path 2, $\hat{h}^M_{<2,3>}$ favors that the coefficients for $a_1^\dagger a_2^\dagger|\psi>$ and $a_1^\dagger a_3^\dagger|\psi>$ have the same sign. Such contradictory phase factor settings in paths 1 and 2 clearly show the existence of phase frustration in the mixed ground state. As configurations of this kind appear only in lattices with more than one closed path, there is no phase frustration in the mixed ground state for 1-dimensional rings.

Any small perturbation from $\hat{h}^{N^I,V}$ has no impact on the mixed ground state as $\hat{h}^{N^I,V}$ is a constant in any mixed subspace. Perturbations from both $\hat{h}^I$ and $\hat{h}^V$ may reduce the degree of degeneracy for the mixed ground state. In the mixed ground state, any perturbation from $\hat{h}^I$ favors a constant or an alternating phase factor arrangement for the connected ionic sites, while any perturbation from $\hat{h}^V$ prefers the

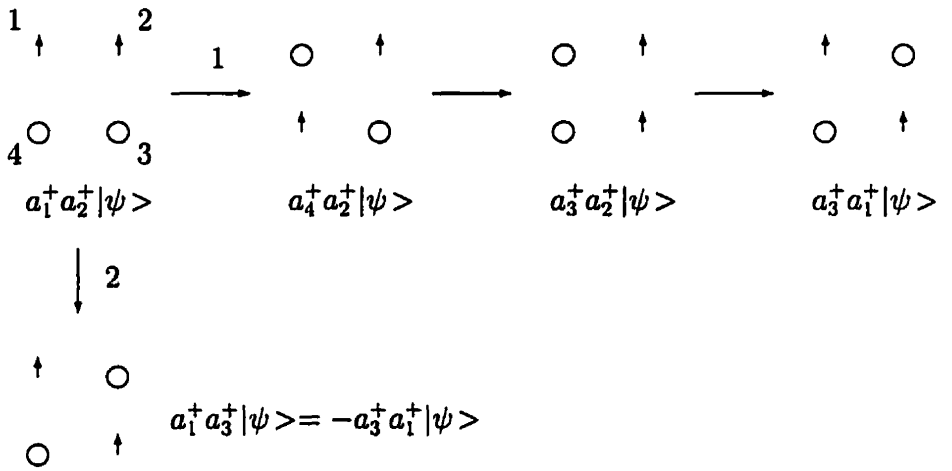

Figure 2.4: Phase Frustration in Mixed Ground States

FM or AFM assignment of the connected valence sites. If the connected ionic sites are not all empty, half of them must be on-site pairing. In that case, the associated mixed ground state is a half-filled state. Because of the phase frustration, the mixed ground state has a very complicated phase factor setting.

Based on the above discussions, we find that there is a mixed quantum phase. It is quite possible that 50% sites are ionic and 50% sites are valence in this mixed quantum phase. In such a quantum phase, the connected ionic sites try to follow the constant or alternating phase role and the connected valence sites try to arrange themselves ferromagnetically or antiferromagnetically. In the mixed quantum phase for 2- and 3-dimensional cubic lattices, frustration exists. It may destroy partially or completely the long-range order that otherwise may occur.

Summary of Quantum Phases for S_{H^2}

As a summary, altogether there are six possible quantum phases for S_{H^2}. They are

the two kinds of superconducting phases characterized by the half-filled constant and alternating phase AGP functions respectively, the FM and AFM phases, the mixed phase and the trivial vacuum phase. Hamiltonians on S_{H^2} for these quantum phases are schematically shown in figure 2.5 Among these quantum phases, the first four

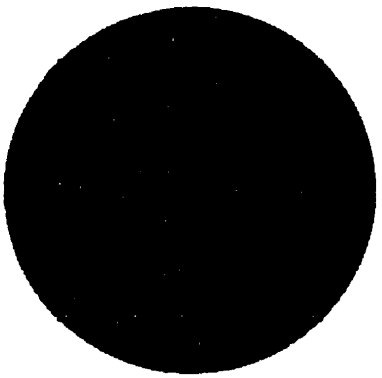

Figure 2.5: The Phase Diagram for S_{H^2}

are exactly half-filled phases and half-filling may also occur in the mixed quantum phase. Thus quantum phases associated with half-filling are a special feature for pure 2-body interactions in S_{H^2}. Collective behavior with some kind of long-range order is another special feature for these quantum phases.

Generally speaking, pure 1-body interactions in H^1 do not preserve on-site pairing. Thus the involvement of pure 1-body interactions will make the sharp picture for these quantum phases become fuzzy. But as long as they are much weaker than the pure 2-body interactions, pure 1-body interactions can not completely destroy the long-range order accompanying the collective behavior and thus can not change the fundamental physics in these quantum phases. As 1-body interactions are not

invariant under particle-hole transformation, perturbations from H^1 may cause some quantum phases of S_{H^2} to move away from the exact half-filling and become near half-filled quantum phases.

It is worth mentioning that for the CPAGP and FM ground states,

$$Q_2^{[0,0]} \mid \psi_{APAGP} >= 0 \quad \text{and} \quad Q_2^{[0,0]} \mid \psi_{FM} >= 0. \tag{2.40}$$

Here, $Q_2^{[0,0]} \in H^1$ is the hopping term in the Hubbard model. Thus any perturbation from $Q_2^{[0,0]}$ will leave both the APAGP and the FM ground states unchanged.

2.4.2 Phase Transitions

As we do not know very much about the mixed phase, here we will only discuss possible phase transitions among the first four quantum phases. Based on the investigation in the last section, the two kinds of superconducting phases are obviously separated quantum phases. Thus no phase transition will occur between them. The same is true for the FM and AFM phases. So the only possible phase transitions are those between each of the superconducting phases and the FM or AFM phase.

In order to investigate such phase transitions, we need to study the intersection of the two basins of attraction for each corresponding phase pair.

The AGP ground state denoted by ϕ_{AGP}^{α} is determined by the ionic Hamiltonian

$$\hat{h}_{AGP}^{\alpha} = -2\alpha\hat{h}_1^I - \frac{1}{4}\hat{h}_2^I. \tag{2.41}$$

Here $\alpha = +1$ or -1 corresponds to the constant or alternating phase, respectively. Let ϕ_V^J be the valence ground state of $\hat{h}^V$, which is the AFM ground state when $J > 0$

or the FM ground state when $J < 0$, and $E_V^J = <\phi_V^J \mid \hat{h}^V \mid \phi_V^J>$. Then, apart from a constant, the Hamiltonian

$$\begin{aligned} \hat{h} &= \hat{h}_\alpha + \xi \hat{h}_J \\ &= \{\hat{h}_{AGP}^\alpha + \frac{n_{ne}}{4}(|\Lambda| + N^{I,V})\} + \xi\{\hat{h}^V - \frac{E_V^J}{2|\Lambda|}(|\Lambda| - N^{I,V})\}, \end{aligned} \tag{2.42}$$

with ξ being a positive coefficient, is pure 2-body. It is easy to see that both ϕ_{AGP}^α and ϕ_V^J are eigenstates of $\hat{h}$ with

$$\hat{h} \mid \phi_{AGP}^\alpha >= 0 \quad \text{and} \quad \hat{h} \mid \phi_V^J >= 0. \tag{2.43}$$

The expectation value for $\hat{h}$ on any ionic or valence state is greater than or equal to zero. Thus $\hat{h} \geq 0$ in both the ionic and the valence subspaces. In any mixed state with n_I ionic and n_V valence sites, ionic-valence boundary always exists. The action of $\hat{h}$ on any mixed configuration does not change the ionic-valence boundary and the mean value for $\hat{h}_{<\mathbf{i},\mathbf{j}>}$ is positive if both **i** and **j** are on the boundary. So the lowest energy state in the mixed subspace with $\{n_I, n_V\}$ is a mixed state that has the smallest possible ionic-valence boundary. In such a state, all the connected ionic sites form a local AGP function determined by $\hat{h}_\alpha$ and all the connected valence sites form a local FM or AFM state determined by $\hat{h}_J$. If we denote by ψ_I^α, ψ_V^J and ψ_B the ionic, valence and boundary parts of the mixed state respectively, the expectation value for $\hat{h}$ on the state can be computed as

$$
\begin{aligned}
<\hat{h}> &= <\psi_I^\alpha \mid \sum_{<i,j>\in I} \hat{h}_{\alpha,<i,j>} \mid \psi_I^\alpha> \\
&\quad +\xi <\psi_V^J \mid \sum_{<i,j>\in V} \hat{h}_{J,<i,j>} \mid \psi_V^J> \\
&\quad + <\psi_B \mid \sum_{<i,j>\in B} \{\hat{h}_{\alpha,<i,j>} + \xi \hat{h}_{J,<i,j>}\} \mid \psi_B> . \qquad (2.44)
\end{aligned}
$$

As $\hat{h}^I_{\alpha,<i,j>}$ is a killer for the associated AGP function,

$$
<\psi_I^\alpha \mid \sum_{<i,j>\in I} \hat{h}_{\alpha,<i,j>} \mid \psi_I^\alpha>= 0. \qquad (2.45)
$$

Thus for small ξ, $< \hat{h} >$ will be dominated by

$$
<\psi_B \mid \sum_{<i,j>\in B} \hat{h}_{\alpha,<i,j>} \mid \psi_B>= \frac{n_B}{2}, \qquad (2.46)
$$

with n_B being the number of nearest neighbor pairs on the boundary. So $< \hat{h} >$ is strictly positive. Thus $<\hat{h}>$ is strictly positive in any mixed subspace.

From the above discussion, we find that ϕ^α_{AGP} and ϕ^J_V are degenerate ground states of $\hat{h}$. So, apart from a constant, $\hat{h}$ is an element in the intersection of the two basins of attraction for these ground states and thus is an element in the intersection of basins of attraction for the corresponding quantum phases. If we gradually vary α away from ± 1 by increasing $|\alpha|$, ϕ^α_{AGP} is deformed smoothly within its own category of half-filled ionic ground states and $\hat{h}$ will remain inside the intersection for these basins of attraction. By further analysis, we found that $\hat{h}^{N^I,V}$ is the only pure 2-body interaction that can break the degeneracy for the ionic and valence ground states. Thus $\hat{h}^{N_I,V}$ is the only interaction that is not contained in the intersection of the two basins of attraction. As a result, the two related quantum phases have a common phase boundary with co-dimension one.

As a summary, we have

Theorem 2.3 *The constant phase superconducting phase and the FM phase, the constant phase superconducting phase and the AFM phase, the alternating phase superconducting phase and the FM phase, the alternating phase superconducting phase and the AFM phase are adjacent phase pairs. Each of these phase pairs has a common phase boundary with co-dimension one.*

In the above discussion, restriction on ξ is introduced mainly to avoid computing $<\psi_V|\sum_{<i,j>\epsilon V}\hat{h}_{J,<i,j>}|\psi_V>$ for the AFM case as it can not be obtained exactly. Further analysis based on results from various numerical computations [16]-[20] strongly supports the idea that $\hat{h}_J$ itself is strictly positive in any mixed subspace and that may remove the restriction on ξ. From this as well as theorem 2.2, we have the following conjecture

conjecture 2.1 *The only possible ground state for the Hamiltonian of the form*

$$\hat{h} = \hat{h}^I + \hat{h}^V + \hat{h}^{N^{I,V}} \tag{2.47}$$

is either an ionic or a valence state.

It is interesting to see that these phase transitions are accompanied by a sudden change of electron distributions. During each of these phase transitions, the system transforms itself from an ionic phase into a valence phase or vice versa without going over any mixed state. This may have something to do with the fact that the superconducting phase and the AFM are adjacent quantum phases in oxide superconducting materials.

2.4.3 The Phase Structure and the Dimensionality

Although our main focus is on the 2-dimensional square lattices as they are closely related to the oxide superconducting materials, the general phase structure obtained above is really dimension independent. The main reason behind such a dimension independent phenomenon may come from the fact that only nearest neighbor interactions have been considered.

However, the dimension independence does not mean that the corresponding quantum phases in 1-, 2- and 3-dimensional cubic lattices always share exactly the same kind of key characteristics. For example, it has been found that the ground state of the AFM Heisenberg Hamiltonian (with $J > 0$) in a 1-dimensional ring does not have the AFM long-range order [55, 56], whereas the ground states of 2- and 3-dimensional AFM Heisenberg Hamiltonians are characterized by the AFM long-range order [16, 57].

Here it is worth paying more attention to $\hat{h}^M$ as it may be the only interaction in S_{H^2} that can cause some dimension dependent phenomena. Recall that $\hat{h}^M$ has a mixed ground state with phase frustration in 2- and 3-dimensional cubic lattices. The phase frustration comes from the fact that different paths connecting two configurations result in different phase factor settings. There is only one closed path connecting two configurations in a 1-dimensional ring. Thus there is no phase frustration in the mixed quantum phase for 1-dimensional cubic lattices. In 2- or 3-dimensional cubic lattices, different closed paths always exist. Thus phase frustration always exists in the corresponding mixed quantum phase. Although we have not figured out a way to

evaluate the phase frustration in mixed quantum phases for 2- and 3-dimensional cubic lattices, it is clear that the degree of the phase frustration is dimension dependent. As phase frustration causes instability, higher degree of phase frustration indicates the smaller basin of attraction for the corresponding mixed quantum phase. Thus the size of basin of attraction for the mixed quantum phase is dimension dependent.

The spherical surface S_{H^2} is covered by the basins of attraction for the six found quantum phases. The size of the basin of attraction for the mixed quantum phase will definitely affect the size of basins of attraction for other quantum phases. Thus the dimensional dependence of the size of the basin of attraction for the mixed quantum phase indicates that the size of the basin of attraction for any other quantum phase may also be dimension dependent. If the relationship between the degree of phase frustration in the mixed ground state and the dimensionality for these lattices is found, it may further help us to explain some other dimension dependent phenomena, such as why the superconducting phase prefers 2-dimensional square lattices.

Chapter 3

The Unique On-site AGP Pairing for the Superconducting Phase

In this chapter, we first investigate some special properties of the AGP functions. Then, we make a conjecture that the on-site AGP pairing is the unique AGP pairing in lattices with cubic symmetry.

3.1 AGP Functions and Their Killers

3.1.1 AGP functions

AGP is the abbreviation for Antisymmetrized Geminal Power, and AGP functions have been extensively studied since the early 1960's [43, 58].

The geminals, or 2-electron wave-functions we will consider, has the form

$$| g>= \sum_{\alpha>0}^{\frac{r_g}{2}} \xi_\alpha a_\alpha^+ a_{\bar{\alpha}}^+ | 0> . \tag{3.1}$$

Where $\{a_\alpha^+, a_{\bar{\alpha}}^+\}$ is a set of creation operators corresponding to a set of orthonormal 1-electron spin orbitals and r_g is the rank of the geminal. α and $\bar{\alpha}$ are called a pair of conjugate spin orbitals which share the same expansion coefficient ξ_α as well as the same occupation number $\lambda_\alpha = \xi_\alpha^* \xi_\alpha \neq 0$. By using the index α and $\bar{\alpha}$ and considering one as positive, the other negative, we avoid double counting in the expansion. By letting $B_\alpha^+ = a_\alpha^+ a_{\bar{\alpha}}^+$, the above expression can be rewritten as

$$| g>= \sum_{\alpha>0}^{\frac{r_g}{2}} \xi_\alpha B_\alpha^+ | 0>, \tag{3.2}$$

which is often referred to as the natural expansion of a geminal.

An AGP function with $n = 2m$ electrons, usually denoted by g^n, is given by

$$| g^n>= \{\sum_{\alpha>0}^{\frac{r_g}{2}} \xi_\alpha B_\alpha^+\}^m | 0> . \tag{3.3}$$

Using the standard form for g, the normalized AGP function can be expressed as

$$| g^n>= S_m^{-1/2} \sum_{0<\alpha_1<\alpha_2<\cdots<\alpha_m} C(\alpha_1, \cdots, \alpha_m) B_{\alpha_1}^+ \cdots B_{\alpha_m}^+ | 0>, \tag{3.4}$$

here the expansion coefficient $C(\alpha_1, \cdots, \alpha_m)$ is given by

$$C(\alpha_1, \cdots, \alpha_m) = \prod_{\alpha \in \{\alpha_1 \cdots \alpha_m\}} \xi_\alpha \tag{3.5}$$

and the normalization constant S_m is given by

$$S_m = \sum_{\alpha_1 < \alpha_2 < \cdots < \alpha_m} \lambda_{\alpha_1} \lambda_{\alpha_2} \cdots \lambda_{\alpha_m}. \tag{3.6}$$

From this definition, we can see that: When $n > r(g)$, g^n is zero; when $n = r(g)$, g^n is a single Slater determinant which is independent of the expansion coefficients of g; and when $n < r(g)$, g^n is a linear combination of Slater determinants. When we talk about AGP wave-functions, we mean the non-trivial case with $n < r_g$. Since an AGP function is a pairing function, it is also called an AGP pairing. Although it is a rather simple function, an AGP function is highly correlated. It is of great interest since it provides a model for superconductivity. The BCS function in the conventional superconductivity theory, when projected to a fixed particle space, is an AGP function.

The 2-body reduced density matrices for general AGP functions were obtained by Coleman in 1965 [43]. Since then, the study and application of AGP functions have gone far beyond the field of superconductivity [59]-[61].

3.1.2 An AGP Function Is Uniquely Determined by Its Killers

If k is an operator, and if

$$k \mid \psi > = 0, \tag{3.7}$$

k is said to be a killer for the wave-function ψ. It is obvious that ψ is a ground state of the Hamiltonian $\hat{h} = k^+k$. Thus the correlation in any ground state ψ is determined by its killer set.

It is well-known that a Slater determinant is completely determined by its killers $\{a_i^+, a_j\}$ where i and j run through all occupied and unoccupied spin orbitals in the Slater determinant, respectively. As a result, the ground state of 1-body interactions can be described by a Slater determinant.

In the linear space of particle-hole operators $a_\alpha^+ a_\beta$, we build a set of killers for the AGP function defined in Eq. (3.4) as

$$k_{\alpha,\bar{\alpha}} = a_\alpha^+ a_{\bar{\alpha}}, \qquad \text{for all } \alpha\ ; \tag{3.8}$$

$$k_{\alpha,\alpha} = a_\alpha^+ a_\alpha - a_{\bar{\alpha}}^+ a_{\bar{\alpha}}, \qquad \text{for all } \alpha > 0\ ; \tag{3.9}$$

$$k_{\alpha,\beta} = \frac{1}{\xi_\beta} a_\alpha^+ a_\beta - sign(\alpha\beta)\frac{1}{\xi_\alpha} a_{\bar{\beta}}^+ a_{\bar{\alpha}}, \tag{3.10}$$

$$\text{with} \quad \alpha > 0,\ \beta > 0,\ \alpha \neq \beta; \quad \text{or} \quad \alpha\beta < 0,\ \alpha > -\beta.$$

These killers form a complete linearly independent basis of killers for g^n with $n = 0$, 2, 4, $\cdots$, r_g in the particle-hole operator space. This killer set is denoted by K_g.

It is significant that any $k \in K_g$ is a second-order homogeneous polynomial in creation and annihilation operators. As a result, g^n is a ground state of a 2-body interaction of the form $\hat{h} = \sum_k^{K_g} k^+k$.

Theorem 3.1 *An AGP function g^n is uniquely determined by its killer set K_g.*

Proof: Let ϕ^n be a wave-function for $n = 2m$ electrons that shares K_g with g^n as its killer set, i.e., $k|\phi^n>=0$ for $k \in K_g$. Then the conditions

$$k_{\alpha,\bar{\alpha}} \mid \phi^n > \;=\; 0 \quad \text{for all } \alpha; \tag{3.11}$$

$$k_{\alpha,\alpha} \mid \phi^n > \;=\; 0 \quad \text{for all } \alpha > 0 \tag{3.12}$$

force ϕ^n to have a pairing identical to that of g^n. In other words, the two orbitals in any conjugate spin orbital pair of g must be empty or doubly occupied simultaneously in any configuration of ϕ^n. Such an n-electron pairing wave-function ϕ^n can be expressed with any $\alpha > 0$ and $\beta > 0$ but $\alpha \neq \beta$ as

$$\begin{aligned} |\phi^n> \;=\; & \sum_{k_1\cdots,k_{m-1}\neq\alpha,\beta} C(\alpha,k_1,\cdots,k_{m-1})B^+_\alpha B^+_{k_1}\cdots B^+_{k_{m-1}}|0> \\ & + \sum_{k_1\cdots,k_{m-1}\neq\alpha,\beta} C(\beta,k_1,\cdots,k_{m-1})B^+_\beta B^+_{k_1}\cdots B^+_{k_{m-1}}|0> \\ & + \sum_{k_1\cdots,k_{m-2}\neq\alpha,\beta} C(\alpha,\beta,k_1,\cdots,k_{m-2})B^+_\alpha B^+_\beta B^+_{k_1}\cdots B^+_{k_{m-2}}|0> \\ & + \sum_{k_1,\cdots,k_m\neq\alpha,\beta} C(k_1,\cdots,k_m)B^+_{k_1}\cdots B^+_{k_m}|0> . \end{aligned} \tag{3.13}$$

It is easy to verify that

$$\begin{aligned} & k_{\alpha,\beta}B^+_\alpha B^+_\beta B^+_{k_1}\cdots B^+_{k_{m-2}}|0>=0, \\ & k_{\alpha,\beta}B^+_{k_1}\cdots B^+_{k_m}|0>=0, \end{aligned} \tag{3.14}$$

and

$$\begin{aligned} k_{\alpha,\beta}B^+_\alpha B^+_{k_1}\cdots B^+_{k_{m-1}}|0> \;&=\; -\tfrac{1}{\xi_\alpha}a^+_\alpha a^+_{\bar{\beta}}B^+_{k_1}\cdots B^+_{k_{m-1}}|0>, \\ k_{\alpha,\beta}B^+_\beta B^+_{k_1}\cdots B^+_{k_{m-1}}|0> \;&=\; \tfrac{1}{\xi_\beta}a^+_\alpha a^+_{\bar{\beta}}B^+_{k_1}\cdots B^+_{k_{m-1}}|0>, \end{aligned} \tag{3.15}$$

Thus,

$$\begin{aligned} k_{\alpha,\beta} \mid \phi^n > \;=\; & \sum_{k_1,\cdots,k_{m-1}\neq\alpha,\beta} -\frac{1}{\xi_\alpha}C(\alpha,k_1,\cdots,k_{m-1})a^+_\alpha a^+_{\bar{\beta}}B^+_{k_1}\cdots B^+_{k_{m-1}}|0> \\ & + \sum_{k_1,\cdots,k_{m-1}\neq\alpha,\beta} \frac{1}{\xi_\beta}C(\beta,k_1,\cdots,k_{m-1})a^+_\alpha a^+_{\bar{\beta}}B^+_{k_1}\cdots B^+_{k_{m-1}}|0> . \end{aligned} \tag{3.16}$$

With the condition

$$k_{\alpha,\beta} \mid \phi^n >= 0, \tag{3.17}$$

it is obvious that

$$\frac{1}{\xi_\alpha} C(\alpha, k_1, \cdots, k_{m-1}) = \frac{1}{\xi_\beta} C(\beta, k_1, \cdots, k_{m-1}) \quad \text{for all } k_1, \cdots, k_{m-1} \neq \alpha, \beta \ . \tag{3.18}$$

As the above relations hold for all α and β, they give the relationship between the coefficients for any two Slater determinants in ϕ^n that can be transformed into each other by switching one pair of electrons. Any two configurations

$$\begin{aligned} &B^+_{\alpha_1} B^+_{\alpha_2} \cdots B^+_{\alpha_m} |0>, \\ &B^+_{\beta_1} B^+_{\beta_2} \cdots B^+_{\beta_m} |0> \end{aligned} \tag{3.19}$$

can be transformed into each other by switching electron pairs. Thus the coefficients for the two configurations satisfy

$$\frac{C(\alpha_1, \alpha_2, \cdots, \alpha_m)}{C(\beta_1, \beta_2, \cdots, \beta_m)} = \frac{\xi_{\alpha_1} \xi_{\alpha_2} \cdots \xi_{\alpha_m}}{\xi_{\beta_1} \xi_{\beta_2} \cdots \xi_{\beta_m}}, \tag{3.20}$$

which is exactly what the coefficients in g^n fulfill (see Eq. (3.5)). Thus $\phi^n = g^n$ and an AGP function is uniquely determined by its killer set K_g. □

3.1.3 The Unique Representation of the 2-body Density Matrix Corresponding to An AGP Wave-Function

The 2-body density matrix for a wave-function ϕ^n can be defined by the equality

$$d^2_{abcd} = <\phi^n \mid a^+ b^+ c d \mid \phi^n> . \tag{3.21}$$

Here the wave-function ϕ^n is called a representation for the matrix d^2_{abcd}. Given a matrix d^2_{abcd}, there need not be a representation ϕ^n so that Eq. (3.21) holds. A density matrix d^2_{abcd} with at least one representation is called n-representable.

Using theorem 3.1, it is very easy to prove the following well-known result on AGP functions.

Theorem 3.2 *The 2-body density matrix for an AGP function has a unique representation.*

Proof: Assume that ϕ^n and g^n share the same 2-body density matrix, that is

$$<\phi^n \mid a^+b^+cd \mid \phi^n>=<g^n \mid a^+b^+cd \mid g^n> . \tag{3.22}$$

For any $k \in K_g$, k^+k can always be expressed as a linear combination of operators a^+b^+cd, a^+b and the identity operator $\hat{e}$ by using fermion commutation relationships. Using the fact that the corresponding 1-body density matrix $<\phi^n|a^+b|\phi^n>$ and the trace $<\phi^n\hat{e} \mid \phi^n>$ are determined by the 2-body density matrix when the particle number is fixed, Eq. (3.22) guarantees that

$$<\phi^n \mid k^+k \mid \phi^n>=<g^n|k^+k|g^n>= 0, \tag{3.23}$$

which implies that

$$k \mid \phi^n>= 0 \qquad \text{for } k \in K_g. \tag{3.24}$$

As an AGP function is uniquely determined by K_g, such a ϕ^n must be g^n. Thus the wave-function that represents the 2-body density matrix corresponding to an AGP function is uniquely determined. □

Using a completely different approach, Coleman obtained this result in 1973 [62]; Rosina also obtained a proof, but only for a restricted class of AGP functions [63]. Our proof is complete and much easier than the previous proofs.

3.2 The Symmetry Properties of AGP Functions and Their Generating Geminals

An AGP function g^n and its generating geminal g are closely related to each other. Here we investigate the symmetry relationship between them. Both spin and spatial symmetries will be addressed. These symmetry properties are very important in determining possible AGP ground states in a system.

3.2.1 Spin Symmetry

Let an arbitrarily chosen z axis be the quantization axis and $\vec{S}^2$, S_z the total spin operator and its z-component for a system. Here spin symmetry for g^n means that it is an eigenstate of $\vec{S}^2$ and S_z with

$$\vec{S}^2 g^n = S(S+1)g^n, \quad S_z g^n = m_s g^n. \tag{3.25}$$

If g^n has spin symmetry, from the above equation, it is obvious that g itself must be an eigenstate of S_z , with

$$S_z\, g = \frac{2m_s}{n} g. \tag{3.26}$$

As the possible eigenvalues of S_z for g are 1, 0, and -1, the possible values for m_s are

$\frac{n}{2}$, 0 and $-\frac{n}{2}$.

Geminals can be classified by spin symmetry. Spin-symmetry-adapted geminals can be labeled by $[s, s_z]$ as ${}^{[1,1]}g$,${}^{[1,0]}g$, ${}^{[1,-1]}g$ and ${}^{[0,0]}g$. Any geminal can be expressed as a linear combination of these geminals.

Theorem 3.3 *If g^n is a spin symmetry state, then g itself must be a geminal with spin symmetry.*

Proof: Let g^n be specified by $[S, M]$, the quantum numbers associated with $\vec{S}^2$ and S_z, respectively. For $M = \frac{n}{2}$ or $-\frac{n}{2}$, it is obvious that the geminal must be either ${}^{[1,1]}g$ when $M = \frac{n}{2}$ or ${}^{[1,-1]}g$ when $M = -\frac{n}{2}$. Thus g has spin symmetry. For $M = 0$, the geminal can be expressed as a linear combination of ${}^{[0,0]}g$ and ${}^{[1,0]}g$. As the coupling of ${}^{[0,0]}g$ and ${}^{[0,0]}g$ always results in singlet, whereas the coupling of ${}^{[0,0]}g$ and ${}^{[1,0]}g$ always results in triplet, g^n can not have spin symmetry unless $g = {}^{[0,0]}g$ or $g = {}^{[1,0]}g$ instead of being the linear combination of the two. In summary, g must be a geminal with spin symmetry. □

It is worth pointing out that the converse statement for the above theorem is not always correct. That is, if g is a geminal with spin symmetry, g^n needs not be a spin state.

Among these spin-symmetry-adapted AGP functions, the singlet AGP function is the most interesting one and the best candidate for the ground state in systems without explicit spin-spin interactions. Possible geminals associated with the singlet AGP function are ${}^{[0,0]}g$ and ${}^{[1,0]}g$ with the singlet geminal being the best candidate as $({}^{[0,0]}g)^n$ is always a singlet whereas $({}^{[1,0]}g)^n$ may or may not be a singlet. So far,

in the study of high-T_c superconductivity, the preferred pairing scheme is the singlet pairing although the BCS-like triplet pairing has not been ruled out.

3.2.2 Spatial Symmetry

Lattice symmetry includes both translation symmetry and point group symmetry. In our investigation, we need to use the following lemma:

Lemma 3.1 *If there are two geminals g_1 and g_2 with $g_1^n = g_2^n$, then $g_1 = g_2$.*

Proof: As $g_1^n = g_2^n$, they share the same killer set K_g. As K_g uniquely determines the associated AGP function, it must be that $g_1 = g_2$. □

Let S denote the space group for a lattice. Spatial symmetry for an AGP function means that for any symmetry operation $s \in S$,

$$sg^n = e^{i\theta(s)} g^n \tag{3.27}$$

with $\theta(s)$ being a real phase factor.

Theorem 3.4 *If g^n has spatial symmetry, then g itself must be a geminal with spatial symmetry.*

Proof: If Eq. (3.27) holds, we have

$$e^{i\theta(s)} g^n = sg^n = \{sg\}^n. \tag{3.28}$$

Let $g_1 = e^{i2\theta(s)/n} g$ and $g_2 = sg$, Eq. (3.28) can be simplified as

$$g_1^n = g_2^n. \tag{3.29}$$

From Lemma 3.1, we have $g_1 = g_2$ and thus

$$sg = e^{i\frac{2\theta(s)}{n}} g. \tag{3.30}$$

So g must be a geminal with spatial symmetry. □

It is obvious that the converse statement is also true which says that if g has spatial symmetry, then g^n must also have spatial symmetry.

3.3 The Unique AGP Pairing in Lattices with Cubic Symmetry

Here we use symmetry properties to investigate what kind of AGP functions may describe quantum phases in lattices with cubic symmetry.

3.3.1 The Geometry Effect on the AGP Ground States

In a system without explicit spin-spin interaction, if a ground state is stable enough to describe a quantum phase, it is usually non-degenerate (excluding spin degeneracy). Such a ground state must be invariant under the action of the space group S and thus must be a symmetry state for a 1-dimensional irreducible representation of S.

In a lattice designated by a vector space $\mathbf{\Lambda}$, every irreducible representation of the translational subgroup $T \in S$ is 1-dimensional and can be specified by a vector $\mathbf{k}$ in the reciprocal lattice space. This means that for any $t_{\mathbf{r}} \in T$ with $\mathbf{r} \in \mathbf{\Lambda}$, we have

$$t_{\mathbf{r}} \psi^{[\mathbf{k}]} = e^{i\mathbf{r}\cdot\mathbf{k}} \psi^{[\mathbf{k}]}, \tag{3.31}$$

here $\psi^{[\mathbf{k}]}$ is a basis function for the irreducible representation specified by $\mathbf{k}$. Under the action of any $p \in P$, where $P \in S$ is the point subgroup for $\mathbf{\Lambda}$, $\mathbf{k}$ is mapped to

$$\mathbf{k_1} = p\mathbf{k}, \tag{3.32}$$

where $\mathbf{k_1}$ may or may not equal $\mathbf{k}$. Thus the action of P on $\mathbf{k}$ creates a set of vectors $\{\mathbf{k}, \mathbf{k_1}, \cdots\}$ called the star of $\mathbf{k}$. The irreducible representation of a space group S can be specified by $\mathbf{k}$ and its star. If the star of $\mathbf{k}$ contains only one vector, that is $\mathbf{k}$ itself, then the irreducible representation specified by $\mathbf{k}$ is 1-dimensional.

Now we will figure out what are those 1-dimensional irreducible representations in lattices with cubic symmetry. For a 2-dimensional square lattice, the point subgroup is C_{4V} and there are only two special vectors $[0,0]$ and $[\pi,\pi]$ which are invariant under the action of C_{4V}. Similarly, for 1- and 3-dimensional cubic lattices, these special vectors are $[0]$, $[\pi]$ and $[0,0,0]$, $[\pi,\pi,\pi]$ respectively. These two kinds of vectors are called constant and alternating phase vectors, respectively, according to the behavior of basis functions for the corresponding irreducible representations under the action of T.

To force an AGP function g^n to be a symmetry state, its generating geminal must be a basis function for a 1-dimensional irreducible representation of S. Thus g can be labeled by either a constant or an alternating phase vector. The corresponding g^n is called a constant or an alternating phase AGP function.

It is significant that there can be only two kinds of AGP ground states in cubic lattices and they are determined purely by lattice symmetry. Lattices with different geometric structure may have different results. For example, on a 2-dimensional

hexagonal lattice, there is only one vector [0, 0] that is invariant under the action of the point subgroup C_{6V}. Thus an alternating phase AGP function can not be a non-degenerate ground state in 2-dimensional hexagonal lattices. It seems that an alternating phase AGP pairing can only occur in lattices with cubic symmetry.

3.3.2 The Unique On-site AGP Pairing

How many AGP functions are there which are spatially invariant in cubic lattices? In order to answer this question, let's define the geminal generator as

$$\eta_{\mathbf{r}'}(\mathbf{k}) = \sum_{\mathbf{r}} e^{i\mathbf{k}\cdot\mathbf{r}} a^{+}_{\mathbf{r}} b^{+}_{\mathbf{r}+\mathbf{r}'}, \tag{3.33}$$

where $\mathbf{r}$, $\mathbf{r}' \in \mathbf{\Lambda}$ and $\mathbf{k}$ is a constant or an alternating phase vector. When acting on vacuum state $|0>$, $\eta_{\mathbf{r}'}(\mathbf{k})$ generates a spatially invariant geminal

$$|g> = \eta_{\mathbf{r}'}(\mathbf{k}) \mid 0>, \tag{3.34}$$

with $|\mathbf{r}'|$ being the distance between the two electrons in each conjugate spin orbital pair. When $\mathbf{r}' = 0$, for example, $\eta_{\mathbf{r}'}(\mathbf{k}) \mid 0>$ is an on-site pairing geminal with a constant or an alternating phase respectively. Let

$$\eta'_{\mathbf{r}'}(\mathbf{k}) = \sum_{\mathbf{r}} e^{i\mathbf{k}\cdot\mathbf{r}} b^{+}_{\mathbf{r}} a^{+}_{\mathbf{r}+\mathbf{r}'}, \tag{3.35}$$

then

$$^{[0,0]}\eta_{\mathbf{r}'}(\mathbf{k}) = \eta_{\mathbf{r}'}(\mathbf{k}) - \eta'_{\mathbf{r}'}(\mathbf{k}) \tag{3.36}$$

and

$$^{[1,0]}\eta_{\mathbf{r}'}(\mathbf{k}) = \eta_{\mathbf{r}'}(\mathbf{k}) + \eta'_{\mathbf{r}'}(\mathbf{k}) \tag{3.37}$$

are generators for spatially invariant singlet and triplet geminals respectively. As $\mathbf{r}'$ goes over $\mathbf{\Lambda}$, ${}^{[0,0]}\eta_{\mathbf{r}'}(\mathbf{k})$ will generate a linear space of all spatially invariant singlet geminals and ${}^{[1,0]}\eta_{\mathbf{r}'}(\mathbf{k})$ will generate a linear space of all spatially invariant triplet geminals. The generators for these singlet and triplet geminals are given by

$$ {}^{[0,0]}\eta(\mathbf{k}) = \sum_{\mathbf{r}'} c_{\mathbf{r}'}\ {}^{[0,0]}\eta_{\mathbf{r}'}(\mathbf{k}) \tag{3.38} $$

and

$$ {}^{[1,0]}\eta(\mathbf{k}) = \sum_{\mathbf{r}'} c_{\mathbf{r}'}\ {}^{[1,0]}\eta_{\mathbf{r}'}(\mathbf{k})\ , \tag{3.39} $$

with $\{c_{\mathbf{r}'}\}$ being a set of arbitrary coefficients.

Will all these symmetry-adapted AGP functions be the ground states of generic Hamiltonians in S_{H^2}? The geometry of cubic lattices demands that g^n with $n = 2m$ and $m = 1, 2, \cdots$ must be with either a constant phase or an alternating phase. But it can not determine $|r'|$, the distance between the two electrons in the pairing. In our investigation of phase structure in Chapter 2, we found two kinds of superconducting phases characterized by the constant and alternating phase AGP pairings, respectively. Both pairings are on-site AGP pairing generated by ${}^{[0,0]}\eta_{\mathbf{r}'}(\mathbf{k})$ with $\mathbf{r}' = 0$. Is on-site AGP pairing the unique AGP pairing in our system? According to theorem 2.1, if g^n is non-degenerate, it must have a unique set of quantum numbers $\{n_I, n_V\}$.

Theorem 3.5 *The AGP function given by* $\{\eta_{\mathbf{r}'}(\mathbf{k})\}^m$ *or* $\{\eta'_{\mathbf{r}'}(\mathbf{k})\}^m$ *with* $\mathbf{r}' \neq 0$ *and* $2 \leq m \leq |\mathbf{\Lambda}|$, *can not have a unique set of* $\{n_I, n_V\}$.

Proof: In $\{\eta_{\mathbf{r}'}(\mathbf{k})\}^m$ or $\{\eta'_{\mathbf{r}'}(\mathbf{k})\}^m$, there are $\binom{|\mathbf{\Lambda}|}{m}$ independent Slater determinants.

Using the expansion expression for AGP functions in Eq. (3.4) and observing quantum numbers for every Slater determinant, it is found that, with $\mathbf{r}' \neq 0$ and $2 \leq m \leq |\Lambda|$, these Slater determinants do not share a unique set of $\{n_I, n_V\}$. Thus the associated AGP function do not have a unique set of $\{n_I, n_V\}$. □

In AGP function of the form $\{ {}^{[0,0]}\eta_{\mathbf{r}'}(\mathbf{k})\}^m$ or $\{ {}^{[1,0]}\eta_{\mathbf{r}'}(\mathbf{k})\}^m$ with $\mathbf{r}' \neq 0$ and $2 \leq m \leq |\Lambda|$, the coefficients for all the configurations are fixed and configurations with different $\{n_I, n_V\}$ always co-exist. Thus the associated AGP function also do not have a unique set of $\{n_I, n_V\}$. For a more general AGP function given by $\{ {}^{[0,0]}\eta(\mathbf{k})\}^m$ or $\{ {}^{[1,0]}\eta(\mathbf{k})\}^m$, it seems that there still can not be a unique set of $\{n_I, n_V\}$ unless

$$ {}^{[0,0]}\eta(\mathbf{k}) = {}^{[0,0]}\eta_{\mathbf{r}'}(\mathbf{k}) \quad \text{with} \quad \mathbf{r}' = 0. \tag{3.40}$$

Although a general proof has not been obtained yet, the above statement has been checked to be correct in a number of cases using a relatively smaller number of lattice sites.

Particle-hole killers for all AGP functions are of the same form and they are given by K_g. In K_g, killers represented by $k_{\alpha,\beta}$ in Eq. (3.11) are the only non-trivial killers, as others are killers for all pairing states. Thus $k_{\alpha,\beta}$ will play a key role in determining the AGP ground state and pure 2-body interactions of the form $k^+_{\alpha,\beta}k_{\alpha,\beta}$ are almost certain to appear in $H_B(g^n)$. For the on-site AGP pairing ground state, such a pure 2-body interaction $\hat{h}_\theta \in H_B(g^n)$ is found to be

$$\hat{h}_\theta = \sum_{<\mathbf{i},\mathbf{j}>} Q^+_{\theta,(<\mathbf{i},\mathbf{j}>)} Q_{\theta,(<\mathbf{i},\mathbf{j}>)}, \tag{3.41}$$

where

$$Q_{\theta,(<i,j>)} = a_i^+ a_j + a_j^+ a_i - \theta(b_i^+ b_j + b_j^+ b_i) \tag{3.42}$$

is a killer for the constant phase AGP function when $\theta = 1$ or alternating phase AGP function when $\theta = -1$. For non on-site AGP pairings, so far we have not found any similar 2-body interaction in S_{H^2}.

The AGP pairing is a coherent pairing whereas the mixed ground state for 2 and 3-dimensional cubic lattices is characterized by phase frustration. This make it even more unlikely that a non on-site AGP pairing can be a mixed ground state in these lattices.

As a summary of the above discussions, we make the following conjecture,

conjecture 3.1 *On-site AGP pairing is the unique AGP pairing in the quantum phases of S_{H^2} for lattices with cubic symmetry.*

It seems that the unique on-site AGP pairing is closely related to the nearest neighbor interactions in our system. If other than nearest neighbor interactions are introduced, the uniqueness of the on-site AGP pairing will probably disappear.

Thus, we suggest that there can be only two kinds of superconducting phases for S_{H^2} in lattices with cubic symmetry. Both of them are characterized by the on-site AGP pairing, but with constant (Cooper pairing) and alternating phases, respectively. They are BCS-like superconducting phases coming from the condensation of singlet electron pairs. If the basins of attraction for these quantum phases are large enough, these superconducting phases may have high transition temperatures.

Chapter 4

Approaching the Ground State with the Lower Bound Method of Reduced Density Matrix Theory

In this chapter, we investigate the lower bound method of reduced density matrix theory. Two numerical algorithms based on a new theorem [53] are developed for solving the central optimization problem in the lower bound method. Numerical computations are performed on 1-dimensional rings to approach the ionic ground state described in Chapter 2. The convergence properties for these algorithms and the tightness of lower bounds to the ground state energy are considered.

4.1 Formulation of the Central Optimization Problem

The von Neumann density operator $\hat{d}$ for the ground state of a fermion system contains all of the information required to compute the ground state properties. One can find $\hat{d}$ by solving the Schrödinger equation, or equivalently by finding the minimizer of the convex problem:

$$\inf_{\substack{\hat{d}\in P \\ <\hat{e},\hat{d}>=1}} <\hat{h},\hat{d}> \tag{4.1}$$

where $\hat{h}$ is the Hamiltonian, $\hat{e}$ is an identity operator, P is a convex set of positive semi-definite operators and $< \cdot,\cdot >$ denotes the trace scalar product for operators on Fock space. $< \hat{e},\hat{d} >= 1$ means that the von Neumann density operator $\hat{d}$ is normalized.

Interactions in most physically interesting systems are up to 2-body. Most of the ground state properties can be obtained from the 2-body reduced density matrix d_n^2 defined in Eq. (1.10) for the ground state. The 2-body reduced density matrix contains a much smaller number of independent parameters than the wave-function (unless n is very small). If r is the total number of 1-particle states, there are $\frac{1}{4}r(r-1)(\frac{1}{2}r(r-1)+1)$ independent entries in the unnormalized 2-body reduced density matrix, while there are $\binom{r}{n}$ independent parameters needed to define an unnormalized wave-function. Furthermore, the symmetry properties of a system usually reduces the number of independent parameters in the reduced density matrix more effectively than in the wave-function. Thus computing the ground state properties by d_n^2 is much

easier than by using a wave-function.

Let a, b, c, $\cdots$, a_r be the annihilators for 1-particle states and $\{\hat{A}_1^p, \hat{A}_2^p, \cdots\}$ be a basis set for a linear space of operators which are p-th order polynomials in creation and annihilation operators. Any up to p-body Hamiltonian $\hat{h}$ can be expressed as

$$\hat{h} = \sum_{i,j} h_{i,j} \hat{A}_i^{p+} \hat{A}_j^p \tag{4.2}$$

with $\{h_{i,j}\}$ being a set of real coefficients. The p-body density matrix d^p can be defined as

$$d^p_{\hat{A}_i,\hat{A}_j} = Tr[\hat{A}_i^{p+} \hat{A}_j^p \hat{d}] \tag{4.3}$$

where Tr is the trace on Fock space. Such a matrix is obviously positive semi-definite. With the same basis set $\{\hat{A}_i^p\}$, we can construct a matrix h from coefficients $\{h_{i,j}\}$. Such a matrix representation for $\hat{h}$ has exactly the same size as the d^p matrix.

The lower bound method of reduced density matrix theory consists in finding a minimizer d^p_* that minimizes the following energy expression:

$$E(d^p) = < h, d^p > \quad \text{with} \quad d^p \in D_0, \tag{4.4}$$

here $< \cdot, \cdot >$ denotes trace scalar product for matrices, i.e., $< h, d^p > = Tr[h^+ d^p]$, and D_0 is a convex set of 'approximately n-representable' p-body density matrices. Since we only have a partial understanding of the n-representability problem, we are forced to carry out the variation in Eq. (4.4) over a set, D_0, somewhat larger than the set of n-representable density matrices. Thus the optimized energy is a lower bound to the ground state energy and the minimizer d^p_* is an approximate p-body reduced density matrix for the corresponding ground state.

The general structure for the central optimization problem in Eq. (4.4) obviously does not depend on p. For convenience, from now on we will use x to replace d^p. Thus the x matrix can be the p-body density matrix for any p. The central optimization problem in Eq. (4.4) can be rewritten with x as

$$E(x) = < h, x > \quad \text{with} \quad x \in D_0, \tag{4.5}$$

From the normalization condition $< \hat{e}, \hat{d} >= 1$, we have $< e, x >=1$, where e is positive and it is a matrix representation for $\hat{e}$ in the same basis set as the x matrix. If a proper basis set for x is chosen, e is a scalar multiple of an identity matrix. The 'approximately n-representable' will mean in the thesis that D_0 is a convex set characterized by (1) $< e, x >= 1$ for any $x \in D_0$, (2) any $x \in D_0$ is positive semi-definite. These conditions are important necessary conditions that x must satisfy in order to be n-representable but are not sufficient.

If the density operator $\hat{d}$ is for a particle conserving system, then all entries of the x matrix describing processes which are not particle conserving, e.g., entries of the form $Tr[a^+b^+c^+d\hat{d}]$ vanish. As a result, the x matrix can be decomposed into a series of smaller blocks. Because of the linear equalities arising from the fermion commutation relations, the entries of the x matrix are not independent but interrelated by a system of linear equalities. For example, when a, b, c, d are distinct,

$$x_{a^+b,c^+d} = Tr[(a^+b)^+c^+d\hat{d}] = Tr[(a^+d^+)^+b^+c^+\hat{d}] = x_{a^+d^+,b^+c^+} \tag{4.6}$$

It is the intertwining of these linear relationship with the positive semi-definiteness of the x matrix that gives D_0 and therefore the central optimization problem a very

complicated structure. Let H be the linear space of real symmetric matrices which have exactly the same block form as the x matrix and P be the set of all positive semi-definite matrices in H. We express all such linear relationships by requiring that $x \in P \cap S^{\perp}$ where S, which we call Pauli subspace, is a suitably chosen subspace of H. Thus in our matrix formulation, the information content of the fermion commutation relations is carried by Pauli subspace S. The elements of S can be interrupted as matrix representations of the zero operator. Let $h = \pi_{S^{\perp}} h$, where $\pi_{S^{\perp}}$ is the orthogonal projector onto $S^{\perp}$, and for convenience we still use h to represent such a projection. Without loss of generality we assume $h \perp e$ and thus $h \in H \cap S^{\perp} \cap e^{\perp}$, as this can always be achieved by translating h by an appropriate scalar multiple of $\pi_{S^{\perp}} e$. Such a translation merely shifts the spectrum of h and does not alter the basic problem in any significant way. Then we can rewrite the central optimization problem in Eq. (4.4) in a completely equivalent but more explicit form as

$$\inf_{\substack{x \in P \cap S^{\perp} \\ <e,x>=1}} <h, x> \tag{4.7}$$

As an example, let's consider the case when the x matrix is a 2-body density matrix for particle conserving systems. Let $\hat{A}_{\alpha\beta} = \frac{1}{2}(\alpha\beta - \beta\alpha)$, $\alpha \neq \beta$ where α, β are either creators or annihilators drawn from the set $\{a^{+}, b^{+}, c^{+}, \cdots, a, b, c, \cdots\}$. With operators $\{\hat{e}, \hat{A}_{\alpha\beta}, \hat{A}_{\alpha\beta}\hat{A}_{\gamma\delta}\}$ as basis set, the x matrix can be expressed by a direct sum of the famous d, q and g matrices:

$$x = d \oplus q \oplus g \tag{4.8}$$

where d and q are real, symmetric and $\binom{r}{2} \times \binom{r}{2}$. Their entries are given by $Tr[\hat{A}^{+}_{ab}\hat{A}_{cd}\hat{d}]$

and $Tr[\hat{A}^{+}_{a^{+}b^{+}}\hat{A}_{c^{+}d^{+}}\hat{d}]$ respectively. The g matrix is given by

$$g = \begin{bmatrix} g_{00} & g_{01} \\ g_{10} & g_{11} \end{bmatrix} \tag{4.9}$$

and $g_{00} = Tr[\hat{e}\hat{d}] = 1$, g_{01} is an r^2 component row vector given by $Tr[\hat{A}_{a^{+}b}\hat{d}]$, $g_{10} = g^{+}_{01}$ and g_{11} is given by $Tr[\hat{A}^{+}_{a^{+}b}\hat{A}_{c^{+}d}\hat{d}]$. Thus g is real, symmetric and $(1+r^2)\times(1+r^2)$. As $<\hat{e},\hat{d}>= 1$, it is easy to compute that $Tr[x] = 1 + \frac{1}{4}r + \binom{r}{2}$. This can be expressed as $<e,x>= 1$, here e is an $\left[1 + \frac{1}{4}r + \binom{r}{2}\right]^{-1}$ multiple of an identity matrix. The convex structure of the x matrix is determined by the positive semi-definiteness of the d, q and g matrices which are the well-known d, q and g n-representability conditions for the 2-body reduced density matrix.

The positive semi-definiteness of the x matrix requires that all the eigenvalues of the x matrix be non-negative. Since the eigenvalues of a matrix are usually non-linear functions of the matrix elements for which no explicit formula exists, the central optimization problem is a distinctly challenging computational problem of minimizing a linear function within a convex domain defined by a finite set of non-linear constraints. The complexity of the problem is enhanced by the fact that any computation of practical value has to deal with a large number of variational parameters.

One very favorable aspect is the convex structure for all x matrices. A point c in a convex C is said to be an extreme point of C if there are no two distinct points c_1 and c_2 in C such that $c = \alpha c_1 + (1-\alpha)c_2$ for some α, $0 < \alpha < 1$. For example, a square is a convex set and the extreme points of the square are its four corners. The solutions for Eq. (4.7) are associated with the extreme points of the convex set

of all x matrices. A non-degenerate solution x_* corresponds to an extreme point of the convex set. A degenerate solution x_* can be expressed as a convex combination of certain extreme points for the convex set

$$x_* = \sum_i^r p_i x_i, \quad \text{with} \quad \begin{cases} 0 \le p_i \le 1, \\ \sum_i^r p_i = 1, \end{cases} \tag{4.10}$$

here $x_1, x_2, \cdots, x_r$ are extreme points and $p_1, p_2, \cdots, p_r$ are corresponding coefficients. Thus convexity ensures that any local minimum is a global solution for the central optimization problem [64].

In principle, the lower bound method applies to any p-body density matrix and can even be used to study the excited states if additional conditions are used to distinguish the excited state investigated from the ground state and other excited states. But so far the focus has been on approaching a ground state by the 2-body density matrix. There are two key criteria for a better lower bound method: tightness of the lower bound and the quickness of convergence. If the lower bound obtained is too far away from the real ground state energy obtained from the FCI wave-function method, the computed result is worthless and new n-representability conditions are needed to further restrict the optimization. Without effective numerical procedures which can solve the central optimization problem with fast convergence, the lower bound method will not be computationally feasible on a large scale. Numerical procedures based on linear programming have been developed and implemented to solve the central optimization problem [51, 52, 65]. These numerical procedures are first-order procedures and numerical experimentation with these procedures in even some small

systems showed rather slow speed of convergence. More effective numerical procedures are still needed before the lower bound method can be put into practical use in large systems. d, q and g conditions have been tested in some small atomic and nuclear systems with varying degree of success [51, 52]. A similar test has never been done in any solid system.

It should be pointed out that the central optimization problem in the lower bound method is only a special case of more general convex problems. Thus effective numerical procedures for solving the convex problem in Eq. (4.7) will not only lead to the solutions in the lower bound method of reduced density matrix theory but also have much more applications in other areas such as linear and nonlinear programming.

4.2 Solving the Central Optimization Problem

4.2.1 Necessary and Sufficient Conditions for the Optimum

The Main Theorem

Here we state a theorem giving necessary and sufficient conditions for the solution of the convex problem defined in Eq. (4.7). Let $K = H \cap S^{\perp} \cap h^{\perp} \cap e^{\perp}$, then we have

Theorem 4.1 *The symmetric matrix x_* is a minimizer of the convex problem if and only if the following conditions are satisfied.*

(1) $x_* \in P \cap S^{\perp}$, $<e, x_*>= 1$,

(2) there is an element $y_* \in P \cap K^{\perp}$ *with* $< h, y_* > > 0$ *which satisfies the matrix equation*

$$x_* y_* = 0. \quad \square \tag{4.11}$$

Note that the condition $< h, y_* > > 0$ guarantees that x_* minimizes the objective function $< h, x >$, not $- < h, x >$. The proof of this theorem is quite straightforward and can be found in [53, 66].

The virtue of this theorem is that it reduces the original convex problem into the problem of solving the matrix equation defined in Eq. (4.11), which is the Euler equation. It should be pointed out that the convex problem defined in Eq. (4.7) does not always have solutions. Whether it has solutions depends upon the specific structure of S. It is found that the convex problem has a solution if and only if $S \cap P = 0$ or equivalently $S^{\perp} \cap \text{int} P$ is not empty. Detailed discussions on the existence of the solutions for the convex problem can be found in [66]. But in physically meaningful systems, there are always solutions. So we only need to find effective methods to get the solutions rather than worry about if there is a solution.

At the optimum, the x_* and its partner y_* can be generally expressed as

$$\begin{aligned} x_* &= -\alpha h + k + \beta \pi_{S^{\perp}} e, \\ y_* &= \alpha' h + s + \beta' e, \end{aligned} \tag{4.12}$$

where $k \in K$, $s \in S$, and α, β, α' and β' are real positive coefficients. It is easy to see that under the normalization condition

$$< e, x_* > = \beta < e, \pi_{S^{\perp}} e > = 1, \tag{4.13}$$

the coefficient β is fixed. The minimizer x_* for $< h, x_* >= -\alpha < h, h >$ should have the largest possible value for α. If the expression for x_* is multiplied by $\frac{1}{\alpha}$,

$$x_* = -h + k + \beta'' \pi_{S^\perp} e, \text{ with } \beta'' = \frac{\beta}{\alpha}. \tag{4.14}$$

The minimizer x_* will have the smallest possible value for $\beta'' > 0$. As $S^\perp \cap \text{int}P \neq 0$, we always can find a $f \in P \cap S^\perp$, and x_* and its partner y_* can be generally re-expressed in a symmetrical form as

$$\begin{aligned} x_* &= -h + k - \lambda(k) f, \qquad k \in K, \\ y_* &= h + s - \omega(s) e, \qquad s \in S. \end{aligned} \tag{4.15}$$

Thus the original problem of minimizing the energy expression $< h, x >$ with $< e, x >= 1$ is equivalent to seeking $k \in K$ that maximizes $\lambda(k) < 0$, the bottom eigenvalue of $-h + k$ given by the matrix eigenvalue equation

$$[-h + k - \lambda(k) f] v = 0, \tag{4.16}$$

and $s \in S$ that maximizes the bottom eigenvalue $\omega(s) < 0$ of the dual problem $h + s$ given by

$$[h + s - \omega(s) e] v = 0. \tag{4.17}$$

It should be pointed out that y_* and h are closely related to each other. Actually the difference between y_* and h comes from (1) the translation of a multiple of e and (2) $s \in S$ which is the matrix representation of the zero operator. Thus y_* can be treated as a very special matrix representation for the original Hamiltonian with

$$< x_*, y_* > = < x_*, h > - \omega(s) < x_*, e > = < x_*, h > + c, \tag{4.18}$$

where c is a constant. What is special here is that y_* is positive semi-definite and orthogonal to the optimized x_*.

In Theorem 4.1, it is the Euler equation that is of importance. Our main interest here is to develop effective numerical algorithms to solve the Euler equation. Let $\dim_{xy}$ be the dimension of the linear space of all matrices (not necessarily symmetric) having the same shape (block structure) as H, then there are $\dim_{xy}$ quadratic equations with $\dim H < \dim_{xy}$ unknowns in the Euler equation. Thus, we are guaranteed by the theorem at least one solution.

Extraneous Solutions for the Euler Equation

As in all quadratic systems, in general there may be more than one solution to the Euler equation. Certainly in most cases there are solutions to the Euler equation where at least one partner of the solution pair x_* and y_* is not positive semi-definite. These solutions do not satisfy the conditions of the central optimization problem defined in Eq. (4.7). So they are referred to as extraneous solutions.

If the Euler equation has a unique solution pair $x_* \geq 0$, $y_* \geq 0$, both theoretical analysis and numerical experimentation have shown that the positivity condition plays little role in searching for these solutions [66]. With carefully chosen seeds, the iterative method will converge rapidly to the desired solutions where both partners are positive semi-definite. Since the positivity condition is very difficulty to impose, this is of considerable importance.

However, in some systems, solutions to the Euler equation are not unique so that

there are either two distinct x_*'s or two distinct y_*'s. Then there are extraneous solutions. If there are two distinct set of solutions $x_* y_*^1 = 0$, $x_* y_*^2 = 0$ with x_*, y_*^1, $y_*^2 \in P$, for example, then there is a solution pair x_*, y_* where y_* is of the form $y_* = t y_*^1 + (1-t) y_*^2$ with t being a real coefficient. It is obvious that such a y_* is a line with respect to t and for some values of t, the matrix $y_* = t y_*^1 + (1-t) y_*^2$ has negative eigenvalues. Thus the degeneracy of solutions to the Euler equation may easily mislead the numerical procedure to extraneous solutions.

Theorem 4.2 *Let x_*, $y_* \in P$ be a desired solution pair to the Euler equation. If there exists an extraneous solution pair x_* and y_{**} where y_{**} has negative eigenvalues, then y_{**} can be expressed as*

$$y_{**} = y_* + s_*, \quad \textit{with} \quad s_* \in S_*, \tag{4.19}$$

and $S_* \subset S$ is the linear space containing all nontrivial solutions to the following matrix equation

$$x_* s_* = 0, \quad \textit{with} \quad s_* \in S. \tag{4.20}$$

Proof: y_{**} can be generally expressed as

$$y_{**} = y_* + s_* + \xi e, \quad \text{with} \quad s_* \in S. \tag{4.21}$$

Since

$$x_* y_{**} = x_* y_* + x_* s_* + x_* \xi e = x_* s_* + x_* \xi e = 0, \tag{4.22}$$

and thus

$$< x_*, y_{**} > = < x_*, s_* > + \xi < x_*, e > = \xi < x_*, e > = 0, \tag{4.23}$$

we have $\xi = 0$ and thus $x_* s_* = 0$. □

According to theorem 4.2, we always can get to the desired solution pair x_*, y_* from x_* and y_{**} by maximizing the bottom eigenvalue of the matrix $y_{**} + s_*$ with $s_* \in S_*$. This procedure referred to as push-up procedure is very useful in searching for desired solutions of the Euler equation.

The situation in which both partners in solutions to the Euler equation are degenerate is very rare and can only be dealt with case by case.

It should be pointed out that extraneous solutions are the direct result of the degeneracy of solutions for the Euler equation. Thus simplifications of any kind on the central optimization problem that reduce the degree of the degeneracy will reduce the risk of getting extraneous solutions.

4.2.2 Symmetry Considerations

Symmetry considerations are very important in the lower bound method. Not only can it simplify the central optimization problem by reducing both the dimensionality of the matrix equation and the risk of getting extraneous solutions dramatically, it may also improve the lower bounds to the ground state.

The Symmetry of x_*

In an n-fermion system, there is usually some kind of symmetry. In the central optimization problem, if the x_* matrix satisfies all the n-representability conditions, the optimization without considerations of symmetry properties will give automatically the ground state with the correct symmetry. Then the consideration of symmetry

is just a matter of convenience, as it reduces the number of independent variational parameters. If, however, the x_* matrix satisfies only a subset of n-representability conditions, the optimized ground state sometimes may not have the correct symmetry. Thus imposing symmetry into the central optimization problem can improve the optimized ground state. Now we consider constraints on n-fermion systems which arise from symmetry considerations. We will consider two types of constraints. The first arises from the requirement that x be invariant under the action of some group (for example x_* is translationally symmetric). The second type of constraint arises when x_* describes an n-fermion system which is an eigenstate of some 1-body operator. For example, we may want to carry out the variation subject to fixed particle number or fixed z-component of the total angular momentum.

In treating the first type of constrained variation, we follow the conventional group theoretical approach, introducing additional block structure in the x_* matrix by choosing a symmetry adapted basis. As a result, H should be redefined as a direct sum of a number of smaller blocks, one corresponding to each of the blocks obtained in the symmetry reduction of the invariant x_* matrix. The effect of this redefinition of H has enormous practical significance since the dimensionality of the problem is reduced considerably. Such a symmetry reduction usually brings additional linear relations among the entries of x_*. The requirement that x_* describe a system which is an eigenstate of some 1-body operator also produces some additional linear relations among the entries of x_*. For example, if such a 1-body operator is the number operator $N = \sum_a a^+ a$ whose eigenvalue n is the number of particles in a system, then

we have

$$\sum_a Tr[(ca)^+ da\hat{d}] = -\sum_a Tr[c^+(\delta_{ad} - da^+)a\hat{d}] = (n-1)Tr[c^+ d\hat{d}], \qquad (4.24)$$

which relates the entries of the d matrix to those of the g matrix. All these additional linear relations among the entries of x_* can be taken into account by expanding the Pauli subspace S. We express both the linear equalities arising from fermion commutation relations and those additional equalities arising from the consideration of the two types of symmetries in terms of the expanded subspace $S \subset H$. Thus $x_* \in H$ has the correct symmetry and satisfies all of the equalities arising from fermion commutation relations if and only if $x_* \perp S$.

It should be pointed out that by redefining the Pauli subspace S, the symmetry of the system is taken into account, but the general structure of the convex problem remains unaltered.

The Symmetry of y_*

The symmetry properties of a system put symmetry constraints only on x_*. Thus y_*, the partner of x_* does not necessarily need to have exactly the same kind of symmetry as x_*. However, the following theorem shows that: symmetry constraints can be put on y_* to further simplify the problem. Here, the symmetry considered is type one only.

Theorem 4.3 *Let G be the symmetry group of a system and $gx_* = x_*$ for any $g \in G$. Then there always exists a symmetry-adapted $y_*^{Sym} \in P \cap K^\perp$ which is positive semi-*

definite and satisfies

$$\begin{aligned} g y_*^{Sym} &= y_*^{Sym}, \quad \text{for } g \in G \\ x_* y_*^{Sym} &= 0. \end{aligned} \tag{4.25}$$

Proof: Let x_* and y_* be the desired solution pair to the Euler equation. As $gx_* = x_*$ for any $g \in G$, if y_* is not degenerate, it is obvious that $gy_* = y_*$. If y_* is degenerate, the action of G on y_* may produce a set of $\{gy_*\}$ with $gy_* \in P \cap K^{\perp}$ and $x_* gy_* = 0$. Let's define

$$y_*^{Sym} = \frac{1}{|G|} \sum_{g \in G} g y_*, \tag{4.26}$$

where $|G|$ is the total number of elements in G. Then, obviously $y_*^{Sym} \in P \cap K^{\perp}$ and it fulfills the equations in (4.25). □

In practice, by considering only symmetry-adapted y_*, we may further reduce the number of variables in the Euler equation by considering only the symmetry-adapted $s \in S$. As the degree of degeneracy for degenerate y_* will also be reduced, symmetry considerations on y_* will also reduce the risk of getting extraneous solutions.

4.2.3 Configuration Interactions in the Lower Bound Method

In the wave-function method, not all configurations contribute equally to the ground state. If only certain important configurations are used in the calculation, the ground state obtained may still be reasonably accurate, but the number of variables involved may be much smaller than that in a full configuration interaction (FCI) calculation. Here, we introduce a similar procedure which will be referred to as the configuration interaction in the lower bound method of reduced density matrix theory.

Recall that the x_* matrix can be expressed as

$$x_* = -h + k - \lambda(k)f, \quad k \in K, \tag{4.27}$$

and the original central optimization problem of minimizing the energy expression $< h, x >$ is equivalent to seeking $k \in K \subset H$ that maximizes $\lambda(k)$, the bottom eigenvalue of $-h + k$ given by

$$[-h + k - \lambda(k)f]v = 0. \tag{4.28}$$

As H is a direct sum of smaller blocks, i.e., $H = \sum_i \oplus H_i$, any $m \in H$ can be expressed as $m = \sum_i \oplus m_i$ with m_i corresponding to block H_i. At the optimum, the optimized $\lambda(k)$ appears only in certain blocks where $x_{*i} = -h_i + k_i - \lambda(k)f_i$ has at least one zero eigenvalue. In other words, $\lambda(k)$ appears only in blocks where x_{*i} is positive semi-definite or equivalently $\lambda(k)$ does not appear in blocks where x_{*i} is positive definite. So it is quite possible that the optimization can be carried out within only blocks where $x_{*i} \geq 0$ at the optimum and the optimized $\lambda(k)$, as well as the optimized x_*, will remain unchanged as long as the number of variables in x_* is not reduced. This procedure can be achieved simply by reformulating H and the basic structure of the convex problem defined in Eq. (4.7) remains unaltered.

Why are blocks with zero eigenvalues at the optimum the most important? The physical meaning can be given as follows: For any x_{*i}, there is a corresponding y_{*i} with $x_{*i}y_{*i} = 0$. If x_{*i} is positive definite, y_{*i} is a trivial zero matrix; Whereas if x_{*i} has zero eigenvalues, then y_{*i} is a matrix representation for an operator of the form $k_i^+ k_i$ where k_i is a linear combination of the basis operators for x_{*i}. As $x_{*i}y_{*i} = 0$

means $Tr[k_i^+ k_i \hat{d}] = 0$, k_i must be a killer operator for the corresponding ground state wave-function. Thus the correlation in the ground state is determined by the killer operators for the ground state. So, important configurations are really determined by killers for the ground state.

If each block x_{*i} is called a configuration, then there will be a FCI calculation by including all blocks of x_* or a non FCI calculation by selecting only certain important blocks in the lower bound method of reduced density matrix theory. This procedure is in exactly the same pattern as that in the wave-function method. As in the wave-function method, the dimensionality of the central optimization problem in Eq. (4.7) in the lower bound method will also be reduced dramatically by removing unimportant configurations.

Now we will discuss in detail about what kind of configurations are not important and thus can be removed from optimizations.

1. If $x_{*i} \geq 0$ as long as certain other blocks in x_* are positive semi-definite, x_i can be removed from the optimization. As an example, if there are several blocks that are exactly the same, then only one such block should remain in the optimization. The requirement that $x_* \geq 0$ comes from n-representability conditions. As $x_{*i} \geq 0$ is no longer an independent condition for $x_* \geq 0$, obviously the removal of this kind of blocks will keep the convex structure of x_* unaltered in the parameter space. Thus the optimization in the reduced space will give exactly the same results as that from FCI optimization. This kind of blocks called type I blocks can be determined by analyzing the convex structure of the x_* matrix.

2. If x_{*i} is strictly positive definite at the optimum, then obviously the corresponding block can also be removed from the optimization without altering the optimized x_*. In other words, the optimization can be performed using only blocks where every corresponding x_{*j} has at least one zero eigenvalue at the optimum. This kind of blocks is referred to as type II block. Generally speaking, removal of type II blocks alters the convex structure of x_*. But it will leave the extreme point associated with the optimum studied unchanged as the extreme point is determined by positive semi-definite blocks. Thus type II blocks are optimum dependent and Hamiltonian dependent. As an optimum is what we seek, in most cases it is almost impossible to figure out exactly how the zero eigenvalues of x_* are distributed among the blocks of x_*. Such a distribution certainly has something to do with the Hamiltonian. So far no general rule on how to locate these zero eigenvalues has been obtained. However in practice, a reasonable guess based on the analysis of the convex structure of x_* and the Hamiltonian can always be made and the optimization can be performed by removing all guessed type II blocks. Then we can check numerically the correctness of the initial guess. If the initial guess is correct, the optimized x_* should be positive semi-definite in the full space H; whereas if the initial guess is not correct, some blocks of x_* will have negative eigenvalues. In the latter case, a new guess can be made by adding blocks where x_* has negative eigenvalues back into the optimization. By repeating this procedure, the desired global optimum can be obtained in a well-controlled reduced linear space and the result obtained are exactly the same as that with the FCI calculation in the lower bound method.

3. If we further remove some blocks where the corresponding x_{*i} has zero eigenvalues at the optimum, the lower bound obtained may be lower than that from the FCI lower bound calculation. This kind of blocks are called type III blocks and will not be investigated numerically in this thesis.

By removing unimportant configurations, the wave-function method will give a different ground state although it may be very close to the ground state from a FCI calculation; On the other side, the lower bound method will give exactly the same ground state as that from a FCI optimization if only type I and type II configurations are to be removed.

4.2.4 Numerical Algorithms for Solving the Euler Equation

$$x_* y_* = 0.$$

Developing efficient numerical procedures for solving the Euler equation defined in Eq. (4.11) is the key problem in the lower bound method. Here we present two numerical algorithms for solving the Euler equation

$$x_* y_* = 0, \qquad \text{with} \qquad x_* \in S^{\perp}, \qquad y_* \in K^{\perp}, \tag{4.29}$$

which is defined in section 4.21. Both x_* and y_* are required to have some fixed but convenient normalization, e.g. $< e, x_* >=< e, y_* >= 1$, where e is as before. This eliminates the trivial solution pair $x_* = 0$, $y_* = 0$ to the Euler equation.

Algorithm 1:

In this algorithm, an iteration procedure based on Newton's method is imple-

mented to solve the Euler equation. In this numerical procedure, x_{i+1} and y_{i+1} in the $(i+1)$-th iteration is determined by

$$\begin{aligned} x_{i+1} &= x_i + t\Delta x_i, \\ y_{i+1} &= y_i + t\Delta y_i, \end{aligned} \tag{4.30}$$

where parameter t is determined by the linear search along the searching direction $\{\Delta x_i, \Delta y_i\}$ to minimize the norm of the matrix

$$x_{i+1}y_{i+1} = x_iy_i + tx_i\Delta y_i + t\Delta x_iy_i + t^2\Delta x_i\Delta y_i, \tag{4.31}$$

where the norm of a matrix m is defined as $||m||^2 = Tr[m^t m]$, and $\{\Delta x_i \in S^\perp, \Delta y_i \in K^\perp\}$ is determined by solving the linearized matrix equation

$$x_iy_i + x_i\Delta y_i + \Delta y_ix_i = 0. \tag{4.32}$$

This is a second order procedure which involves solving $\dim_{xy}$ simultaneous linear equations with $\dim(H) < \dim_{xy}$ unknowns in each iteration. Finally x, y converge to the desired solution pair x_*, y_*.

Algorithm 2.

From a starting pair x_0 and y_0, we are to reduce $||xy||^2$ with

$$\begin{aligned} x &= x_0 + s^\perp \quad \text{with} \quad s^\perp \in S^\perp, \\ y &= y_0 + k^\perp \quad \text{with} \quad k^\perp \in K^\perp. \end{aligned} \tag{4.33}$$

Let $\pi_{S^\perp}$, $\pi_{K^\perp}$ be the orthogonal projectors onto $S^\perp$ and $K^\perp$, respectively. As

$$xy = x_0y_0 + x_0k^\perp + s^\perp y_0 + s^\perp k^\perp, \tag{4.34}$$

the best $s^\perp \in S^\perp$ to reduce $||xy||^2$ is given by $s_1^\perp = \pi_{S^\perp}(x_0y_0^2)$ with $s_1^\perp y_0$ being the orthogonal projection of x_0y_0 onto the linear space $S^\perp y_0$, and the best $k^\perp \in K^\perp$ to

reduce $||xy||^2$ is given by $k_1 = \pi_{K^\perp}(x_0^2 y_0)$ with $x_0 k_1^\perp$ being the orthogonal projection of $x_0 y_0$ onto the linear space $x_0 K^\perp$. This procedure is schematically shown in the first two pictures in figure 4.1.

If we define the linear space spanned by $s_1^\perp$ as $S_1^\perp$, which is a subspace of $S^\perp$, and the linear space spanned by $k_1^\perp$ as $K_1^\perp$, which is a subspace of $K^\perp$, we can carry out the reduction of $||xy||^2$ in these 1-dimensional linear spaces $S_1^\perp$, $K_1^\perp$ with

$$\begin{aligned} x &= x_0 + s^\perp \quad \text{with} \quad s^\perp \in S_1^\perp, \\ y &= y_0 + k^\perp \quad \text{with} \quad k^\perp \in K_1^\perp. \end{aligned} \tag{4.35}$$

As $s^\perp$ and $k^\perp$ vary only within $S_1^\perp \subset S^\perp$ and $K_1^\perp \subset K^\perp$, $||xy||^2$ may not be reduced to zero but to a local minimum with respect to $S_1^\perp$ and $K_1^\perp$. At the local minimum, xy should be orthogonal to both $S_1^\perp y$ and $xK_1^\perp$, thus the optimized $s^\perp$ and $k^\perp$ can be obtained by solving the following equations

$$\begin{aligned} <xy \mid xk^\perp> &= 0, \\ <xy \mid s^\perp y> &= 0. \end{aligned} \tag{4.36}$$

These nonlinear equations can be solved iteratively with Newton's method in exactly the same way as described in algorithm 1. The procedure described above is schematically shown in the third picture of figure 4.1.

Further, we can define $S_i^\perp = \text{span}\{s_1^\perp, s_2^\perp, \cdots, s_i^\perp\}$, $K_j^\perp = \text{span}\{k_1^\perp, k_2^\perp, \cdots, k_j^\perp\}$ where $s_i^\perp$, $k_j^\perp$ are determined by projecting xy^2 and $x^2 y$ from the previous local minimum (with respect to $S_{i-1}^\perp$, $K_{j-1}^\perp$) onto $S^\perp$ and $K^\perp$, respectively. At the previous local minimum, xy is orthogonal to both $S_{i-1}^\perp y$ and $xK_{j-1}^\perp$, which is equivalent to $xy^2 \perp S_{i-1}^\perp$ and $x^2 y \perp K_{j-1}^\perp$. So the new bases $s_i^\perp$ and $k_j^\perp$ are orthogonal to $S_{i-1}^\perp$ and

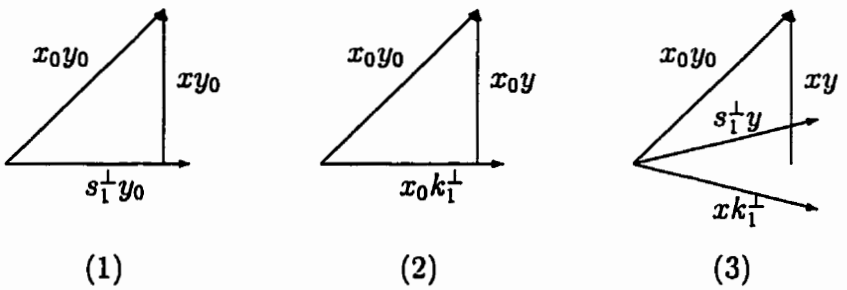

Figure 4.1: Schematic Illustration for Algorithm 2

$K_{j-1}^\perp$, respectively. Thus both $\{s_1^\perp, s_2^\perp, \cdots, s_i^\perp\}$ and $\{k_1^\perp, k_2^\perp, \cdots, k_j^\perp\}$ are orthogonal basis sets which are very convenient in computations. In this way, we generate a series of expanded subspaces of $S^\perp$ and $K^\perp$ with

$$\begin{aligned} S_1^\perp \subset \quad S_2^\perp \subset \cdots \subset \quad S^\perp, \\ K_1^\perp \subset \quad K_2^\perp \subset \cdots \subset \quad K^\perp. \end{aligned} \tag{4.37}$$

In the computation, the reduction of $||xy||^2$ begins at the left side and is carried out step by step from the left to the right of the subspace chains in (4.37) consecutively. In the step with $s^\perp \in S_i^\perp$ and $k^\perp \in K_j^\perp$, searching for the local minimum involves solving $i+j$ simultaneous linear equations with $i+j$ unknowns in each iteration.

In each step of the expansion for the subspaces in (4.37), the new bases are created by projections in exactly the same way as creating $s_1^\perp$ and $k_1^\perp$. Thus they are the best bases to further reduce $||xy||^2$. Finally the global minimum with $x_*y_* = 0$ is reached. As Newton's method is used to solve the nonlinear equations, this algorithm is also a second-order numerical procedure and therefore has fast convergence near the minimum.

By comparison, the first algorithm is simpler and more straightforward. In nu-

merical procedure, it needs relatively less number of iterations to get to the global minimum. The main disadvantage of this algorithm is that the number of linear equations in each iteration grows faster as the system becomes larger and larger. That may cause this algorithm to slow down in large systems. The second algorithm seems a little more complicated. In the numerical procedure, it involves finding the best bases by projection, reducing $||xy||^2$ in well-controlled smaller subspaces and expanding the subspaces step by step. It needs relatively more iterations to converge to the global minimum. But as the new bases in each step of the expansion are always the best, the reduction of $||xy||^2$ in each step is very effective. Actually we do not need to go very far along the subspace chains before the global minimum is reached. In other words, the global minimum can be reached within much smaller carefully chosen subspaces of $S^{\perp}$ and $K^{\perp}$. Thus the total number of linear equations involved is much less than those in algorithm 1.

It is expected that algorithm 2 will work much faster than algorithm 1 in large systems. Not only will it offer a very effective numerical procedure to make the lower bound method of reduced density matrix theory a real computationally feasible method in large scale, but it will also have much more applications in other linear and non-linear optimization problems.

In a series of numerical experiments, x and y were symmetric matrices with dimensions up to 30 and there were up to 465 independent variational parameters. Both algorithms showed fast convergence. In the case where x and y were 30×30 symmetric matrices with 465 variational parameters, both algorithms needed about 20 iterations

to converge to the desired solutions. In the numerical procedure from algorithm 2, the global minimum was reached in the reduced subspaces whose combined dimension was about 20. Such a dimension is much lower than the full dimension 465. As a result, the number of equations involved there was much less than that in algorithm 1 and algorithm 2 worked much faster than algorithm 1. These results agree very well with our expectation.

4.3 Application of the Lower Bound Method to 1-dimensional Rings

Here, the lower bound method will be applied to 1-dimensional rings to compute the ground state determined by the ionic Hamiltonian $\hat{h}^I$ in Eq. (2.16). The Hamiltonian reads

$$\hat{h}^I = \alpha_1^I \hat{h}_1^I + \alpha_1^I \hat{h}_2^I, \tag{4.38}$$

where α_1^I and α_2^I are real coefficients, and $\hat{h}_1^I$ and $\hat{h}_2^I$ given by

$$\begin{aligned} \hat{h}_1^I &= \textstyle\sum_{<i,j>}(a_i^+ b_i^+ b_j a_j + a_j^+ b_j^+ b_i a_i), \\ \hat{h}_2^I &= \textstyle\sum_{<i,j>}(e_{a_i e_{a_j}} + e_{b_i e_{b_j}} + e_{a_i e_{b_j}} + e_{a_j e_{b_i}}). \end{aligned} \tag{4.39}$$

From the investigation in chapter 2, we know that the ground state of $\hat{h}^I$ is an ionic state consisting of empty and on-site pairing ionic lattice sites. Requiring that $\hat{d}$ is a density operator for an ionic state in 1-dimensional rings will put an additional constraint on the corresponding x matrix defined in Eq. (4.3). All elements of the x matrix that do not preserve the number of on-site pairings will vanish. For example,

$Tr[(a_{\mathbf{r}}b_{\mathbf{r}})^{+}b_{\mathbf{r}}a_{\mathbf{r}'}\hat{d}] = 0$ if $a_{\mathbf{r}}$, $b_{\mathbf{r}}$ are annihilators on site $\mathbf{r}$ with spin up and down respectively and $a_{\mathbf{r}'}$ is an annihilator on another site $\mathbf{r}'$. Our main interest is the half-filled ionic ground state which is the main characteristic of the superconducting quantum phases for S_{H^2} in lattices with cubic symmetry. So only rings with an even number of lattice sites will be considered.

The main purpose of our investigation is:

(1) to further test the numerical procedures we presented above.

(2) to seek and test proper n-representability conditions which are manageable but still give reasonably tight lower bounds to the ground state energy, as well as good approximations to the corresponding reduced density matrix in the system.

The success of such an investigation will make a big step forward towards applying the lower bound method of reduced density matrix theory to 2-dimensional square lattices and other more complicated physical systems. Efficient numerical procedures based on the main theorem will have applications beyond the lower bound method of reduced density matrix theory.

4.3.1 The Lower Bound Method with the 2-body Density Matrix

As $\hat{h}^I$ is pure 2-body, the natural choice for the lower bound method is the 2-body density matrix defined in Eq. (4.8). Such a 2-body density matrix x should be invariant under the particle-hole transformation T_{PH}. Thus all entries of x of the form $Tr[\hat{A}^1\hat{d}]$, where $\hat{A}^1$ is a pure 1-body operator, will vanish. As a result, the x matrix

is completely determined by pure 2-body operators and further the corresponding d- and q-matrices are equivalent with

$$Tr[(ab)^+ cd\hat{d}] = Tr[(a^+b^+)^+ c^+ d^+ \hat{d}]. \tag{4.40}$$

Because of the translational symmetry in the system and because of the fact that the ground state investigated is an ionic ground state, there are $|\Lambda|$ independent variables in x which are associated with $|\Lambda|$ pure 2-body operators in a ring with $|\Lambda|$ sites. These variables can be defined as

$$\begin{aligned} \alpha_i &= Tr[e_{a_1} e_{a_{1+i}} \hat{d}], \\ \beta_i &= Tr[4(a_1 b_1)^+ a_{1+i} b_{1+i} \hat{d}] \end{aligned} \qquad \text{with i} = 1, 2, \cdots, \frac{|\Lambda|}{2}. \tag{4.41}$$

It is the constraint on these variables that completely determines the convex structure of the x matrix.

Let $r = 2|\Lambda|$ denote the rank of 1-particle states, the dimension of the x matrix is $2\binom{r}{2} + 1 + r^2$. By removing all type I blocks, the dimension of the x matrix is reduced to $\frac{7}{2}|\Lambda|$. In the reduced x matrix, there are two $|\Lambda| \times |\Lambda|$ blocks whose basis set can be chosen as $\{\sqrt{2}\, a_i b_i,\ i = 1, 2, \cdots, |\Lambda|\}$ and $\{e_{a_i},\ i = 1, 2, \cdots, |\Lambda|\}$, respectively; $|\Lambda|$ 2×2 blocks whose bases are given by $\{a_1^+ a_{1+i},\ b_{1+i}^+ b_1\}$ with $i = 1, 2, \cdots |\Lambda|/2$; and $|\Lambda|$ 1×1 blocks whose bases are given by $\{a_1 a_{1+i}\}$ with $i = 1, 2, \cdots, |\Lambda|$. Because of its special symmetric form, the x matrix can be diagonalized by an unitary transformation independent of the variables $\{\alpha_i,\ \beta_i,\ i = 1, 2, \cdots, |\Lambda|/2\}$. So the constraint condition $x \geq 0$, which is equivalent to requiring that all eigenvalues of the x matrix be greater than or equal to zero, becomes a set of linear constraints on

these variables. Thus, the approximately n-representable region in which $x \geq 0$ is a polyhedron. This makes the investigation of the convex structure of x much easier.

$|\Lambda| = 2$ Case

For $|\Lambda| = 2$, the simplest case in 1-dimensional rings with an even number of sites, the reduced x matrix is determined by α_1 and β_1. It can be expressed as

$$x = \sum_{i=1}^{4} \oplus x_i \tag{4.42}$$

with

$$\begin{aligned} x_1 &= \begin{bmatrix} 1 & \beta_1/2 \\ \beta_1/2 & 1 \end{bmatrix}, \qquad x_2 = \begin{bmatrix} 1 & \alpha_1 \\ \alpha_1 & 1 \end{bmatrix}, \\ x_3 &= \begin{bmatrix} 1-\alpha_1 & \beta_1 \\ \beta_1 & 1-\alpha_1 \end{bmatrix}, \quad x_4 = \begin{bmatrix} 1+\alpha_1 \end{bmatrix}. \end{aligned} \tag{4.43}$$

This x matrix can be diagonalized by an unitary transformation

$$U = \sum_{i=1}^{4} \oplus U_i \tag{4.44}$$

with

$$\begin{aligned} U_1 &= \begin{bmatrix} \frac{1}{\sqrt{2}} & \frac{1}{\sqrt{2}} \\ \frac{1}{\sqrt{2}} & -\frac{1}{\sqrt{2}} \end{bmatrix}, \quad U_2 = \begin{bmatrix} \frac{1}{\sqrt{2}} & \frac{1}{\sqrt{2}} \\ \frac{1}{\sqrt{2}} & -\frac{1}{\sqrt{2}} \end{bmatrix}, \\ U_3 &= \begin{bmatrix} \frac{1}{\sqrt{2}} & \frac{1}{\sqrt{2}} \\ \frac{1}{\sqrt{2}} & -\frac{1}{\sqrt{2}} \end{bmatrix}, \quad U_4 = \begin{bmatrix} 1 \end{bmatrix}. \end{aligned} \tag{4.45}$$

The convex structure of the x matrix is determined by the non-negativity of all eigenvalues of x, that is

$$\begin{aligned} 1 \pm \beta_1/2 \geq 0, \qquad & 1 \pm \alpha_1 \geq 0, \\ 1 - \alpha_1 \pm \beta_1 \geq 0, \qquad & 1 + \alpha_1 \geq 0. \end{aligned} \tag{4.46}$$

Such a convex set is schematically shown by the triangle $V^0 V_-^2 V_+^2$ in figure 4.2 where at any point inside the triangle, $x > 0$ and at any point on the triangle boundary, $x \geq 0$. V^0, V_+^2, and V_-^2 are three extreme points of the convex set and thus correspond to possible desired solutions in the lower bound method.

It is easy to check that this convex set is n-representable. Any point outside the convex is not n-representable and thus is forbidden. The lower bound method gives exactly the same ground state as that from the FCI wave-function method. Among those extreme points, V^0 with $\{\beta_1, \alpha_1\} = \{0, 1\}$ corresponds to the vacuum ground state, V_+^2 with $\{\beta_1, \alpha_1\} = \{+2, -1\}$ and V_-^2 with $\{\beta_1, \alpha_1\} = \{-2, -1\}$ correspond to the half-filled AGP ground states with constant and alternating phases, respectively. Here, it is worth mentioning a very special point C with $\{\beta_1, \alpha_1\} = \{0, -1\}$. This point corresponds to the checkerboard ground state and happens to be degenerate with the AGP ground states in this case.

$|\Lambda| = 4$ Case

For $|\Lambda| = 4$, the x matrix is determined by $\{\alpha_1, \alpha_2, \beta_1, \beta_2\}$ and the blocks in the reduced x matrix are given by

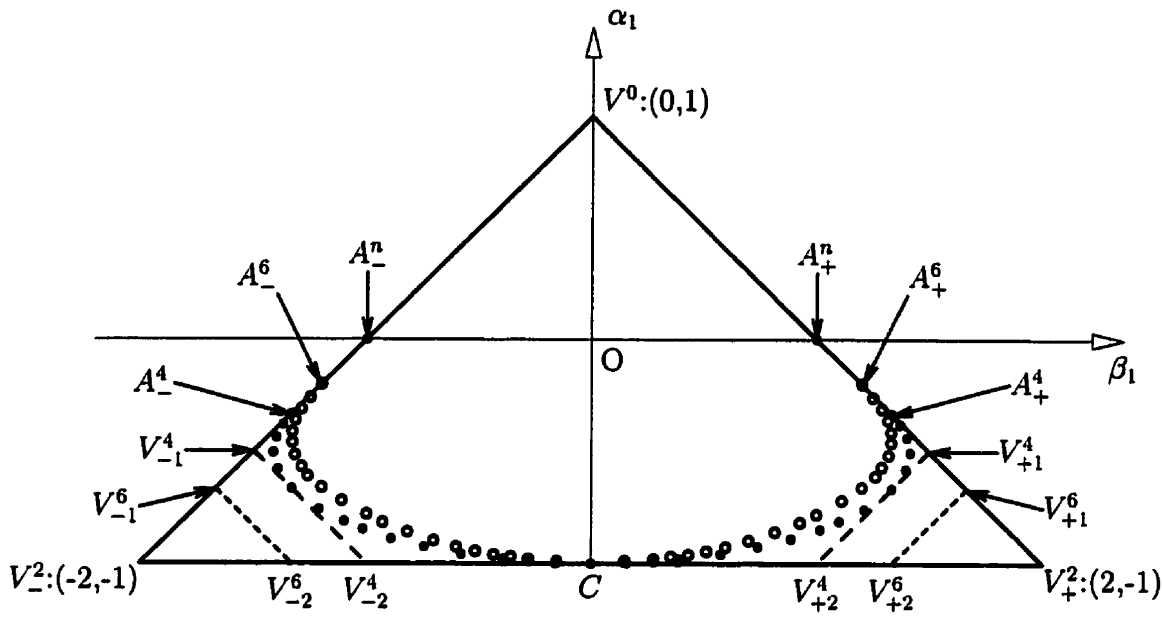

Figure 4.2: The Approximately n-representable Region from the 2-body Density Matrix

$$\begin{bmatrix} 1 & \beta_1/2 & \beta_2/2 & \beta_1/2 \\ \beta_1/2 & 1 & \beta_1/2 & \beta_2/2 \\ \beta_2/2 & \beta_1/2 & 1 & \beta_1/2 \\ \beta_1/2 & \beta_2/2 & \beta_1/2 & 1 \end{bmatrix}, \qquad \begin{bmatrix} 1 & \alpha_1 & \alpha_2 & \alpha_1 \\ \alpha_1 & 1 & \alpha_1 & \alpha_2 \\ \alpha_2 & \alpha_1 & 1 & \alpha_1 \\ \alpha_1 & \alpha_2 & \alpha_1 & 1 \end{bmatrix}, \tag{4.47}$$

$$\begin{bmatrix} 1-\alpha_i & \beta_i \\ \beta_i & 1-\alpha_i \end{bmatrix}, \qquad [1+\alpha_i], \quad \text{with} \quad \mathrm{i} = 1 \text{ and } 2.$$

In exactly the same procedure as in $|\Lambda| = 2$ case, the convex structure of the x matrix is determined by the non-negativity of all its eigenvalues, that is found to be

$$
\begin{aligned}
&1 \pm \beta_1 + \beta_2/2 \geq 0, \qquad && 1 - \beta_2/2 \geq 0, \\
&1 \pm 2\alpha_1 + \alpha_2 \geq 0, \qquad && 1 - \alpha_2 \geq 0, \\
&1 - \alpha_i \pm \beta_i \geq 0, \qquad && 1 + \alpha_i \geq 0 \quad \text{with} \quad \text{i=1, 2.}
\end{aligned}
\tag{4.48}
$$

The convex set determined by these linear constraints is a polyhedron with five extreme points. The projection of this polyhedron onto the plane spanned by $\{\alpha_1, \beta_1\}$ is a polygon with the projections of the five extreme points as its five vertexes. As the ground state energy depends only on α_1 and β_1, the ground state in the lower bound method is best described by such a polygon. In figure 4.2, this polygon is schematically given by $V^0 V^4_{+1} V^4_{+2} V^4_{-2} V^4_{-1}$ where V^0, V^4_{+1} V^4_{+2}, V^4_{-2} and V^4_{-1} are the projections of the five extreme points. The associated values of $\{\alpha_1, \alpha_2, \beta_1, \beta_2\}$ at these extreme points corresponding to V^0, V^4_{+1} V^4_{+2}, V^4_{-2} and V^4_{-1} are given in table 4.1.

In order to compare the results from the lower bound method and the wave-function method, the projections onto the $\beta_1\alpha_1$ plane of the n-representable half-filled ionic ground states from the FCI wave-function computation are also schematically shown with small disks in figure 4.2. There A^4_+, A^4_- correspond to the half-filled AGP ground states with constant and alternating phases, respectively, and C corresponds to the checkerboard ground state. The associated values of $\{\alpha_1, \alpha_2, \beta_1, \beta_2\}$ for these special points are also given in table 4.1.

$|\Lambda| = 6$ Case

Despite the increase in dimensionality, both the block structure and the convex structure of x are found to be similar to that in $|\Lambda| = 2$, 4 cases. In this case, the

	V^0	C	A^4_+	A^4_-	V^4_{+1}	V^4_{-1}	V^4_{+2}	V^4_{-2}
α_1	1	-1	$-\frac{1}{3}$	$-\frac{1}{3}$	$-\frac{1}{2}$	$-\frac{1}{2}$	-1	-1
α_2	1	1	$-\frac{1}{3}$	$-\frac{1}{3}$	0	0	1	1
β_1	0	0	$\frac{4}{3}$	$-\frac{4}{3}$	$\frac{3}{2}$	$-\frac{3}{2}$	1	-1
β_2	0	0	$\frac{4}{3}$	$\frac{4}{3}$	1	1	0	0

Table 4.1: Values for Some Special Points with $|\Lambda| = 4$

polygon from the lower bound method is schematically given by $V^0V^6_{+1}V^6_{+2}V^6_{-2}V^6_{-1}$ in figure 4.2 where V^0, V^6_{+1}, V^6_{+2}, V^6_{-2} and V^6_{-1} correspond to five extreme points of the convex set. The n-representable half-filled ionic ground states are also given schematically with small circles in figure 4.2 where A^6_+, A^6_- and C correspond to the half-filled AGP ground states with constant and alternating phases and the checkerboard ground state respectively. The associated values of $\{\alpha_1, \alpha_2, \alpha_3, \beta_1, \beta_2, \beta_3\}$ at these special points are given in table 4.2.

Fixing Particle Number

In the above investigations, the number of electrons is not fixed in order to facilitate the study for the convex structure of x. If the number of electrons is fixed to $|\Lambda|$ (half-filling), an additional linear condition will arise from

$$Tr[N\hat{d}] = |\Lambda| \quad \text{with} \quad N = \sum_i^{|\Lambda|}(a_i^+a_i + b_i^+b_i)\,. \tag{4.49}$$

	V^0	C	A^6_+	A^6_-	V^6_{+1}	V^6_{-1}	V^6_{+2}	V^6_{-2}
α_1	1	-1	$-\frac{1}{5}$	$-\frac{1}{5}$	$-\frac{2}{3}$	$-\frac{2}{3}$	-1	-1
α_2	1	1	$-\frac{1}{5}$	$-\frac{1}{5}$	0	0	1	1
α_3	1	-1	$-\frac{1}{5}$	$-\frac{1}{5}$	$\frac{1}{3}$	$\frac{1}{3}$	-1	-1
β_1	0	0	$\frac{6}{5}$	$-\frac{6}{5}$	$\frac{5}{3}$	$-\frac{5}{3}$	$\frac{4}{3}$	$-\frac{4}{3}$
β_2	0	0	$\frac{6}{5}$	$\frac{6}{5}$	1	1	0	0
β_3	0	0	$\frac{6}{5}$	$-\frac{6}{5}$	$\frac{2}{3}$	$-\frac{2}{3}$	$-\frac{2}{3}$	$\frac{2}{3}$

Table 4.2: Values for Some Special Points with $|\Lambda| = 6$

This condition will put an additional linear constraint on the variables with

$$Tr[\sum_i^{|\Lambda|} e_{a_i} \sum_j^{2|\Lambda|} e_{a_j} \hat{d}] = Tr[(2N - 2|\Lambda|)(2N - 2|\Lambda|)\hat{d}] = 0, \tag{4.50}$$

which means that

$$1 + 2 \sum_i^{\frac{|\Lambda|}{2}-1} \alpha_i + \alpha_{\frac{|\Lambda|}{2}} = 0. \tag{4.51}$$

It has been checked that the values of variables on all the extreme points mentioned above except V^0, which corresponds to the vacuum ground state, satisfy the condition in Eq. (4.51). This indicates that the ground states obtained from the lower bound method are half-filled automatically. Thus adding condition in Eq. (4.51) to further constrain the x matrix will not improve the lower bounds to the ground state energy as well as the approximations to the corresponding reduced density matrix.

Numerical Computations

Numerical procedures based on the two algorithms presented in the previous section are implemented to compute the ground state in the 1-dimensional rings discussed above. In most situations, the numerical procedures are not very sensitive to the starting points. An arbitrarily chosen starting pair $\{x_0, y_0\}$ with $x_0 \geq 0$, $y_0 \geq 0$ will lead to the desired solutions with fast convergence. The optimized x_* corresponds to one of the extreme points for the corresponding convex set. But for certain special $\hat{h}^I$, degeneracy exists for the ground state. The desired x_* no longer simply corresponds to one of the extreme points but corresponds to a line segment connecting two extreme points. In $|\Lambda| = 6$ case, for example, all points on the line segment $V^6_{-2}V^6_{+2}$ correspond to the degenerate ground states of $\hat{h}^I$ with $\alpha^I_1 = 0$, $\alpha^I_2 \geq 0$. Thus, there are extraneous x_{**} on the extension of the line segment. In this kind of situation, carefully chosen starting points, in which both partners are positive semi-definite and very close to the desired solutions, and the push-up procedure based on Theorem 4.2 are needed to get to the desired solutions.

The highly symmetric AGP ground states are found to be the most difficult ones to compute numerically. As the AGP ground states have much higher degree of symmetry and thus have many more zero eigenvalues in x^{AGP}_* than other ground states, not only every x^{AGP}_* itself is highly degenerate, its partner y^{AGP}_*, which is the positive semi-definite killer of x^{AGP}_* with $y^{AGP}_* x^{AGP}_* = 0$ at the optimum, is also highly degenerate. Thus there is much more chance to get to the extraneous solutions. As there is much higher degree of symmetry in the solid state, the lower

bound calculation may be more difficult in solid systems than in atomic and nuclear systems.

Although the systems computed are not very large, numerical tests have already shown that algorithm 2 had an equally fast speed of convergence as algorithm 1. This again indicates that algorithm 2 will be a much faster numerical procedure than algorithm 1 when systems become larger and larger.

Discussions and Conclusions

As a summary of the above investigation, we have the following conclusions:

1. As is shown in figure 4.2, the projection onto the $\alpha_1\beta_1$ plane of the n-representable region in a 1-dimensional rings is bounded by two line segments meeting at V^0 and a smooth curve connecting the other ends of the segments ($|\Lambda| = 2$ is an exception). Every point in such a smooth curve represents a half-filled ionic ground state. The middle point C corresponds to the checkerboard ground state and the two end points correspond to the half-filled AGP ground states with constant and alternating phases, respectively. As the number of sites in the ring increases, the corresponding n-representable region will shrink. As a result, the middle point C remains unchanged and all other points on the curve move inwards. The two end points go approaching to A^n_+ and A^n_- which correspond to the half-filled AGP ground states with constant and alternating phases respectively for $|\Lambda| \longrightarrow \infty$.

2. On the other side, the projection onto the $\alpha_1\beta_1$ of the approximately n-representable region obtained from the lower bound method is a polygon. The half-

filled ionic ground states are represented by several line segments which connect the extreme points of the corresponding convex set non-smoothly. Point C, and the points corresponding to the AGP ground states are the only points corresponding to the n-representable half-filled ionic ground states. As the number of sites in a ring increases, the approximately n-representable region will expand. The extreme points with $\beta_1 > 0$ and $\beta_1 < 0$ approach to V_+^2 and V_-^2, respectively. As a result, for $|\Lambda| \longrightarrow \infty$, the polygon for the approximately n-representable region will be represented by the triangle $V^0V_+^2V_-^2$.

3. From the above discussion, it is obvious that: as the number of sites in a ring increases, the approximately n-representable region from the lower bound method will go in the opposite direction to the n-representable region. This strongly indicates that the d-, q- and g-conditions for the 2-body density matrix in the lower bound method are not good enough to give reasonably tight lower bounds to the ground state energy as well as good approximations to the corresponding 2-body reduced density matrix in 1-dimensional rings. So more n-representability conditions are needed in order to give a better description of the ground states using the lower bound method.

4.3.2 The Lower Bound Method with the 3-body Density Matrix

Now it is clear that more n-representability conditions have to be introduced into the lower bound method in order to get better results. But what are the n-representability conditions which are important to the ground state and still manage-

able in the system. There are two alternatives: one is to introduce more necessary n-representability conditions for the 2-body reduced density matrix , the other is to use the p-body density matrix with $p > 2$ in the lower bound method. The following analysis on the ionic ground state for $\mathbf{\Lambda} = 4$ strongly indicates that the second alternative is a better choice in our system.

The 3-body Reduced Density Matrix for $|\mathbf{\Lambda}| = 4$

Let the pair creation and annihilation operators be

$$B_i^+ = a_i^+ b_i^+, \quad B_i = a_i b_i, \tag{4.52}$$

then the wave-function for the n-representable half-filled ionic ground state in the ring with $|\mathbf{\Lambda}| = 4$ can be generally expressed as

$$|\phi_g(\xi)>= \left[(B_1^+ B_3^+ + B_2^+ B_4^+) + \xi(B_1^+ B_2^+ + B_2^+ B_3^+ + B_3^+ B_4^+ + B_4^+ B_1^+)\right] |0>, \tag{4.53}$$

with $0 \leq |\xi| \leq 1$. When $\xi = 0$, $\phi_g(\xi)$ is the checkerboard ground state; and when $\xi = +1$ or -1, $\phi_g(\xi)$ is the AGP ground state with a constant or an alternating phase. We build a set of killer operators for $\phi_g(\xi)$ as:

$$\begin{aligned}
k_{1,\hat{\alpha}} &= (\xi b_2^+ b_1 - a_1^+ a_2)\hat{\alpha}, & k_{2,\hat{\alpha}} &= (b_2^+ b_1 - \xi a_1^+ a_2)\hat{\alpha}^+, \\
k_{3,\hat{\alpha}} &= (\xi a_2^+ a_1 - b_1^+ b_2)\hat{\alpha}, & k_{4,\hat{\alpha}} &= (a_2^+ a_1 - \xi b_1^+ b_2)\hat{\alpha}^+, \\
k_{5,\hat{\alpha}} &= (\xi a_2^+ b_1 + a_1^+ b_2)\hat{\alpha}, & k_{6,\hat{\alpha}} &= (a_2^+ b_1 + \xi a_1^+ b_2)\hat{\alpha}^+, \\
k_{7,\hat{\alpha}} &= (\xi b_2^+ a_1 + b_1^+ a_2)\hat{\alpha}, & k_{8,\hat{\alpha}} &= (b_2^+ a_1 + \xi b_1^+ a_2)\hat{\alpha}^+,
\end{aligned} \tag{4.54}$$

with

$$\hat{\alpha} \in \{a_1^+,\ b_4^+,\ a_3,\ b_3\}. \tag{4.55}$$

Keep in mind that the operator

$$k_9 = \sum_i^{\Lambda}(e_{a_i} + e_{b_i}) \tag{4.56}$$

is a killer for all half-filled states. From these killer operators, we can build a Hamiltonian

$$\hat{h}_\xi = (1-\xi^2)k_9^+ k_9 + \sum_i^8 \sum_{\hat{\alpha}} k_{i,\hat{\alpha}}^+ k_{i,\hat{\alpha}}. \tag{4.57}$$

Obviously $\hat{h}_\xi$ is positive semi-definite and it is also a killer operator for $\phi_g(\xi)$. Thus $\phi_g(\xi)$ is the ground state of $\hat{h}(\xi)$. $\hat{h}_\xi$ can be further expressed as

$$\begin{aligned}\hat{h}(\xi) &= 16\left[2 - \xi\sum_i^{\Lambda}(-B_i^+ B_{i+1} - B_{i+1}^+ B_i) + \frac{1-2\xi^2}{8}\sum_i^{\Lambda}(e_{a_i} + e_{b_i})(e_{a_{i+1}} + e_{b_{i+1}})\right] \\ &= 16\left[2 - \xi\hat{h}_1^I + \frac{1-2\xi^2}{8}\hat{h}_2^I\right].\end{aligned} \tag{4.58}$$

Apart from a constant, $\hat{h}(\xi)$ is exactly the ionic Hamiltonian $\hat{h}^I$ in Eq. (4.38). The most striking feature of $\hat{h}(\xi)$ is that: in its expression (4.57), any k_i is a polynomial in creation and annihilation operators of degree less than or equal to 3 and thus is a basis operator for the 3-body density matrix.

Let $x_{\phi_g(\xi)}$ be the n-representable 3-body density matrix corresponding to $\phi_g(\xi)$ and $h(\xi)$ be the positive semi-definite matrix representation of $\hat{h}(\xi)$ in the same basis set as $x_{\phi_g(\xi)}$. As $\hat{h}(\xi)$ is a killer of $\phi_g(\xi)$, we have

$$x_{\phi_g(\xi)} h(\xi) = 0. \tag{4.59}$$

This means that if we use the 3-body density matrix to replace the 2-body density matrix in the convex problem defined in Eq. (4.7), then $x_{\phi_g(\xi)}$, $h(\xi)$ will be the desired solution pair for the Euler Equation. Thus the ground states obtained in the lower

bound method with entries of the 3-body density matrix as variational parameters will be exactly the same as that from the FCI wave-function method.

This important result strongly indicates that the 3-body density matrix is a good candidate to replace the 2-body density matrix in the lower bound method.

The 3-body Density Matrix in the Lower Bound Method

In the cases of $|\mathbf{\Lambda}| > 4$, no 3-body killer operator with similar form as that in Eq. (4.57) has been found. This means that the 3-body density matrix corresponding to the ground state obtained from the lower bound method will probably not be exactly the same as that from the wave-function method. However, the significant improvement of the lower bound in the $|\mathbf{\Lambda}| = 4$ case strongly suggests that the lower bound method with entries of the 3-body density matrix as variational parameters may give much tighter lower bounds to the ground state energy as well as much better approximations to the corresponding ground state in the system.

The 3-body density matrix x is determined by up to 3-body operators. It can be generally decomposed as

$$x = Tr[\hat{A}^0\hat{d}] + Tr[\hat{A}^1\hat{d}] + Tr[\hat{A}^2\hat{d}] + Tr[\hat{A}^3\hat{d}], \tag{4.60}$$

where $\hat{A}^0$, $\hat{A}^1$, $\hat{A}^2$ and $\hat{A}^3$ are scalar, pure 1-, 2- and 3-body operators, respectively. As the Hamiltonian studied is invariant under particle-hole transformation, both $Tr[\hat{A}^1\hat{d}]$ and $Tr[\hat{A}^3\hat{d}]$ vanish. Thus the number of independent variables in the 3-body density matrix is exactly the same as that in the 2-body density matrix. From the definition in Eq. (4.3), it is obvious that all the blocks from the 2-body density matrix will be

included in the 3-body density matrix . Thus the dimensionality of the problem is increased. The general structure of the convex problem defined in Eq. (4.7) remains unaltered.

For $|\Lambda| = 4$, after removing all type I blocks, new blocks in the reduced x matrix are given by

$$\begin{bmatrix} 1-\alpha_1 & \beta_1/2 & \beta_2/2 & \beta_1/\sqrt{2} & -\beta_1/\sqrt{2} & 0 & 0 \\ \beta_1/2 & 1-\alpha_2 & \beta_1/2 & \beta_2/2 & 0 & -\beta_2/\sqrt{2} & 0 \\ \beta_2/2 & \beta_1/2 & 1-\alpha_1 & \beta_1/\sqrt{2} & 0 & 0 & -\beta_1/\sqrt{2} \\ \beta_1/\sqrt{2} & \beta_2/\sqrt{2} & \beta_1/\sqrt{2} & 1 & \alpha_1 & \alpha_2 & \alpha_1 \\ -\beta_1/\sqrt{2} & 0 & 0 & \alpha_1 & 1 & \alpha_1 & \alpha_2 \\ 0 & -\beta_2/\sqrt{2} & 0 & \alpha_2 & \alpha_1 & 1 & \alpha_1 \\ 0 & 0 & -\beta_1/\sqrt{2} & \alpha_1 & \alpha_2 & \alpha_1 & 1 \end{bmatrix}, \quad (4.61)$$

with $\{2b_1(a_ib_i)^+,\ -\sqrt{2}a_1^+,\ \sqrt{2}a_1^+e_{a_i},\ \mathrm{i} = 2,\ 3,\ 4\}$ as bases;

$$\begin{bmatrix} 1+\alpha_1 & \beta_1/2 & \beta_2/2 \\ \beta_1/2 & 1+\alpha_2 & \beta_1/2 \\ \beta_2/2 & \beta_1/2 & 1+\alpha_1 \end{bmatrix}, \quad (4.62)$$

with $\{2a_1^+(a_ib_i)^+,\ \mathrm{i} = 2,\ 3,\ 4\}$ as bases; and

$$\begin{bmatrix} 1-\alpha_2 & \beta_1 & \beta_2 & 0 \\ \beta_1 & 1-2\alpha_1+\alpha_2 & \beta_1 & 0 \\ \beta_2 & \beta_1 & 1-\alpha_2 & 0 \\ 0 & 0 & 0 & 1+2\alpha_1+\alpha_2 \end{bmatrix}, \tag{4.63}$$

with $\{2\sqrt{2}a_1^+a_2^+a_3,\ 2\sqrt{2}a_1^+b_3^+b_2,\ 2\sqrt{2}b_3^+a_2^+b_1,\ 2\sqrt{2}a_1a_2a_3\}$ as bases.

It has been checked that at extreme points V_{+1}^4, V_{-1}^4, V_{+2}^4 and V_{-2}^4, these blocks all have negative eigenvalues and bigger negative eigenvalues are always found in the first and third blocks. By further analysis of the exact solution, we found that these two blocks alone will be enough to give the desired solutions in the lower bound method.

As the number of sites increases, the block structure in the reduced x matrix is found to be similar to that for $|\Lambda| = 4$. There are two big blocks whose dimensions increase linearly with $|\Lambda|$ and whose bases are given by $\{2b_1(a_ib_i)^+,\ -\sqrt{2}a_1^+,\ \sqrt{2}a_1^+e_{a_i},$ i $= 2, 3, \cdots, |\Lambda|\ \}$ and $\{2a_1(a_ib_i)^+,$ i $= 2, 3, \cdots, \Lambda\}$ respectively. There are a series of 4×4 blocks, whose basis set is given by $\{2\sqrt{2}a_{i_1}^+a_{i_2}^+a_{i_3},\ 2\sqrt{2}a_{i_1}^+b_{i_3}^+b_{i_2},\ 2\sqrt{2}b_{i_3}^+a_{i_2}^+b_{i_1},$ $2\sqrt{2}a_{i_1}a_{i2}a_{i_3}\}$ with $i_1 \neq i_2 \neq i_3$. The three indices can be associated with a special configuration. For example, in the case with $|\Lambda| = 6$, there are three 4×4 blocks given by

$$\begin{bmatrix} 1-\alpha_2 & \beta_1 & \beta_2 & 0 \\ \beta_1 & 1-2\alpha_1+\alpha_2 & \beta_1 & 0 \\ \beta_2 & \beta_1 & 1-\alpha_2 & 0 \\ 0 & 0 & 0 & 1+2\alpha_1+\alpha_2 \end{bmatrix}, \tag{4.64}$$

$$\begin{bmatrix} 1+\alpha_1-\alpha_2-\alpha_3 & \beta_2 & \beta_3 & 0 \\ \beta_2 & 1-\alpha_1-\alpha_2+\alpha_3 & \beta_1 & 0 \\ \beta_3 & \beta_1 & 1-\alpha_1+\alpha_2-\alpha_3 & 0 \\ 0 & 0 & 0 & 1+\alpha_1+\alpha_2+\alpha_3 \end{bmatrix}, \tag{4.65}$$

$$\begin{bmatrix} 1-\alpha_2 & \beta_2 & \beta_2 & 0 \\ \beta_2 & 1-\alpha_2 & \beta_2 & 0 \\ \beta_2 & \beta_2 & 1-\alpha_2 & 0 \\ 0 & 0 & 0 & 1+3\alpha_2 \end{bmatrix}. \tag{4.66}$$

The basis sets for these three blocks are

$$\begin{aligned} &\{2\sqrt{2}a_1^+a_2^+a_3,\ \ 2\sqrt{2}a_1^+b_3^+b_2,\ \ 2\sqrt{2}b_3^+a_2^+b_1,\ \ 2\sqrt{2}a_1a_2a_3\}, \\ &\{2\sqrt{2}a_1^+a_2^+a_4,\ \ 2\sqrt{2}a_1^+b_4^+b_2,\ \ 2\sqrt{2}b_4^+a_2^+b_1,\ \ 2\sqrt{2}a_1a_2a_4\}, \\ &\{2\sqrt{2}a_1^+a_3^+a_5,\ \ 2\sqrt{2}a_1^+b_5^+b_3,\ \ 2\sqrt{2}b_5^+a_3^+b_1,\ \ 2\sqrt{2}a_1a_3a_5\}, \end{aligned} \tag{4.67}$$

that are associated with three configurations schematically shown in (1), (2) and (3) of figure 4.3, respectively.

By further analysis , we found that: at extreme points V_{+1}^6, V_{-1}^6, V_{+2}^6 and V_{-2}^6, these blocks have negative eigenvalues and bigger negative eigenvalues are always in

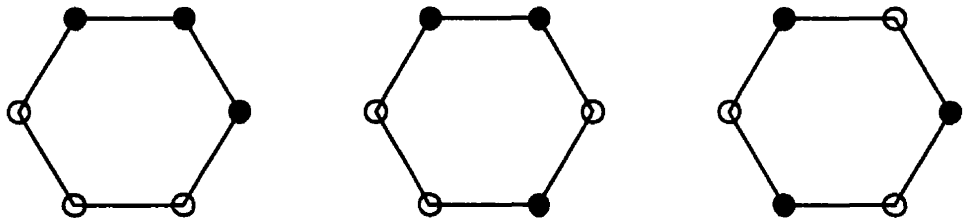

Figure 4.3: Some Configurations in the 3-body Density Matrix for $\Lambda = 6$

the first big block and the 4×4 block associated with configuration (1) in figure 4.3 . It seems that the positive semi-definite condition for the second big block is contained in the first big block and the 4×4 block associated with configuration (1) with three connected nearest neighbor sites is much more important than other 4×4 blocks in determining the lower bound to the ground state in the system. So it is quite possible that the bottom eigenvalues of the 3-body density matrix for a 1-dimensional ring can always be determined in the two blocks mentioned above. This means that: killer operators for the approximately n-representable ground state, which determine the correlation in the ground state, are linear combinations of the basis operators for the two blocks. Thus these blocks are the most important configurations in the 3-body density matrix x. This statement will be checked numerically in our computation. If it is true, the lower bound computation with the 3-body density matrix will be simplified dramatically in our system.

Numerical Computations with the 3-body Density Matrix

Direct lower bound computations with entries of the 3-body density matrix as

variational parameters are done for 1-dimensional rings with $|\Lambda| = 6$, 8 and 10. With circles and disks to represent the computed results for the half-filled ionic ground states from the wave-function method and the lower bound method respectively, the projections onto the $\beta_1\alpha_1$ plane of the computed correlation holes for $|\Lambda|$ =6, 8, 10 are schematically given in figures 4.4, 4.5 and 4.6, respectively. From these figures, it is quite clear that the approximately n-representable region are very close to their n-representable counterparts. In order to give a complete comparison, the ground state energies and the values of variables corresponding to the ground state of $\hat{h}^I$ in Eq. (4.38) with $\alpha_1^I = -1$ and $\alpha_2^I = 0$ for $|\Lambda| = 6$, 8, 10 are given in table 4.3. These results show that the lower bounds obtained are very tight and the approximately n-representable 3-body density matrices corresponding to the half-filled ionic ground states are very close to their n-representable counterparts.

In numerical computations, numerical procedures from both algorithms showed a fast speed of convergence. Actually as the dimensionality of the 3-body density matrix is reduced efficiently by removing type I blocks, the speed of convergence here is almost as fast as that in the lower bound method with the 2-body density matrix.

Numerical lower bound computations with only the two most important configurations discussed above are also carried out. The results obtained are exactly the same as those from the FCI lower bound computations. This proved numerically our prediction that the bottom eigenvalues of the 3-body density matrices corresponding to the half-filled ionic ground states are determined by these most important configurations.

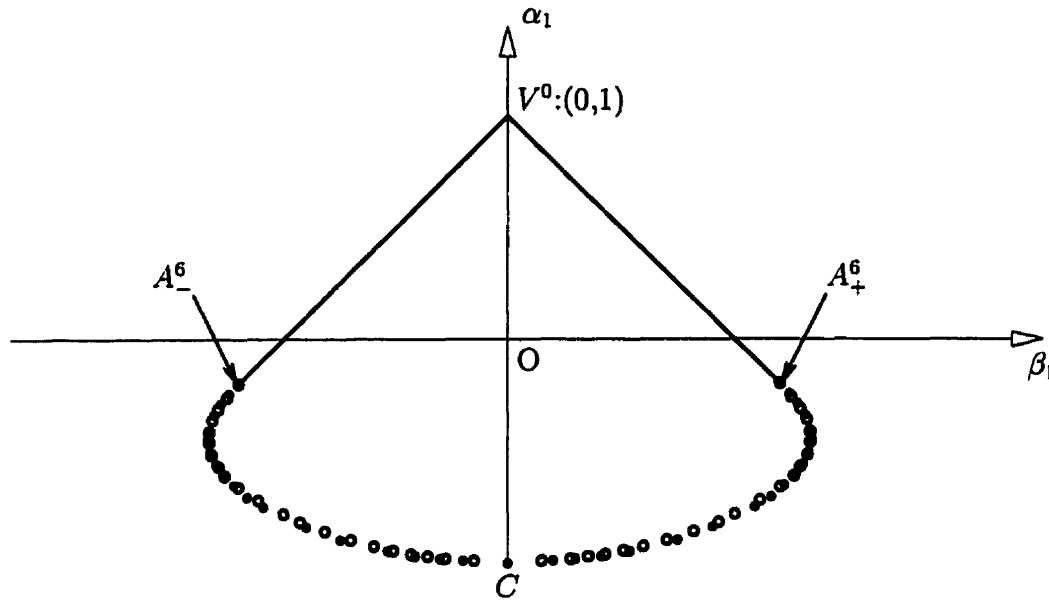

Figure 4.4: n-representable Region from the 3-body Density Matrix for $|\Lambda| = 6$

Conclusions

From these computed results, we find that: the lower bound method with entries of the 3-body density matrix as variational parameters works very well in our system. Not only does the computed approximately n-representable region have correct behavior, i.e., the approximately n-representable region will shrink as the number of sites increases, but also the lower bounds obtained are extremely tight and the optimized 3-body density matrices are very close to their n-representable counterparts. The significant improvement of the results from the 2-body density matrix to the 3-body density matrix shows that the 3-body density matrix in the lower bound method is a much better choice. The tightness of the lower bounds and the closeness of the computed values of all variables to those from the wave-function method strongly

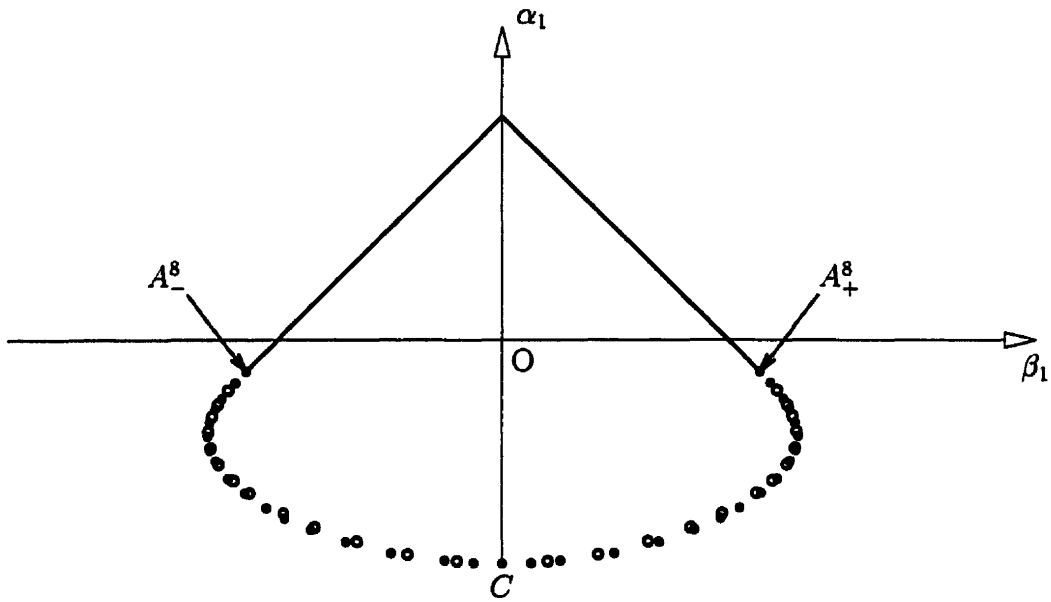

Figure 4.5: n-representable Region from the 3-body Density Matrix for $|\mathbf{\Lambda}| = 8$

indicate that the lower bound method with the p-body density matrix for larger p can not further improve the results very much. Thus the lower bound method with the 3-body density matrix is the best choice for the 1-dimensional system.

As pure 2-body nearest neighbor interactions in 1-, 2- and 3-dimensional cubic lattices share a lot of common characteristics, almost all the strategies used in the lower bound computation for 1-dimensional rings can be transferred into computations for 2- and 3-dimensional cubic lattices. Among these strategies, the idea of lower bound computations using only a small number of most important configurations is especially important. It has enormous practical significance since the dimensionality of the problem can be reduced considerably. The second numerical algorithm is a second-order numerical procedure and it is proved both theoretically and numerically to have a very fast speed of convergence even in large systems. So it is quite reason-

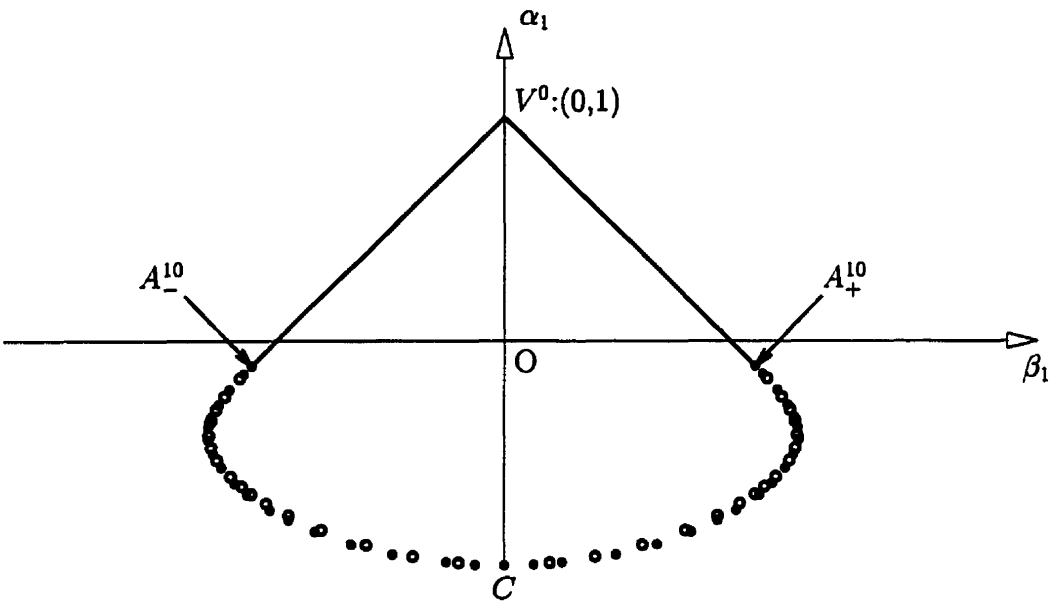

Figure 4.6: n-representable Region from the 3-body Density Matrix for $|\Lambda| = 10$

able to predict that direct lower bound computations in 2-dimensional square lattices will be achieved soon.

	$\|\Lambda\| = 6$		$\|\Lambda\| = 8$		$\|\Lambda\| = 10$	
	W-Function	L-Bound	W-Function	L-Bound	W-Function	L-Bound
α_1	-0.4444	-0.4474	-0.4268	-0.4304	-0.4189	-0.4229
α_2	0.0000	0.0218	0.0000	-0.0208	0.0000	0.0200
α_3	-0.1111	-0.1489	-0.0732	-0.1065	-0.0609	-0.0901
α_4			0.0000	0.0322	0.0000	0.0269
α_5					-0.0401	-0.0678
β_1	1.3333	1.3354	1.3066	1.3107	1.2944	1.2997
β_2	0.8889	0.8826	0.8535	0.8469	0.8380	0.8309
β_3	0.8889	0.9102	0.7886	0.7897	0.7401	0.7433
β_4			0.7372	0.6823	0.6601	0.6182
β_5					0.6142	0.6472
E_g	-4.0000	-4.0061	-5.2263	-5.2428	-6.4722	-6.4987

Table 4.3: Values for the Ground State of $\hat{h}^I$ with $\alpha_1^I = -1$, $\alpha_2^I = 0$

Chapter 5

Conclusions

By considering Pauli's principle and the nearest neighbor interactions, we found a seven-dimensional linear space H of all spin-invariant up to two-body nearest neighbor interactions in a class of lattices where all nearest neighbor pairs are equivalent. We classified these interactions into pure one-body which belong to H^1, a two-dimensional subspace of H, and pure two-body which belong to H^2, a five-dimensional subspace of H.

We studied the phase structure for pure two-body interactions in S_{H^2}. We found a very simple way to label quantum phases for S_{H^2} by a unique set of quantum numbers.

By simply using good quantum numbers and the idea of basin of attraction, we found six quantum phases of S_{H^2} in lattices with cubic symmetry. These quantum phases are a FM phase, an AFM phase, two superconducting phases characterized by the constant and alternating phase AGP functions, respectively, the mixed phase

where half of the sites are ionic and the other half are valence and the trivial vacuum quantum phase. Half-filling and collective behavior with some kind of long-range order are the main features for these quantum phases.

By analyzing the relationship between the basins of attraction for each of the adjacent phase pairs, we found that phase transitions are very likely to occur between each of the superconducting phases and the FM or AFM phase.

Both superconducting phases found are BCS-like superconducting states which are characterized by the condensate of coherent electron pairs. The on-site AGP pairing seems to be the unique AGP pairing in the system. Thus the on-site AGP pairing plays a key role in the superconducting phases. The uniqueness of the on-site AGP pairing is a very important conjecture. The proof or disproof of this conjecture will help us to gain a deeper understanding about the relationship between the AGP pairing and the quantum phases in cubic lattices. This will further help us to understand better about superconductivity in these lattices.

We formulated the central optimization problem in the lower bound method of reduced density matrix theory into a convex problem. Two numerical algorithms based on the main theorem are presented and programmed to solve the central optimization problem. Numerical procedures from both algorithms are second-order procedures. They exhibit a fast speed of convergence in our numerical computations. Both theoretical analysis and numerical experimentation show that numerical procedure from algorithm 2 will work even faster in large systems.

Numerical computations with the lower bound method are carried out to approach

both the two-body and the three-body reduced density matrices corresponding to the ionic ground states in one-dimensional rings. With the two-body density matrix, the results obtained show that: the lower bounds are not very close to the ground state energy from the full configuration wave-function method. The situation will become even worse as the number of sites increases. Thus, the most commonly used d, q and g n-representability conditions are not good enough to give reasonably tight lower bounds to the ground state as well as good approximations to the corresponding n-representable two-body density matrix in the system.

Both theoretical analysis and numerical computation show that the lower bound method with the three-body density matrix is the best choice for our system. Although the number of variables in the three-body density matrix is exactly the same as that in two-body density matrix, the lower bound obtained is very tight and the optimized three-body density matrix is very close to its n-representable counterpart.

Numerical computations with only the most important configurations are also carried out. The results obtained are exactly the same as those from the full configuration lower bound computations and the dimensionality of the computation is reduced dramatically.

As pure two-body nearest neighbor interactions in one-, two- and three-dimensional cubic lattices share a lot of common characteristics, almost all the strategies used in the lower bound computation for one-dimensional rings can be transferred into computations for higher-dimensional cubic lattices. From the computed results and conclusions for one-dimensional rings, it is reasonable to predict that direct lower bound

computation in two-dimensional square lattices is around the corner. The application of the lower bound method to other more complicated systems is not very far away.

It is found that the size of the basin of attraction for the mixed quantum phase is dimension dependent because of the fact that the degree of phase frustration in the mixed quantum phase depends on the dimensionality of the lattice. This will further affect the size of the basins of attraction for other quantum phases and thus will be the cause for some dimension dependent phenomena of the system. The exact relationship between the size of basin of attractions and the dimensionality can be determined by numerical computations. It may further explain why the superconducting phase prefers two-dimensional square lattices and if it is possible for the superconducting phase to occur in three-dimensional lattices.

The numerical procedure from algorithm 2 is proved to be a very efficient numerical procedure, especially for large systems. It will not only help to make the lower bound method of reduced density matrix theory to become a computationally feasible method in large scale but should also have more applications in other linear and nonlinear optimization problems.

After all, our work makes it one step closer to achieving the dream of replacing the wave-function method with the lower bound method of reduced density matrix theory.

Bibliography

[1] H. Kamerlingh-Onnes, Comm. Phys. Lab. Leiden, 10, 120b (1911); 12, 122b and 124c (1911).

[2] L. R. Testardi, J. H. Wernick and W. A. Royer, Solid State Commun. 15, 1 (1974).

[3] J. Bardeen, L. N. Cooper and J. R. Schrieffer, Phys. Rev. 108, 1175 (1957).

[4] J. B. Bednorz and K. A. Müller, Z. Phys. B 64, 189 (1986).

[5] L. Gao, Y. Y. Xue, F. Chen, Q. Xiong, R. L. Meng, D. Ramirez, C. W. Chu, J. H. Eggert and H. K. Mao, Phys. Rev. B 50, 4260 (1994).

[6] A. Santoro, in High Temperature Superconductivity, J. W. Lynn et al. Eds., (Springer-Verlag, 1990), pp. 84-121.

[7] P. B. Allen, in High Temperature Superconductivity, J. W. Lynn et al. Eds., (Springer-Verlag, 1990), pp. 303-342.

[8] W. Heisenberg, Z. Phys. 49, 619 (1928).

[9] P. O. Löwdin, Rev. Mod. Phys. 34, 80 (1962).

[10] T. Freltoft, G. Shirane, S. Mitsuda, J. P. Remeika and A. S. Cooper, Phys. Rev. B 37, 137 (1988).

[11] C. Stassis, B. N. Harmon, T. Freltoft, G. Shirane, S. K. Sinha, K. Yamada, Y. Endoh, Y. Hidaka and T. Murakami, Phys Rev. B 38, 9291 (1988).

[12] D. C. Johnston, J. P. Stokes, D. P. Goshorn, J. T. Lewandowski, Phys Rev. B 36, 4007 (1987).

[13] D. Vaknin, S. K. Sinha, D. E. Moncton, D. C. Johnston, J. M. Newsam, C. R. Safinya, and H. E. King, Jr., Phys Rev. Lett. 58, 2802 (1987).

[14] Y. J. Uemura, C. E. Stronach, D. C. Johnston, M. S. Alvarez and D. P. Goshorn, Phys Rev. Lett. 59, 1045 (1987).

[15] D. R. Harshman, G. Aeppli, G. P. Espinosa, A. S. Cooper, J. P. Remeika, E. J. Ansaldo, T. M. Riseman, D. Ll. Williams, D. R. Noakes, B. Ellman and T. F. Rosenbaum, Phys Rev. B 38, 852 (1988).

[16] E. Manousakis, Rev. Mod. Phys. 63, 1 (1991).

[17] E. Dagotto and A. Moreo, Phys. Rev. B 38, 5087 (1988).

[18] Z. Liu and E. Manousakis, Phys. Rev. B 40, 11437 (1989).

[19] D. Huse, Phys. Rev. B 37, 2380 (1988).

[20] P. W. Anderson, Phys. Rev. 86, 694 (1952).

[21] S. Liang, B. Doucot, and P. W. Anderson, Phys. Rev. Lett. 61, 365 (1988).

[22] P. W. Anderson, Science 235, 1196 (1987).

[23] A. H. MacDonald, S. M. Girvin and D. Yoshioka, Phys Rev. B 37, 9753 (1988).

[24] J. E. Hirsch, Phys. Rev. Lett. 54, 1317 (1985).

[25] P. W. Anderson, in Frontiers and borderlines in many-particle physics : Varenna on Lake Como, Villa Monastero, July 7-17, 1987, edited by R.A. Broglia and J.R. Schrieffer, (Elsevier Science Pub. Co., 1988).

[26] F. A. Valentine, Convex Sets, McGraw-Hill Book Comp. Inc., New York (1964).

[27] P. O. Löwdin, Phys. Rev. 97, 1474 (1955).

[28] A. J. Coleman, Rev. Mod. Phys. 35, 668 (1963).

[29] J. E. Mayer, Phys. Rev. 100, 1579 (1955).

[30] R. H. Tredgold, Phys. Rev. 105, 1421 (1957).

[31] R. V. Ayres, Phys. Rev. 111, 1453 (1958).

[32] A. J. Coleman, in Density Matrices and Density Functionals, Proceedings of A. John Coleman Symposium, edited by R. Erdahl and V. H. Smith, Jr., (D. Reidel, Dordrecht, 1987), pp. 5-20.

[33] A. J. Coleman, Can. Math. Bull. 4, 209 (1961).

[34] C. Garrod and J. K. Percus, J. Math. Phys. 5, 1765 (1964).

[35] A. J. Coleman, J. Math. Phys. 13, 214 (1972).

[36] R. Erdahl, J. Math. Phys. 13, 1608 (1972).

[37] R. Erdahl, in Density Matrices and Density Functionals, Proceedings of A. John Coleman Symposium, edited by R. Erdahl and V. H. Smith, Jr., (D. Reidel, Dordrecht, 1987), pp. 51-71.

[38] P. O. Löwdin, in Density Matrices and Density Functionals, Proceedings of A. John Coleman Symposium, edited by R. Erdahl and V. H. Smith, Jr., (D. Reidel, Dordrecht, 1987), pp. 21-49.

[39] C. N. Yang, Rev. Mod. Phys. 34, 694 (1962).

[40] O. Penrose and L. Onsager, Phys. Rev. 104, 576 (1956).

[41] F. Bloch, Phys. Rev. 137, A787 (1965).

[42] J. M. Blatt, Prog. Theor. Phys. 23, 447 (1960).

[43] A. J. Coleman, J. Math. Phys. 6, 1425 (1965).

[44] F. Bopp, Z. Phys. 156, 348 (1959).

[45] E. G. Weidemann, Nucl. Phys. 65, 559 (1965).

[46] R. L. Hall and H. R. Post, Proc. Phys. Soc. A69, 936 (1956); A79, 819(1962); A90, 381 (1967).

[47] R. L. Hall, Proc. Phys. Soc. A91, 16 (1967).

[48] M. V. Mihailović and M. Rosina, Nucl. Phys. A130, 386 (1969).

[49] E. R. Davidson, J. Math. Phys. 10, 725 (1969).

[50] L. Kijewski, Phys. Rev. 6, 31 (1972).

[51] C. Garrod, M. V. Mihailović and M. Rosina, J. Math. Phys. 16, 868 (1975).

[52] M. V. Mihailović and M. Rosina, Nucl. Phys. A237, 221 (1975).

[53] R. Erdahl, Rep. Math. Phys. 15, 147 (1979).

[54] R. Erdahl, Int. J. Quantum Chem. 13, 697 (1978).

[55] H. A. Bethe, Z. Phys. 71, 205 (1931).

[56] R. L. Orbach, Phys. Rev. 112, 309 (1958).

[57] T. Kennedy, E. H. Lieb and B. S. Shastry, J. Stat. Phys. 53, 1019 (1988).

[58] J. M. Blatt, Prog. Theor. Phys. 23, 447 (1960).

[59] J. Linderberg and Y. Öhrn, Int. J. Quantum Chem. 12, 161 (1977).

[60] J. V. Ortiz, B. Weiner and Y. Öhrn, Int. J. Quantum. Chem. Symp. 15, 113 (1981).

[61] E. Sangfelt, H. Kurtz, N. Elander and O. Goscinski, J. Chem. Phys. 81, 3976 (1984).

[62] A. J. Coleman, Rep. Math. Phys. 4, 113 (1973).

[63] M. Rosina in Reduced Density Operators with Application to Physical and Chemical Systems II, R. M. Erdahl, Ed. (Queen's Papers on Pure and Applied Mathematics, No. 40, 1974), p. 50.

[64] D. G. Luenberger, Introduction to Linear and Nonlinear Programming, Addison-Wesley Pub. Co., Reading, Mass. (1973).

[65] M. Rosina and C. Garrod, J. Comp. Phys. 18, 300 (1975).

[66] R. Erdahl, "Optimal Design Of A Real Symmetric Matrix" to be published.

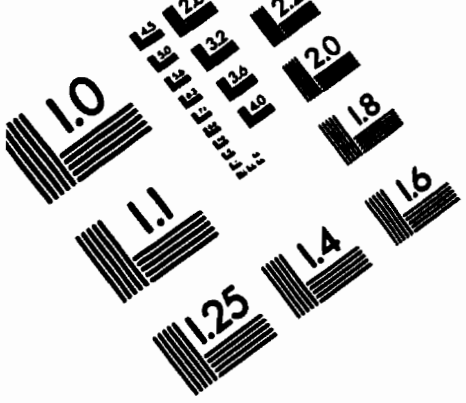

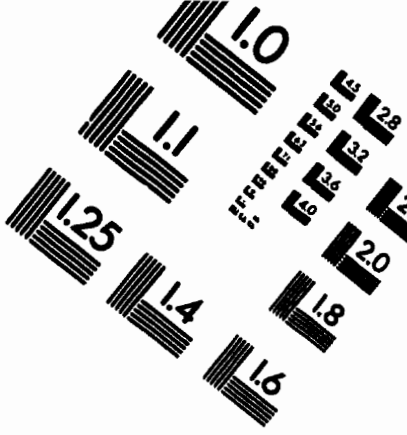

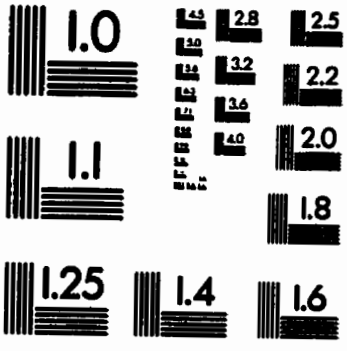

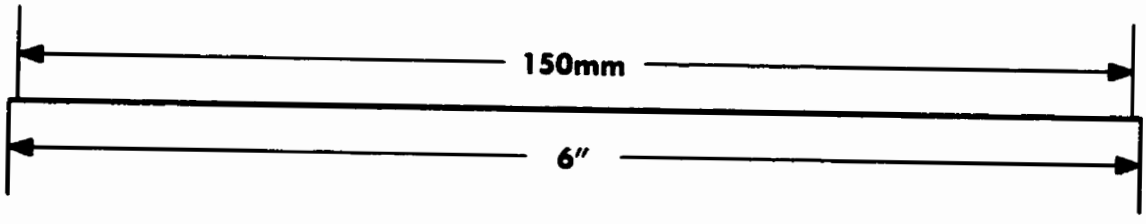

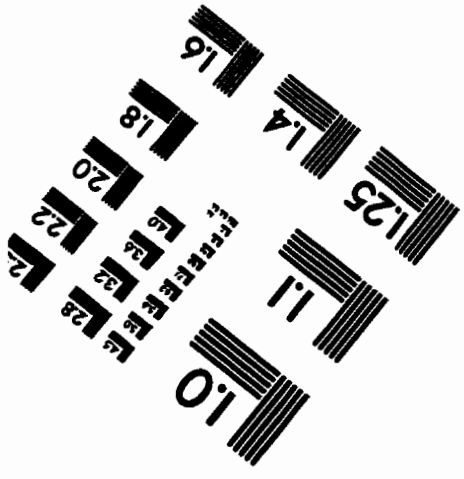

APPLIED IMAGE, Inc
1653 East Main Street
Rochester, NY 14609 USA
Phone: 716/482-0300
Fax: 716/288-5989